

Pharmacology of a Novel Biased Allosteric Modulator for NMDA Receptors

Lina Kwapisz

Thesis submitted to the faculty of the Virginia Polytechnic Institute and State University
in partial fulfillment of the requirements for the degree of

Master of Science
In
Biomedical and Veterinary Sciences

B. Costa, Co-Chair
B. Klein
M. Theus
C. Reilly

April 28th of 2021
Blacksburg, VA

Keywords: NMDAR, allosteric modulation, CNS4, glutamate

Pharmacology of a Novel Biased Allosteric Modulator for NMDA Receptors

Lina Kwapisz

ABSTRACT

NMDA glutamate receptor is a ligand-gated ion channel that mediates a major component of excitatory neurotransmission in the central nervous system (CNS). NMDA receptors are activated by simultaneous binding of two different agonists, glutamate and glycine/ D-serine¹. With aging, glutamate concentration gets altered, giving rise to glutamate toxicity that contributes to age-related pathologies like Parkinson's disease, Alzheimer's disease, amyotrophic lateral sclerosis, and dementia^{88,95}. Some treatments for these conditions include NMDA receptor blockers like memantine¹³⁰. However, when completely blocking the receptors, there is a restriction of the receptor's normal physiological function⁵⁹. A different approach to regulate NMDAR receptors is through allosteric modulators that could allow cell type or circuit-specific modulation, due to widely distributed GluN2 expression, without global NMDAR overactivation^{59,65,122}.

In one study, we hypothesized that the compound CNS4 selectively modulates NMDA diheteromeric receptors (GluN2A, GluN2B, GluN2C, and GluN2D) based on (three) different glutamate concentrations. Electrophysiological recordings carried out on recombinant NMDA receptors expressed in xenopus oocytes revealed that 30 μ M and 100 μ M of CNS4 potentiated ionic currents for the GluN2C and GluN2D subunits with 0.3 μ M Glu/100 μ M Gly. However, when using 300 μ M Glu/100 μ M Gly, CNS4 inhibited the relative response in the GluN2D subunit and had no effect on the remaining subunits. CNS4 reduced the response to glutamate alone for GluN2A but increased it for GluN2B and did not appear to replace glutamate. Another set of electrophysiological recordings measuring current-voltage relationship was made in order to understand ion flow across the channel in the presence of CNS4. 100 μ M CNS4 numerically increased the ionic inward current through the channel pore with more positive membrane potential, reflected by a significant difference in reversal potential values, in the GluN2C and GluN2D subunits. CNS4 also exhibited a non-voltage dependent activity and it did not appear to compete with magnesium which naturally blocks the receptor.

Finally, the effect of CNS4 on calcium uptake and cellular viability was studied in neurons from primary rat brain culture. Cortical and striatal neurons were given excessive doses of synthetic agonist NMDA in order to hyperactivate native NMDAR. In the calcium assay, 100 μ M of CNS4 significantly increased calcium uptake when given with 300 μ M NMDA compared with NMDA alone in cortex and when given with 100 μ M and 300 μ M NMDA in striatum. In the MTS assay, CNS4 did not alter neuronal viability in either cortical or striatal neurons compared with NMDA alone. Also, when CNS4 was used in non treated neurons it did not alter neuronal viability. Findings from the primary brain culture let us conclude that CNS4 could facilitate calcium influx and possibly be non toxic for neurons.

Pharmacology of a Novel Biased Allosteric Modulator for NMDA Receptors

Lina Kwapisz

GENERAL AUDIENCE ABSTRACT

NMDA ionotropic glutamate receptors are predominately expressed in the central nervous system (CNS). These receptors are activated by glutamate and glycine/ D-serine¹. With aging, glutamate concentration in the synapse gets altered giving rise to toxic environments for neurons that can contribute to age-related pathologies like Parkinson's disease, Alzheimer's disease, amyotrophic lateral sclerosis, and dementia^{88,95}. Some treatments of these conditions include the receptor blockers like memantine¹³⁰. However, when completely blocking the receptors, there is a restriction of the receptor's normal physiological function⁵⁹. A different approach to regulate NMDAR is through allosteric modulators that are compounds that modulate the receptor function without competing with endogenous agonists^{59,65,122}.

In this study, we hypothesized that the compound CNS4 selectively modulates NMDAR based on glutamate concentration. Electrophysiological recordings on stage four xenopus oocytes helped us to identify the dose-dependent activity of CNS4 and we found that 30 and 100 μ M of CNS4 selectively potentiates ionic currents for GluN2C and GluN2D subunits with 0.3 μ M Glu/100 μ M Gly but inhibited currents for only GluN2D with 300 μ M Glu/100 μ M Gly. Following this, a current-voltage plot was made to examine the channel activity of CNS4. We found a numerical increase of ionic inward current through the channel pore with more positive membrane potential values in the GluN2C and GluN2D subunits. Also, the effect of CNS4 on the ion current activity changed based on glutamate concentration, and CNS4 did not exhibit a voltage-dependent activity, which is a positive feature for compounds that target the receptor¹³³.

Finally, to better understand the effect of the compound CNS4 in primary neurons in a toxic environment, a rat brain neuronal culture was made. Increasing doses of NMDA with constant 100 μ M CNS4 increased cellular Ca²⁺ influx in a dose-dependent manner. Particularly, 100 μ M CNS4 with 300 μ M NMDA exhibited a significant increase in Ca²⁺ influx in both cortical and striatal neurons compared with 300 μ M NMDA alone. However, when used alone, 100 μ M CNS4 did not have an effect on the amount of Ca²⁺ influx. In addition, CNS4 plus NMDA did not increase viability compared to NMDA alone, and CNS4 alone did not proportionally reduce neuronal viability.

DEDICATION

To God, my father Luis, my twin sister Camila and my husband Peter. To my friends, specially Brittney, for all the work and emotional support. Thank you for always being there for me.

ACKNOWLEDGEMENTS

First of all, I would like to acknowledge my lab. Dr. Costa has been a good advisor and without his guidance this work couldn't have been possible. I also want to thank Brittney for all her support with all experiments and for her friendship.

I thank my committee members Dr. Theus, Dr. Klein and Dr. Reilly for their feedback and help along the way.

TABLE OF CONTENTS

ABSTRACT	ii
GENERAL AUDIENCE ABSTRACT	iii
DEDICATION	iv
ACKNOWLEDGEMENTS	v
TABLE OF CONTENTS	vi
LIST OF FIGURES	viii
LIST OF TABLES	xiii
LIST OF ABBREVIATIONS	xiv
CHAPTER ONE: GENERAL INTRODUCTION	1
INTRODUCTION	1
NMDA RECEPTOR SUBUNITS	1
NMDA RECEPTOR SUBUNITS IN DEVELOPMENT	2
NMDA RECEPTOR STRUCTURE	3
NMDA RECEPTOR ENDOGENOUS AGONISTS	6
<i>GluN1</i>	7
<i>GluN2</i>	7
<i>GluN3</i>	8
GATING, LIGAND-BINDING AND CHANNEL PROPERTIES	8
SYNAPTIC PLASTICITY	11
CHAPTER 2: LITERATURE REVIEW	12
CHANGES IN SYNAPTIC GLUTAMATE CONCENTRATION	12
DISORDERS ASSOCIATED WITH NMDA RECEPTORS	13
NMDA RECEPTOR PHARMACOLOGY	21
<i>SYNTHETIC AGONISTS</i>	21
<i>COMPETITIVE ANTAGONISTS</i>	22
<i>NONCOMPETITIVE ANTAGONISTS</i>	24
<i>CHANNEL BLOCKERS</i>	24
<i>ALLOSTERIC REGULATION</i>	26
CHAPTER 3: DOSE DEPENDENT ACTIVITY OF CNS4	31
INTRODUCTION	31
<i>The need for allosteric regulation based on glutamate concentration</i>	31
<i>CNS4</i>	32
SPECIFIC AIM 1:	33
MATERIALS AND METHODS	33
Oocytes:	33
<i>Solutions</i>	33
<i>Compounds</i>	33

<i>NMDAR Constructs</i>	34
<i>Oocyte Processing</i>	34
<i>Electrophysiological Recordings for Dose Response Curve (DRC)</i>	35
<i>Statistics</i>	37
RESULTS	37
CONCLUSION.....	42
CHAPTER 4: CNS4 CHANNEL ACTIVITY IN NMDA RECEPTORS.....	56
INTRODUCTION	56
<i>Understanding NMDAR channel properties</i>	56
SPECIFIC AIM 2	57
MATERIALS AND METHODS.....	57
Oocytes:	57
<i>Solutions</i>	57
<i>Compounds</i>	58
<i>NMDAR Constructs</i>	58
<i>Oocyte Processing</i>	58
<i>Electrophysiological Recordings for Current Voltage (IV) plot</i>	59
<i>Statistics</i>	60
RESULTS	61
CONCLUSION.....	65
CHAPTER 5: CNS4 ACTIVITY IN PRIMARY NEURONS.....	75
INTRODUCTION	75
SPECIFIC AIM 3.....	76
MATERIALS AND METHODS.....	76
<i>Neuronal culture</i>	76
<i>Calcium assay</i>	78
<i>MTS tetrazolium cell proliferation assay</i>	78
<i>Statistics</i>	79
RESULTS	80
CONCLUSION.....	83
CHAPTER 6: CONCLUSION.....	90
REFERENCES.....	94

LIST OF FIGURES

Figure 1. 1 Schematic diagram showing heteromeric structure of NMDAR. The amino-terminal domain (ATD) comprises binding site for Zn ²⁺ . Ligand-binding domain (LBD) composed of extracellular segments S1 and S2 which binds agonist glutamate (GluN2) and co-agonist glycine (GluN1 and GluN3). The transmembrane domain (TMD) is formed by three transmembrane helices (M1, M3 and M4) and one loop (M2) which form a channel pore. The highly diversified intracellular C-terminal domain (CTD), is labeled . (Hashimoto K, 2017 [2]) used under fair used, 2020.	6
Figure 1. 2 NMDA Receptor Subtype Deactivation Kinetics. NMDAR currents recorded from transfected HEK cells with a brief application of 1mM of glutamate. Ranking order from faster to slower: GluN2A> GluN2B > GluN2C > GluN2D. (Paoletti, 2011 [11]) Used under fair use 2020.	10
Figure 3. 1 CNS4 (4-fluoro-N-(2-(pyridin-3-yl)piperidine-1-carbonothioyl) benzamide chemical structure	34
Figure 3. 2 Kwapisz L (2020) Picture of a “clamped” oocyte using two-electrode voltage clamp electrophysiology. Costa lab, Virginia Tech.....	35
Figure 3. 3 GluN2A (blue), GluN2B (red), GluN2C (pink) and GluN2D (green) relative response with increasing doses of CNS4 (1µM, 3µM, 10µM, 30µM and 100µM) in Agonist solution (0.3µM Glu/ 100µM Gly). Statistical significance was determined comparing means of the evoked response using Agonist solution alone in at least five oocytes with every CNS4 increasing doses at the alpha level $p < 0.05(*)$ and using a one-way ANOVA Tukey’s multiple comparisons.	45
Figure 3. 4 Traces from GluN2C (pink) and GluN2D (green) dose response curve recordings with increasing doses of CNS4 (1µM, 3µM, 10µM, 30µM and 100µM) in agonist solution (0.3µM Glu/ 100µM Gly), every trace represents a single experiment using one oocyte.	46
Figure 3. 5 Relative response (y axis) of the GluN2A (blue), GluN2B, (red), GluN2C (pink) and GluN2D (green) in Agonist solution with increasing doses of CNS4 converted to the logarithmic scale (x axis). The GluN2D subunit exhibits the greatest increase in relative response.....	47
Figure 3. 6 GluN2A (blue), GluN2B (red), GluN2C (pink) and GluN2D (green) relative response with increasing doses of CNS4 (1µM, 3µM, 10µM, 30µM and 100µM) in Agonist max solution (100µM Glu/ 100µM Gly). Statistical significance was determined comparing means of the evoked response using Agonist max solution alone in at least five oocytes with every CNS4 increasing doses at the alpha level $p < 0.05(*)$ and using a one-way ANOVA Tukey’s multiple comparisons.	48
Figure 3. 7 Traces from GluN2C (pink) and GluN2D (green) dose response curve recordings with increasing doses of CNS4 (1µM, 3µM, 10µM, 30µM and 100µM) in agonist max solution (100µM Glu/ 100µM Gly), every trace represents a single experiment using one oocyte.	49
Figure 3. 8 Relative response (y axis) of the GluN2A (blue), GluN2B, (red), GluN2C (pink) and GluN2D (green) in Agonist max solution with increasing doses of CNS4	

converted to the logarithmic scale (x axis). The GluN2A subunit exhibits the greatest increase in relative response, however, it was non statistically significant..... 50

Figure 3. 9 GluN2A (blue), GluN2B (red), GluN2C (pink) and GluN2D (green) relative response with increasing doses of CNS4 (1µM, 3µM, 10µM, 30µM and 100µM) in Agonist super max solution (300µM Glu/ 100µM Gly). Statistical significance was determined comparing means of the evoked response using Agonist super max solution alone in at least five oocytes with every CNS4 increasing doses at the alpha level $p < 0.05(*)$ and using a one-way ANOVA Tukey's multiple comparisons..... 51

Figure 3. 10 Traces from GluN2C (pink) and GluN2D (green) dose response curve recordings with increasing doses of CNS4 (1µM, 3µM, 10µM, 30µM and 100µM) in agonist super max solution (300µM Glu/ 100µM Gly), every trace represents a single experiment using one oocyte 52

Figure 3. 11 Relative response (y axis) of the GluN2A (blue), GluN2B, (red), GluN2C (pink) and GluN2D (green) in Agonist super max solution with increasing doses of CNS4 converted to the logarithmic scale (x axis). The GluN2D subunit exhibits the greatest decrease in relative response..... 53

Figure 3. 12 Top, Traces from GluN2A subunit with Agonist max solution, glycine alone (100µM), glutamate alone (100µM), glycine + CNS4 (100µM each) and glutamate + CNS4 (100µM each) representing a single experiment using one oocyte. **Bottom**, GluN2A relative response with Agonist max, glutamate alone (100µM), glutamate + CNS4 (100µM each), glycine alone (100µM) and glycine + CNS4 (100µM each). Statistical significance was determined comparing means of the evoked response with every solution in at least five oocytes at the alpha level $p < 0.05(*)$ using ANOVA Tukey's multiple comparisons test. 54

Figure 3. 13 Top, Traces from GluN2A subunit with Agonist max solution, glycine alone (100µM), glutamate alone (100µM), glycine + CNS4 (100µM each) and glutamate + CNS4 (100µM each) representing a single experiment using one oocyte. **Bottom**, GluN2A relative response with Agonist max, glutamate alone (100µM), glutamate + CNS4 (100µM each), glycine alone (100µM) and glycine + CNS4 (100µM each). Statistical significance was determined comparing means of the evoked response with every solution in at least five oocytes at the alpha level $p < 0.05(*)$ using ANOVA Tukey's multiple comparisons test 55

Figure 4. 1 Explanatory diagram of ion movement across the cell membrane (green line) when doing IV plot electrophysiology. The y axis represent electrophysiological responses in current which is measured in amperes, negative values represent inward current (ions going outside the cell). The x axis represent different membrane holding potential, negative values are plotted in the left and positive values to the right. The red circle points out when the Y axis is equal to zero, meaning that no ions are crossing the cell membrane, this is referred as Reversal potential. 60

Figure 4. 2 Upper two, current (x axis) and voltage (y axis) relationship of CNS4 (100µM) in the GluN2A subunit in the presence and absence of Agonist solution (0.3µM Glu/100µ Gly) and in the presence and absence of 40µM MgCl₂, allowing visualizing of the ion movements across the channel. **Bottom**, comparison of reversal potential from at least five recordings in the presence and absence of CNS4 in the GluN2A subunit .

Statistical comparison of the reversal potential was determined at the alpha level $p < 0.05(*)$ using one way ANOVA Tukey's multiple comparisons test 67

Figure 4. 3 Upper two, current (x axis) and voltage (y axis) relationship of CNS4 (100 μ M) in the GluN2B subunit in the presence and absence of Agonist solution (0.3 μ M Glu/100 μ Gly) and in the presence and absence of 40 μ M MgCl₂ , allowing visualizing of the ion movements across the channel. **Bottom**, comparison of reversal potential from at least five recordings in the presence and absence of CNS4 in the GluN2B subunit . Statistical comparison of the reversal potential was determined at the alpha level $p < 0.05(*)$ using one way ANOVA Tukey's multiple comparisons test. 68

Figure 4. 4 Upper two, current (x axis) and voltage (y axis) relationship of CNS4 (100 μ M) in the GluN2C subunit in the presence and absence of Agonist solution (0.3 μ M Glu/100 μ Gly) and in the presence and absence of 40 μ M MgCl₂ , allowing visualizing of the ion movements across the channel. **Bottom**, comparison of reversal potential from at least five recordings in the presence and absence of CNS4 in the GluN2C subunit . Statistical comparison of the reversal potential was determined at the alpha level $p < 0.05(*)$ using one way ANOVA Tukey's multiple comparisons test. 69

Figure 4. 5 Upper two, current (x axis) and voltage (y axis) relationship of CNS4 (100 μ M) in the GluN2D subunit in the presence and absence of Agonist solution (0.3 μ M Glu/100 μ Gly) and in the presence and absence of 40 μ M MgCl₂ , allowing visualizing of the ion movements across the channel. **Bottom**, comparison of reversal potential from at least five recordings in the presence and absence of CNS4 in the GluN2D subunit . Statistical comparison of the reversal potential was determined at the alpha level $p < 0.05(*)$ using one way ANOVA Tukey's multiple comparisons test. 70

Figure 4. 6 Upper two, current (x axis) and voltage (y axis) relationship of CNS4 (100 μ M) in the GluN2A subunit in the presence and absence of Agonist max solution (100 μ M Glu/100 μ Gly) and in the presence and absence of 40 μ M MgCl₂ , allowing visualizing of the ion movements across the channel. **Bottom**, comparison of reversal potential from at least five recordings in the presence and absence of CNS4 in the GluN2A subunit . Statistical comparison of the reversal potential was determined at the alpha level $p < 0.05(*)$ using one way ANOVA Tukey's multiple comparisons test. 71

Figure 4. 7 Upper two, current (x axis) and voltage (y axis) relationship of CNS4 (100 μ M) in the GluN2B subunit in the presence and absence of Agonist max solution (100 μ M Glu/100 μ Gly) and in the presence and absence of 40 μ M MgCl₂ , allowing visualizing of the ion movements across the channel. **Bottom**, comparison of reversal potential from at least five recordings in the presence and absence of CNS4 in the GluN2B subunit . Statistical comparison of the reversal potential was determined at the alpha level $p < 0.05(*)$ using one way ANOVA Tukey's multiple comparisons test. 72

Figure 4. 8 Upper two, current (x axis) and voltage (y axis) relationship of CNS4 (100 μ M) in the GluN2C subunit in the presence and absence of Agonist max solution (100 μ M Glu/100 μ Gly) and in the presence and absence of 40 μ M MgCl₂ , allowing visualizing of the ion movements across the channel. **Bottom**, comparison of reversal potential from at least five recordings in the presence and absence of CNS4 in the GluN2C subunit . Statistical comparison of the reversal potential was determined at the alpha level $p < 0.05(*)$ using one way ANOVA Tukey's multiple comparisons test. 73

Figure 4. 9 Upper two, current (x axis) and voltage (y axis) relationship of CNS4 (100 μ M) in the GluN2D subunit in the presence and absence of Agonist max solution

(100 μ M Glu/100 μ Gly) and in the presence and absence of 40 μ M MgCl₂, allowing visualizing of the ion movements across the channel. **Bottom**, comparison of reversal potential from at least five recordings in the presence and absence of CNS4 in the GluN2D subunit. Statistical comparison of the reversal potential was determined at the alpha level $p < 0.05(*)$ using one way ANOVA Tukey's multiple comparisons test. 74

Figure 5. 1 Kwapisz L (2020) Pictures of E19 rat embryo dissection with anatomic characterization of different brain regions. **A.** Ventral view of an E19 brain rat under the microscope, (1) optic chiasm (2) Left hemisphere (3) midbrain (4) spinal cord. **B.** Ventral view of one of the two hemispheres separated from the brain (1) brain cortex (2) striatum. **C.** Ventral view of one hemisphere with (1) cortex region separated from (2) striatum region. Costa Lab, Virginia Tech..... 77

Figure 5. 2 Cortex Ca²⁺ assay in neurons previously treated with NMDA to induce hyperactivation of NMDAR with increasing doses of NMDA and constant 100 μ M CNS4. Every treatment group had eight dots representing the eight wells of every column of the 96well plate, color of starts on top of the dots represent the group that is being compared with. The presence of CNS4 (100 μ M) did not alter Ca²⁺ uptake compared to control, however, increased Ca²⁺ uptake when used with NMDA (300 μ M). Statistical difference was determined through at the alpha level $p < 0.05(*)$ using one way ANOVA Tukey's multiple comparisons. 85

Figure 5. 3 Striatum Ca²⁺ assay in neurons previously treated with NMDA to induce hyperactivation of NMDAR with increasing doses of NMDA and constant 100 μ M CNS4. Every treatment group had eight dots representing the eight wells of every column of the 96well plate, color of starts on top of the dots represent the group that is being compared with. The presence of CNS4 (100 μ M) did not alter Ca²⁺ uptake compared to control, however, increased Ca²⁺ uptake when used with NMDA (100 μ M and 300 μ M). Statistical difference was determined through at the alpha level $p < 0.05(*)$ using one way ANOVA Tukey's multiple comparisons. 86

Figure 5. 4 Cortex MTS Assay in neurons previously treated with NMDA to induce hyperactivation of NMDAR. Y axis represents quantification of cellular metabolic activity measured at OD 490nm, X axis represent treatment groups and color of starts represent the group that is being compared with. NMDA (100 μ M) reduced metabolic activity in neurons compared with control. Increasing doses of CNS4 (1, 10 and 100 μ M) with NMDA (100 μ M) did not have an effect in neuronal viability compared with NMDA (100 μ M) alone. Statistical differences were done comparing means of every treatment group with ANOVA Tukey's multiple comparisons test at the alpha level $p < 0.05(*)$. 87

Figure 5. 5 Striatum MTS Assay in neurons previously treated with NMDA to induce hyperactivation of NMDAR. Y axis represents quantification of cellular metabolic activity measured at OD 490nm, X axis represent treatment groups and color of starts represent the groups and color of starts represent the group that is being compared with. NMDA (100 μ M) reduced metabolic activity in neurons compared with control and memantine (50 μ M) increased it. Increasing doses of CNS4 (1, 10 and 100 μ M) with NMDA (100 μ M) did not have an effect in neuronal viability compared with NMDA (100 μ M) alone. Statistical differences were done comparing means of every treatment group with ANOVA Tukey's multiple comparisons test at the alpha level $p < 0.05(*)$. 88

Figure 5. 6 Cortex and Striatum MTS assay in untreated neurons versus 100 μ M CNS4.
Statistical difference was determined with unpaired T-Test P (<0.001) 89

LIST OF TABLES

Table 1. 1 Gating and Ligand-Binding Properties of the GluN2 subtypes at the ATD. (Glasgow et al, 2015 [18]) Used under fair use, 2020.	9
Table 1. 2 Channel Properties of the GluN2 subtypes at the LBD and TMD. (Glasgow et al, 2015 [18]) Used under fair use, 2020.	10
Table 3. 1 Protocol followed for the CNS4 dose response experiment and the amount of oocytes used.	37

LIST OF ABBREVIATIONS

AD	Alzheimer's disease
ALCAR	Acetyl-L-Carnitine
AMPA	α -Aminio-hydroxy-5-methyl-4-isoxazole propionic acid
ASD	Autism spectrum disorder
ATD	Amino-terminal domain
BDNF	Brain-derived neurotrophic factor
CaMKII	Calcium/calmodulin-dependent protein kinase II
CaMKIII	Eukaryotic elongation factor 2 (eEF2) kinase
CNS	Central nervous system
CTD	Carboxyl-terminal domain
D-AP5	D- [-]-2-amino-5-phosphonopenatnoid acid
D-AP7	D- [-]-2-amino-7-phosphonopenatnoic acid
5,7-DCK	5,7-dicholorokynurenic acid
DCS	D-cycloserine
DRG	Dorsal Root Ganglia
GluR	Glutamate receptor
iGluR	Ionotropic glutamate receptor
L	Leucine
LBD	Ligand-binding domain
LID	L-DOPA-induced-dyskinesia
LTD	Long-term depression
LTP	Long-term potentiation
mGluR	Metabotropic glutamate receptor
MK-801	[PCP, dizocilpine maleate]
mTOR	The mammalian target of rapamycin
NMDA	N-methyl-d-aspartate
PAS	Pregnanolone sulfate
PCP	Phencyclidine
PD	Parkinson's Disease
PKA	Protein kinase A
PKC	Protein kinase C
P_{open}	Maximal channel open probability
S	Serine
SCZ	Schizophrenia
SNC	Substance nigra zona compacta
TMD	Transmembrane domain
UBP	1-(phenanthrene-2-carbonyl) pyrazine-2,3-dicarboxylic acid
V_m	Voltage membrane potential

CHAPTER ONE: GENERAL INTRODUCTION

INTRODUCTION

The NMDA subtype of glutamate receptor is a ligand-gated and voltage sensitive ion channel that mediates a major component of excitatory neurotransmission in the central nervous system (CNS). NMDA receptors are activated by simultaneous binding of two different agonists, glutamate and glycine/ D-serine¹. NMDA receptors are widely distributed at all stages of development and are critically involved in normal brain functions, including neuronal development and synaptic plasticity¹. NMDA receptors have also been implicated in the pathogenesis of several neurological and psychiatric disorders including Alzheimer's disease (AD), epilepsy, bipolar disorder and schizophrenia (SCZ)⁴.

NMDA RECEPTOR SUBUNITS

Functional NMDA receptors are hetero-tetramers formed by the co-assembly of four poly-peptide chains referred as subunits. Based on the nomenclature of International Union of Basic and Clinical Pharmacology NMDA receptor subunits are classified as GluN1, GluN2A, GluN2B, GluN2C, GluN2D, GluN3A and GluN3B. Further, the genome that encodes each of these subunits are, according to Human Genome Organization, classified as GRIN1, GRIN2A, GRIN2B, GRIN2C, GRIN2D, GRIN3A and GRIN3B².

The NMDAR GluN1 subunit is encoded by one gene, four different genes encoding GluN2 subunits (GluN2A, GluN2B, GluN2C and GluN2D), and GluN3 subunits (GluN3A and GluN3B) arise from two different genes^{11, 12}. NMDAR form a tetrameric

structure containing two or three different subunits¹⁰, which allows the formation of complexes that can be either diheteromeric (with two subunits e.g. GluN1/GluN2) or triheteromeric (with three subunits e.g. GluN1/GluN2/GluN3)¹¹. The presence of various NMDAR subunits leads to different combinations of subunit assembly that allows variation in physiological roles in different neuronal cell types and brain regions, e.g. two GluN1s with two GluN2As form the subunit GluN2A^{2, 12}.

NMDA RECEPTOR SUBUNITS IN DEVELOPMENT

NMDAR subunits manifest different expression and distribution patterns in brain development at different periods of time^{14, 15}. In order to identify these changes, a technique called in situ hybridization is performed. This hybridization technique uses a complementary RNA probe as label to a specific section of tissue, allowing the detection of specific signals from the different NMDAR subunits^{14, 15, 16}.

The GluN1 subunit has low neonatal expression (1-2 months) that gradually increases until adulthood in human beings¹⁵. GluN1 is widely expressed in almost all neuronal cells of brain and spinal cord being more predominant in cortex and hippocampus^{11, 14, 15}. The GluN2A subunit doesn't have detectable signals in embryos^{14, 15}. Abundance of this subunit is very low in fetus, relatively higher in neonates, and rapidly increases soon after birth. In adult humans (~ 20 years), GluN2A is mainly expressed in cortex and sub-cortical regions^{14, 15}. Regarding the GluN2B subunit, in contrast to GluN2A, there is an age-dependent decrease in expression from neonatal to infant period^{14, 15}. In the embryos, GluN2B subunits are widely expressed in telencephalic and thalamus regions and spinal cord; in adulthood however, the expression is confined to parahippocampal gyrus^{14, 15}. There is a switch in receptor expression from GluN1/GluN2B to GluN1/GluN2A in the

cortex, hippocampus and cerebellum in the first week of postnatal life¹⁹. This switch is important for synaptic formation in development and is due to agonist (glutamate and glycine) binding.¹⁹ The GluN2C subunit is not detectable in embryos and exhibits an intense adulthood expression in cerebellar cortex^{14, 15}. The GluN2D subunit embryonically is widely expressed in brainstem regions, cortex of the olfactory bulb, and spinal cord^{11,15}. GluN2B expression gradually increases until the postnatal day-7 but after the second week of birth decreases again and gets narrowed to the diencephalon and brainstem^{11, 15}. The GluN3A subunit expression is low before birth, peaks in the postnatal period (2-6 months), and decreases again in adulthood¹¹. GluN3B subunit expression is low in the postnatal period, but it constantly rises until adulthood. GluN3B subunit is predominantly expressed in the brain stem and spinal cord¹¹. In general, GluN2B, GluN2D, and GluN3A are predominant in postnatal life versus GluN2A and GluN2C which are more abundant in adulthood¹⁹.

NMDA RECEPTOR STRUCTURE

NMDA ionotropic receptors are obligate heterotetramers that typically comprise two glycine-binding GluN1 subunits and two glutamate-binding GluN2 subunits⁵. Every subunit has an extracellular amino-terminal domain (ATD) that is also referred to as NTD, a ligand-binding domain (LBD), a transmembrane domain (TMD) and a carboxyl terminal domain also referred to as an intracellular C-terminal domain (CTD) (Figure 1.1)⁶.

The ATD has a bilobed shape that resembles a kidney-like structure composed of two domains that can be either open or shut; this change of conformation allows or inhibits the receptor function since it can favor the opening of the channel pore but is not essential

for channel activity^{2,7}. The ATD controls pharmacological and kinetic properties². ATD comprises the binding site of inhibitory Zn²⁺ for GluN2A and of ifenprodil-binding for GluN2B².

The clamshell like structure of LBD is formed by two discontinuous extracellular segments (S1 and S2)⁷. The S1 peptide is located between the ATD and the first membrane-associated domain (M1), and the S2 segment is located between the third and fourth membrane-associated domains (M3 and M4)⁷. The LBD binds with the endogenous neurotransmitter agonist glutamate and coagonist glycine¹¹². Binding of both glycine and glutamate is essential to maximally activate the NMDAR¹¹². Glutamate binds with the GluN2 subunit (GluN2A, GluN2B, GluN2C and GluN2D) and it is thought to stabilize a closed conformation of the two lobes of the LBD¹¹². Glycine or D-serine binds with GluN1 and GluN3 subunits^{2,7}. Some studies have shown that partial agonists also can favor the closure of the S1S2 clamshell, allowing the design of novel therapeutics in the glycine binding site¹¹². Glycine binding site affinity to GluN1 differs between NMDAR subunits based on the co-assembling GluN2 subunit¹¹². Notably, the GluN1/GluN3 receptors can be fully activated by glycine alone¹¹².

The TMD is formed of three transmembrane helices (M1, M3 and M4) and one re-entrant loop (M2) conforming to a channel pore^{2,9}. The NMDAR channel is blocked by Mg²⁺ under physiological membrane resting potential of about -70mV^{2,9}. At depolarizing membrane potential Mg²⁺ block is expelled, allowing the movement of divalent (Ca²⁺) and monovalent cationic ions like Na⁺ and K⁺ across the channel. Ca²⁺ entry into the cell induces intracellular signal transduction in the neurons². An appropriate level of Ca²⁺ influx into neurons is necessary for survival; however, excessive influx of Ca²⁺ activates

Ca²⁺ dependent proteases and lipases that depolarizes mitochondrial membrane inducing neuronal damage and death².

The length of CTD varies among the NMDAR subunits^{8,17}. The total number of amino acids forming CTD ranges from 900 to over 1480 based on the subunit, and the number of amino acids determines the size of the intracellular carboxyl terminal^{8,17}. The GluN1 subunit has four different carboxyl-termini derived from alternative splicing^{2,8}. The CTD provides interaction sites for intracellular proteins that regulate trafficking, internalization and signal transduction, which is important for appropriate synaptic formation^{2,8}.

The NMDAR channel pore has a structural asymmetry among subunits; it can be noted in the extracellular vestibule between the tip of the M3 segment and the M2 loop^{2,13}. The M2 loop turns into an α -helix that diagonally links the GluN1 and the GluN2 segments^{2,13}. This turn in the M2 segment differs among subunits, and results in structural and activation differences among NMDAR subunits^{2,13}.

The pore asymmetry allows the channel to be permeable to Ca²⁺ but not Mg²⁺¹³. Ca²⁺ permeability is facilitated by the M2 loop that forms a narrow constriction, big enough to allow Ca²⁺ to flow but at the same time being obstructive for Mg²⁺. This characteristic is essential for the Mg²⁺ voltage-dependent channel block¹³

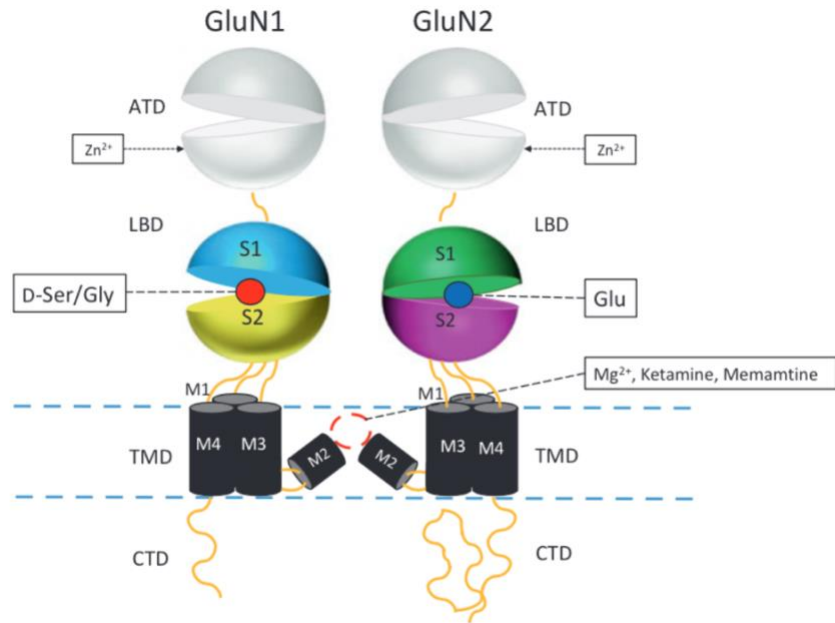


Figure 1. 1 Schematic diagram showing heteromeric structure of NMDAR. The amino-terminal domain (ATD) comprises binding site for Zn²⁺. Ligand-binding domain (LBD) composed of extracellular segments S1 and S2 which binds agonist glutamate (GluN2) and co-agonist glycine (GluN1 and GluN3). The transmembrane domain (TMD) is formed by three transmembrane helices (M1, M3 and M4) and one loop (M2) which form a channel pore. The highly diversified intracellular C-terminal domain (CTD), is labeled . (Hashimoto K, 2017 [2]) used under fair used, 2020.

NMDA RECEPTOR ENDOGENOUS AGONISTS

Glutamate participate in excitatory neurotransmission in the mammalian brain and spinal cord and its action occurs through glutamate receptors (GluR) inducing excitatory neurotransmission and intracellular signal transduction^{2, 3}. GluR is classified into ionotropic (iGluR) and metabotropic (mGluR) and their difference is based on their speed of neurotransmission and signaling mechanism². The iGluRs are ligand-gated ion channels permeable to cations Na⁺, K⁺, and Ca²⁺ that can be pharmacologically classified

into three different classes, namely α -amino-3-hydroxy-5-methyl-4-isoxasolepropionic acid (AMPA) receptors, kainite receptors and NMDAR¹.

Normal function of iGluR is needed for activity dependent processes of neurodevelopment, sensory and cognitive function³². NMDAR requires two agonists for activation, glutamate which binds the GluN2 subunits and glycine which binds the GluN1 subunit²⁹. Unproper glutamate function its involved in neuropathological conditions like ischemia, epilepsy, SCZ, chronic pain and AD³⁷. Due to glutamate importance in normal function and its involvement in different pathological conditions, several compounds have been developed to specifically target the different NMDAR subunits, however, a selective agonist that specifically distinguishes between subunits has not been developed³⁷.

GluN1

Agonist that binds with the GluN1 subunit binds in the LBD within the cleft between the S1 and S2 domains (Figure 1-1)^{1,3}. D-serine, which is synthesized in the astrocytes, serves as an endogenous ligand for NMDAR in the brain³¹. Proper levels of D-serine are crucial in brain physiology since hypofunction of NMDAR-mediated signaling pathways is implicated in pathologies like SCZ³²

GluN2

The NMDAR channel opening is primarily determined by glutamate binding to the GluN2 subunit. However, GluN1 subunit is needed as a co-agonist for receptor opening and activation³⁴. GluN2 subunits are activated by endogenous agonists glutamate and aspartate¹⁹

D-aspartate is a neurotransmitter that can activate post-synaptic NMDAR³⁶. D-aspartate is an endogenous agonist that enhances hippocampal NMDAR-dependent long-term potentiation (LTP)³⁵

GluN3

The GluN3 subunit binds with glycine and also partially binds with D-serine like the GluN1 subunit³⁸. GluN3 subunits, by co-assembling with GluN1, form a functional excitatory glycine receptors¹³⁸.

GATING, LIGAND-BINDING AND CHANNEL PROPERTIES

Each NMDAR subunit has unique structural and functional properties^{16,17,18}. The subunit composition determines the conformational changes of ligand binding, activation and desensitization^{19,20}. Three patterns have been suggested for the NMDAR assembly. The first one suggests that GluN1-GluN1 and GluN2-GluN2 homodimers form first and then coassemble to form the tetrameric receptor. Second model suggests that the GluN1-GluN1 homodimer forms a folded complex to which the two GluN2 monomers are added to form the tetramer. The third model suggests an initial formation of the GluN1-GluN2 heterodimer and then subsequent tetramerization¹⁹.

Diheteromeric NMDAR e.g, GluN2A, GluN2B, GluN2C and GluN2D, are classified based on channel gating, and ligand-binding¹⁸. The GluN2 ATD site regulates the differences of the NMDAR subunits in gating and ligand-binding properties. These properties include the maximal channel open probability (P_{open}) upon ligand binding, agonist potency, sensitivity to endogenous inhibitors like Zn^{2+} and protons, and deactivation kinetics, which describe the course of synaptic currents in synaptic

physiology (see **Table 1-1**)^{18,19}. An example of the difference in gating and channel properties between subunits is presented in **Figure 1-2**. This figure shows a brief application of saturating concentration of glutamate (1mM) on Human Embryonic Kidney (HEK) cells' recombinant NMDAR. Every subunit shows a distinct deactivation time course. GluN2A being the fastest deactivating subtype followed by GluN2B, the subunits GluN2C and GluN2D manifest slower deactivation times¹¹.

There is also another way to classify NMDAR, based on channel properties. The specific structural component that determines these differences is located at the proximal end of the M3 region. This site is often referred as the S/L site¹⁹. The “S” refers to serine in the GluN2A or GluN2B subunits, and the “L” refers to leucine (L) in the GluN2C and GluN2D subunits. The S/L site controls subtype differences in Mg²⁺ sensitivity, Ca²⁺ permeability, single-channel conductance and inherent voltage dependence (V_m) of channel gating (see **Table 1-2**)^{18,19}.

NMDAR Subtype	Maximal P _{open}	Agonist Potency	Deactivation Kinetics	Zn ²⁺ Sensitivity	Proton Sensitivity
GluN1/2A	High	Low	Fast	High	Medium
GluN1/2B	Medium	Medium-Low	Medium	Medium	High
GluN1/2C	Low	Medium-high	Medium	Low	Low
GluN1/2D	Low	High	Low	Low	High

Table 1. 1 Gating and Ligand-Binding Properties of the GluN2 subtypes at the ATD.

(Glasgow et al, 2015 [18]) Used under fair use, 2020.

NMDAR Subtype	Mg ²⁺ Sensitivity	Ca ²⁺ Permeability	Single Channel Conductance	Inherent V _m Dependence
GluN1/2A	High	High	High	Strong
GluN1/2B	High	High	High	Strong
GluN1/2C	Medium	Medium-high	Medium- high	None
GluN1/2D	Medium	Medium-High	Medium- high	None

Table 1. 2 Channel Properties of the GluN2 subtypes at the LBD and TMD. (Glasgow et al, 2015 [18]) Used under fair use, 2020.

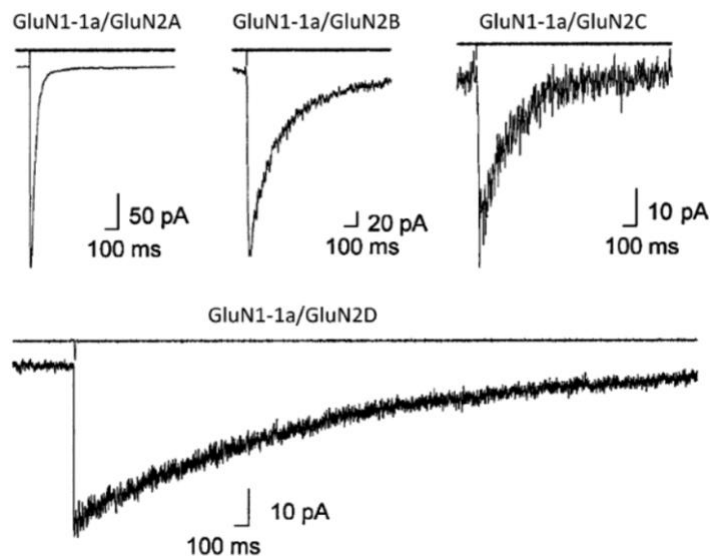


Figure 1. 2 NMDA Receptor Subtype Deactivation Kinetics. NMDAR currents recorded from transfected HEK cells with a brief application of 1mM of glutamate. Ranking order from faster to slower: GluN2A > GluN2B > GluN2C > GluN2D. (Paoletti, 2011 [11])

Used under fair use 2020.

SYNAPTIC PLASTICITY

NMDAR are expressed in the functional synapse and extrasynaptically and their presence is widely distributed throughout the CNS¹⁹. When the cell membrane has a negative resting potential, Mg²⁺ enters into the extracellular vestibule and blocks the entry of other ions through the NMDAR^{21,22}. Once the depolarization process begins, the membrane potential reaches a positive value expelling the Mg²⁺ block and allowing ions like Na⁺ and Ca²⁺ to enter the cell within hundreds of milliseconds²¹.

NMDAR is also involved in the processes of long-term synaptic plasticity²¹. This process determines how every synaptic transmission between two neurons changes based on its activity and it is a key aspect in the process of learning and memory²¹. The activity-dependent long-term change that occurs in the synapse can either strengthen the connection between two neurons, known as long-term potentiation (LTP), or depress it, known as long-term depression (LTD), both processes are synapse specific^{21,22,23}.

The iGluR are mainly expressed in the postsynaptic dendritic spines, but they can also be found in the presynaptic terminals^{21,22}. Presynaptic NMDAR are crucial in the induction of presynaptic LTP²². These receptors receive endogenous glutamate from either the same terminal bouton (homosynaptic regulation) or the neighborhood terminal bouton (heterosynaptic modulation)^{21,22}. Presynaptic NMDAR enhance both spontaneous and evoked glutamate (excitatory) and GABA (inhibitory) transmitter release by direct depolarization of the presynaptic terminal or by increasing Ca²⁺ permeability²².

CHAPTER 2: LITERATURE REVIEW

CHANGES IN SYNAPTIC GLUTAMATE CONCENTRATION

Glutamate (Glu) is the major excitatory neurotransmitter in the CNS, and it is involved in normal functions like motor behavior, cognition, and emotion⁸⁸. Synaptic glutamate levels fluctuate as a result of pulsatile release and rapid reuptake mechanisms⁹². Under normal conditions, Astrocytes release glutamate via calcium dependent exocytosis⁹³.

There are numerous mechanisms in which glutamate can be released in the CNS; including gap junction hemichannels, swelling-activated anion channels, activation of purinergic receptors and cysteine-glutamate exchanges⁹⁴.

There is an estimate of a tonic basal concentration of extracellular glutamate that ranges from 0.02 to 20 μ M⁹¹. However, based on the method applied to measure glutamate the concentration can be slightly different⁹², for example, when measuring plasma glutamate levels, the range is estimated around 150 μ M, when measuring cerebrospinal fluid glutamate levels are around 10 μ M, and intracellular glutamate concentration can reach close to 10mM⁹². Also, glutamate concentration in the synaptic cleft after action potential can exceed 1mM for less than 10 seconds and rapidly return to resting values less than 20nM⁹¹.

Several studies indicate that cerebral cortex exhibits an age-related decrease in glutamate concentration⁸⁹. With aging reduction of glutamate in the motor cortex has been correlated with neuronal loss and neuronal shrinkage, being associated with age-related pathologies like Parkinson's disease, AD, amyotrophic lateral sclerosis (ALS) and dementia^{88,95}. In ALS, for example, there is neuronal injury characterized by a loss of

motor neurons in the motor cortex, brainstem, and spinal cord, resulting in progressive muscle weakness and death⁹⁰. Therapeutic strategies that can prevent glutamate-mediated toxicity have been reported to slow down the ALS progression⁹⁰. For this reason, drugs that could modulate glutamate-induced neurotoxicity are being considered for the treatment of glutamate-toxicity mediated conditions^{88,90}.

DISORDERS ASSOCIATED WITH NMDA RECEPTORS

NMDAR have an important role in neuronal death that occurs soon after ischemic stroke⁵⁶. Even though stroke is a multifactorial disorder, NMDAR-mediated excitotoxicity due to excessive calcium influx has been proposed to be a primary cause of comorbidities⁵⁷. Meanwhile, therapeutic agents like GluN2B-selective antagonists have been proposed as treatment options for stroke, cerebral ischemia, and traumatic brain injury¹².

Additionally, NMDAR are involved in pain sensation⁵⁸. NMDAR are expressed in dorsal root ganglia (DRG) of the spinal cord, and widely distributed in the brain⁵⁸. While conducting the pain signals, there will be a release of endogenous glutamate from the nerve terminals of primary sensory afferent neurons that will activate NMDAR facilitating the sensation of pain and related behavior⁵⁸. In particular, the GluN2B subunit has been suggested to play an important role in pain sensation⁵⁸. Also, it has been observed in animal models of pain that NMDAR channel blockers like memantine, ketamine and MK801 attenuate neuropathic pain⁵⁸.

NMDAR hyperactivation is implicated in neurodegenerative conditions like AD^{12,59}.

Accumulation of excessive amounts of beta amyloid (A β) is considered to be the cause

of cognitive impairment with this condition; and a relationship between NMDAR and A β has been suggested⁵⁹. Therapeutic agents like memantine, which is an uncompetitive NMDAR blocker, is being used as a treatment for AD, by blocking the receptor the NMDAR-related deleterious effects of A β can be minimized⁵⁹. However, complete blockade of NMDAR restricts their normal normal physiological function as well⁵⁹.

Another condition related with NMDAR hyperactivation is Parkinson's disease (PD), which is the second most common age-related disease after AD^{12,61}. PD is a progressive neurodegenerative disorder due to the deterioration of pigmented dopaminergic neurons located at the substantia nigra pars compacta, producing clinical symptoms like cognitive impairment and motor disturbances⁶¹. One example of a frequent motor complication is L-DOPA-induced-dyskinesia (LID)¹². This condition involves NMDAR through the enhancement of synaptic GluN2A expression and shift of GluN2B from synaptic to extrasynaptic locations that modifies the fine regulation of receptor numbers and subunit composition resulting in altered synaptic strength¹². In addition, patients with PD have higher serum glutamate concentrations than healthy people⁶². It has been suggested then that drugs that modulate glutamate concentration in the GLuN2A and GluN2B NMDAR subunits could have a promising therapeutic use^{12,61}.

Excessive NMDAR activity is also implied in the pathogenesis of conditions like Huntington's disease (HD), a disorder characterized by the degeneration of striatal medium-sized spiny neurons resulting in changes of mood and mental abilities⁶⁰. Pathophysiology of this condition in animal models involves the GluN2B subunit increased expression and resulting excitotoxicity⁶⁰.

Depression is another disorder correlated with abnormal NMDAR dysfunction^{62,63}. Pathophysiology of depression involves dysregulation of the mammalian target of rapamycin (mTOR) and a decrease in brain-derived neurotrophic factor (BDNF)^{62,63,64}. Current treatment of depression involves NMDAR antagonist ketamine and NMDAR uncompetitive antagonist memantine⁶¹. However, memantine has lower affinity than ketamine to NMDAR, especially in the GluN2B subunit⁶². Ketamine, shows anti-depressive attributes through increase in phosphorylated extracellular signal-regulated kinase and protein kinase B, signaling pathways that are linked with the activation of mTOR signaling⁶³. This protein activates local protein synthesis, maturation and function of new spine synapses⁶³. Ketamine also blocks NMDAR at rest and deactivates eukaryotic elongation factor 2 (eEF2) kinase, or CaMKIII, attenuating CaMKIII phosphorylation^{63,64}. Further, ketamine produces antidepressant response within hours that can be sustained per days^{63,64}. However, ketamine adverse effects like delirium and hallucinations limit its use as chronic treatment for depression⁶².

In addition to depression, NMDAR are also associated with white matter damage. This damage can be present in chronic and acute conditions like cerebral palsy, traumatic neuronal injury, and multiple sclerosis^{64,65}. The GluN3A subunit is expressed in glia and responds mostly to glutamate activation exhibiting also less sensitivity to Mg²⁺ blockage (like the GluN2C subunit), suggesting greater glutamate activation dependency even in the absence of strong depolarization^{65,67}. For this reason, GluN3A or GluN2C selective antagonists would be ideal as therapeutic agents for preventing white matter excitotoxicity damage with less possible side effects, like hallucinations, than broad-spectrum NMDAR antagonists^{65,66}.

Overall, hyperactivation of NMDAR leads to excitotoxicity that gives rise to several clinical conditions as discussed above. On the contrary, pathogenesis of other type of conditions could evolve when the receptor is hypo-activated¹². Some of these conditions include autism, cognitive impairments, SCZ and anti-NMDAR encephalitis¹².

Autism spectrum disorder (ASD) is a group of conditions that include reduced social interaction, communication, and limited and repetitive behaviors⁶⁸. ASD is a heritable disorder involving the mutation of the SHANK2 gene, which allows expression of a synaptic signaling adaptor protein, Shank2⁶⁹. Both, mutations in gene SHANK2 and molecular unbalances from disruption in the *ProSAP2/Shank3* gene, result in molecular alterations of glutamatergic synapses^{69,70}. Mutations of the SHANK2 gene reduce normal glutamate synaptic function and lead to the development of abnormal behaviors like impaired social interaction, hyperactivity and intellectual disability^{68,69,70}. Normalization of NMDAR function with partial agonists improved social interaction and abnormal behaviours⁶⁸. Overall, it has been proposed that the development of drugs to modulate hypoactivated NMDAR could offer a novel strategy to treat ASD^{68,70}.

In cognitive impairments, there is also an NMDAR hypoactivation component⁷³. Under physiological conditions, NMDAR are involved in memory formation through synaptic plasticity²¹ and the GluN2B subunit in particular has been suggested to have an important role in spatial learning and LTP⁷¹. However, age related reduction of GluN2B subunit expression in cortex and hippocampus alters long term potentiation (LTP) leading to a deficit in spatial learning^{72,73}. In general, aged animals exhibit less glutamate binding to the NMDAR, which is correlated with abnormal LTP leading to altered memory function^{74,75}. It has been proposed that a decline in NMDAR in the synaptic pool of

prefrontal and frontal brain regions can contribute to age-related deficiencies in spatial learning and passive avoidance. The decline in NMDAR could be a compensatory mechanism from neurons to avoid NMDAR-related excitotoxicity in aging brain^{73,74}. Changes in NMDAR expression has more impact to the aging brain than other glutamatergic receptors like AMPA^{73,74}. Not all NMDAR subtype expression declines in elderly people, and even if some NMDAR are being expressed, they might be insufficient to generate LTP essential for cognitive function⁷³. For this reason, it has been proposed that the development of treatments that could prevent or reverse effects of aging on the NMDAR may help to improve memory failure when aging⁷³. Some of the interventions that enhance NMDAR expression include treatment with acetyl-L-carnitine (ALCAR), a compound essential for long-chain fatty acid uptake and utilization in mitochondria⁷⁵. ALCAR has antiaging effects because it improves agonist binding to the NMDAR in hippocampus and striatum⁷⁵. Likewise, the chronic use of antioxidants like Vitamin E has antiaging effects⁷⁷. Vitamin E is present in the cell membrane and could improve receptor lipid environment that results in better glutamate binding to the NMDAR in the cortex, hippocampus, and striatum⁷⁷. Another example is the use of memantine which could improve memory⁷⁸. Memantine can cause a selective block of extrasynaptic NMDAR, particularly the GluN2C and GluN2D subunits⁷⁶. It has been suggested as well that the ideal treatment for memory loss could be through enhancement of NMDAR normal function⁷³.

Another key disease which involves NMDAR dysfunction is SCZ. The disease is a psychotic disorder characterized by positive, negative and cognitive symptoms⁸². Positive symptoms include delusions, hallucinations, paranoia and psychosis; and negative

symptoms include lack of affection, impaired attention, social withdraw and cognitive impairments^{80,82}. A major hypothesis for the pathophysiology of this disease involves dopamine dysfunction⁸⁰. Even though treatment with dopamine receptor blockers reduced positive psychotic symptoms, it does not avoid unwanted adverse side effects like sleepiness and compulsive behaviors⁸²

Glutamate dysfunction has been proposed as well as an explanatory hypothesis for the disease⁸⁰ Hypofunction of NMDAR results in dopaminergic abnormalities⁸² and reduced NMDAR activity on inhibitory neurons leads to disinhibition of glutamate release⁷⁹.

Notably, some patients with SCZ have low glutamate levels in cerebrospinal fluid, supporting the glutamate hypofunction hypothesis⁸². In particular, underexpression of the GluN2A subunit has been linked with this disorder⁸¹. The GluN2A subunit is widely distributed in the cerebral cortex, and when experimental mice lack this subunit in the anterior cingulate cerebral cortex, they shown altered behaviors like hyperlocomotion⁸¹. Similarly, when the GluN2A subunit is being underexpressed, there is a disturbance in glutamatergic inputs onto GABA interneurons via the NMDAR that result in GABA neurotransmission disturbances. These characteristics are present in cerebral cortex neurons from patients with both SCZ and bipolar disorder⁸¹

Because of the possible involvement of NMDAR on SCZ, glutamate regulation provides a novel approach since it could effectively control both positive and negative symptoms⁸². When healthy individuals are experimentally intoxicated with phencyclidine (PCP) they manifest schizophrenic symptoms like hallucinations^{79,82}. For instance, PCP, MK-801, and Ketamine, all NMDAR antagonists, worsen psychotic symptoms in schizophrenic patients^{80,82}. A different approach to treat SCZ has been made with the use

of NMDAR agonists⁸². Controversially, direct glutamate NMDAR stimulation can lead to excitotoxicity, thus glycine site binding compounds like agonists D-serine and D-cycloserine are being studied to improve NMDAR function⁸². A different approach includes targeting the glycine binding site in order to modulate NMDAR function⁸². In general, the development of NMDAR modulatory compounds is still being studied since allosteric modulators may offer superior efficacy with less danger of downregulation⁸². A final example of conditions related to NMDAR hypofunction takes place in anti NMDAR encephalitis, which is a relatively new auto-immune disease⁸³. This can be lethal encephalitis associated with antibodies against the NMDAR⁸⁴. Several neuronal and psychiatric symptoms are present, like seizures, a decline of consciousness, paranoid, delusional thinking, agitation, changes in speech, autonomic imbalance, and dyskinesia (abnormal movements)^{83,84,85}. Symptoms are similar to those present when attenuating NMDAR with antagonists like Ketamine that causes psychosis⁸⁴. Because this condition presents psychiatric-like symptoms, people are often misdiagnosed with an acute psychotic break or drug abuse. However, symptoms deteriorate rapidly over the days presenting a lack of conscious responsiveness that can lead to death⁸⁵. This disorder affects mostly women with a history of ovarian tumor teratoma, but it can also be seen in men, young people, and children⁸³. An immunological trigger has been described as a starting cause for this condition⁸³. It has been proposed that antibodies target mainly the GluN1 subunit at the NTD, resulting in a selective decrease of the surface density of the NMDAR, leading to the receptor internalization^{83,84}. Nevertheless, the antibodies do not affect AMPA receptors, neither the number of synapses, dendritic spines, dendritic complexity or cell survival⁸⁴. It has

been proved that the loss of glutamate receptors eliminates NMDA-mediated synaptic function, resulting in altered learning, memory loss, and abnormal movements⁸⁴. Also, the use of purified immunoglobulin type G (IgG) in mice impairs normal glutamate transmission *in vivo*⁸⁵. The EphB receptor tyrosine kinase is important to synapse formation and its activation promotes the association of EphB with NMDAR that may help with synapse formation⁸⁶. Additionally, when extrasynaptic GluN2B is reduced, it is consistent with an antibody-induced receptor cross-linking that follows receptor endocytosis⁸⁵. Those distinct changes correlated with the expression of schizophrenic symptoms⁸⁶. On the positive side, anti-NMDA-receptor-encephalitis can be serologically diagnosed and successfully treated⁸³. The internalization of the receptor is reversible with the removal of antibodies from neuronal culture⁸⁵ and even though symptoms are severe, after treatment with corticosteroids, cyclophosphamide, or rituximab, 80% of patients fully recover⁸⁵.

The antibodies that induce seizures in anti-NMDAR encephalitis offer a model for testing therapies in autoimmune seizures⁸⁷. Since this immune response leads to NMDAR under expression, special attention has been put into NMDAR potentiators to treat this condition⁸³.

In summary, strong efforts have been made to develop therapeutic drugs that can modulate NMDAR. However, NMDAR blockers like memantine or ketamine can exhibit undesirable side effects^{59,61}. Since NMDAR participates in many physiological functions, a complete blockage is not ideal because too little activation alters normal cell function⁶¹. On the other hand, special attention has been put into compounds that can potentiate the NMDAR in disorders associated with NMDAR hypofunction. However, hyperactivation

of the receptor could lead to excitotoxicity^{59,65}. The ideal therapeutic agent, then, should be able to carefully tune the receptors without eliminating their normal function⁶⁵.

NMDA RECEPTOR PHARMACOLOGY

NMDAR structure provides several sites for drug interaction⁸². Over the years, agonist and antagonist compounds have been developed to target all NMDAR. However, a more selective targeting that involves subunit specificity remains the ideal goal since some diseases are subunit dependent⁸². For example, SCZ⁸¹ and Parkinson's Disease when there is GluN2A dysfunction⁶¹ and in GluN3A dysfunction in depression⁶³. In general, compounds that can target NMDAR specific subunits and that can modulate NMDAR normal function are ideal⁸². It has been suggested that there is a need for compounds that can modulate glutamate receptor function based on glutamate-activity, by either reducing or enhancing function progressively in response to a varying glutamate stimulus⁷⁹.

SYNTHETIC AGONISTS

NMDAR agonists enhance receptor activity⁸². These compounds have been proposed to be used as a treatment in conditions like autism and SCZ in which hypo-NMDAR activation is present⁸². Hence, NMDAR potentiators have been suggested to treat some of the conditions related to the receptor hypoactivation⁸². It is important to point out that traditional agonists may cause harm in presynaptic and postsynaptic glutamate neurotransmission⁷⁹. Glutamate synapses are highly dynamic, and sudden activation or overstimulation might facilitate neurotoxicity⁷⁹.

In the GluN1 subtype, D-cycloserine (DCS) is a partial glycine agonist, having a positive effect on cognition, fear extinction, and motor dysfunction^{19,33}. DCS has a greater response in the GluN2C subunit compared to the GluN2A, GluN2B and GluN2D subunits³³.

The GluN2 subunits have different functional properties that result in different subunit efficacy⁴⁰. In general, GluN2 synthetic agonists show less potency in the GluN2A subunit and more potency in the GluN2D subunit, leaving the GluN2B and GluN2C subunits with intermediate potency values⁴⁰. An example of this is the synthetic agonist N-methyl-D-aspartate, which has more potency for GluN2D than GluN2A¹⁹. SYM 208, another synthetic agonist, also potentiates the GluN2D subunit more since it needs 46 times less to reach the EC₅₀ value than in the GluN2A subunit⁴¹. Some other synthetic agonists like L-Homocysteinsulfinate, D-Homocysteinsulfinate, Ibotenate, and *trans*-ADC1 express similar potency patterns^{19,42}.

COMPETITIVE ANTAGONISTS

NMDAR antagonists are compounds that functionally inhibit NMDAR by acting at either agonist binding domain, allosteric sites, and ion channel pore. These compounds have the potential to be used in disorders that result from glutamate-induced excitotoxicity like ischemia, epilepsy and pathologic pain states⁸². Overall, special attention has been brought to subunit-specific compounds like selective GluN2B antagonist since these compounds could minimize side effects and improve therapeutic efficacy⁸².

Two examples of general NMDAR competitive antagonists are D-AP5 (D-[-]-2-amino-5-phosphonopentanoic acid) and D-AP7 (D-[-]-2-amino-7-phosphonopentanoic acid)⁹⁶. D-AP5 shows a reduction in synaptic potentiation in the CA1 region of hippocampus,

following a high-frequency stimulation on the Schaeffer collateral input, and, minimal effect was observed on synaptic potentials at low stimulation frequencies⁹⁷. Thus demonstrating the role of NMDAR in initiating of LTP⁹⁷. In general, NMDAR antagonists prevent the loss of inappropriate synapses and strengthen correct synapses⁹⁷. Both D-AP5 and D-AP7 have been indicated to treat anxiety since they have anxiolytic, antidepressant, and antinociceptive effects⁹⁶. However, unwanted side effects like memory impairment, psychosis, and sedation can be present⁹⁶.

On the GluN1 subunit, antagonist binding to the LBD works by stabilizing an open-cleft conformation between the S1 and S2 structures when glycine is bound (Figure 1-1)³⁹. An example of this conformational change happens with the antagonist 7-chlorokynureic acid (5,7-DCKA)³⁹. Another example is the noble gas xenon that has been proposed to inhibit NMDAR with direct interaction in the glycine binding site, providing anesthetic effects⁴³.

Alongside, on the GluN2 subunit, compounds that selectively target different GluN2 subtypes are challenging to achieve since the glutamate-binding pocket is mostly conserved, making difficult the identification of subtype-specific ligands⁴⁴. Nevertheless, there are some antagonist compounds that exhibit more affinity towards certain GluN2 subtypes, for example, the antagonist 3-((R)-2-carboxypiperazin-4-yl)-propyl-1-phosphonic acid that has more affinity for GluN2A than for GluN2C and GluN2D⁴⁴. Likewise, conantokin peptides can be both competitive and noncompetitive and have more affinity towards the GluN2A subunit⁴⁶. Another example is the antagonist 1-(phenanthrene-2-carbonyl) pyrazine-2,3-dicarboxylic acid (UBP141), which has a higher affinity for GluN2C and GluN2D subunits⁴⁵

NONCOMPETITIVE ANTAGONISTS

Ifenprodil was the first subunit-selective antagonist for the NMDAR, it is voltage-independent and inhibits the GluN2B subunit⁴⁷. Under normal circumstances, the bilobed structure of the GluN2 ATD opens and rearranges the GluN1-GluN2 ATD heterodimeric interface, forming an active receptor that gates the channel⁹⁸. Ifenprodil binds to the ATD domain of the GluN2B subunit, specifically at the N-terminal leucine/isoleucine/valine-binding protein (LIVBP)-like domain. In this domain there are various residues that are hydrophobic and hydrophilic that control inhibition by ifenprodil, however, its exact mechanism has not fully been elucidated⁹⁹. Ifenprodil has derivatives that also interact with the GluN2B subunit like besonprodil (CI-1041) and traxoprodil (CP-101,606)⁴⁸. Another example of noncompetitive antagonist is Dynorphin A, which has more potency in the GluN2A subunit⁵⁰. And finally, ethanol that inhibits the receptor activation, which is correlated with neuronal and cognitive impairment seen in alcohol intoxication⁴⁹

CHANNEL BLOCKERS

Uncompetitive antagonists like channel blockers obstruct the NMDAR when the channel is open and functions in a use-dependent way. The longer the receptor is open the more inhibition will be produced⁵¹. An example of an uncompetitive antagonist channel blocker is Mg^{2+} , which naturally blocks NMDAR¹¹. However, its affinity is lower for the GluN2C and GluN2D subunits^{2,51}. When the uncompetitive antagonists get trapped in the pore they are called “trapping blockers”⁵¹. An example of this are ketamine, memantine, and [PCP, dizocilpine maleate] (MK-801)⁵¹.

Ketamine, or 2-(2-chlorophenyl)-2-(methylamino) cyclohexan-1-one was first used in 1962. The chemical composition of this compound is closely related to the drug phencyclidine (PCP) which is a hallucinogen¹⁰⁰. There are two forms of ketamine, (*S*)-ketamine or esketamine and (*R*)-ketamine or areketamine¹⁰⁰. Ketamine has been shown to have antidepressant effects in patients with Major Depressive disorder (MDD) for a sustained period of time¹⁰⁰. However, due to ketamine's psychoactive properties its distribution is strictly managed¹⁰⁰.

Memantine is another example of NMDAR channel blockers. It was first synthesized in 1960s but in the 1970s it was found that it affected the CNS¹⁰¹. Memantine, like blocker MK-80, binds within the vestibule of the ion channel, thus promoting the closure of the ion channel gate, lodging between the M3-helix-bundle and the M-2 pore loops, resulting in a blockage for ion permeation¹⁰⁹. Once memantine blocks the NMDAR, the channel closes, "trapping" memantine inside the channel. This blockage does not compete with agonist binding sites¹⁰¹. Memantine inhibits the NMDAR with an IC₅₀ of 1 μM, and at high concentrations (between 10 to 50 μM) affects serotonin and dopamine uptake, nicotinic acetylcholine receptors, serotonin receptors and voltage-activated sodium channels¹⁰¹. Memantine has shown therapeutic potential to be used for the treatment of neurodegenerative diseases like AD⁵¹.

Even though Ketamine and Memantine are both channel blockers, they exhibit different clinical properties¹⁰¹. Ketamine causes memory deficits, strongly reproduces the symptoms of SCZ and in higher doses can cause cell death, not to mention that it is also a widely abused substance due to its psychotic properties¹⁰². On the contrary, memantine is clinically better tolerated, even though it also has psychotic effects in general, has

fewer side effects, and is a less abused substance compared with ketamine¹⁰³. Both compounds have different effects on channel gating and even though they are channel blockers, it is thought that memantine interact with a more shallow site in the TMD than keamine. Continuously, ketamine has a higher concentration spike that can explain psychotic properties that are linked with NMDAR hyperactivation leading to excitotoxicity¹⁰¹.

A different illustration of NMDAR antagonist is the channel blocker phencyclidine (PCP) which induces psychotic states that resemble schizophrenic symptoms, and that can persist over several weeks even with drug discontinuation¹⁰⁸. This compound along with NMDA antagonist dizocilpine (MK-801) have been used as models to study SCZ¹⁰⁸, nevertheless, MK-801 discontinuation will not sustain psychotic symptoms over time like PCP does and this could be explained with PCP's ability to inhibit not just NMDAR but also to alter normal dopamine transporter and vesicular dopamine uptake as well¹⁰⁸. The NMDAR blocker MK-801 binds within the vestibule of the ion channel, thus promoting the closure of the ion channel gate, lodging between the M3-helix-bundle and the M-2 pore loops, resulting in a blockage for ion permeation¹⁰⁹. It is important to point out that inadequate glutamate transmission has been proposed as a model for SCZ mainly involving NMDAR function and the need of compounds that can modulate the receptors based on glutamate concentration could be ideal¹⁰⁸.

ALLOSTERIC REGULATION

An allosteric compound modulates the receptor function instead of fully blocking it, like some antagonists, or over activating it, like some agonists¹⁹. Allosteric modulators can be

positive, which increase receptor activation affinity, or negative, which decrease receptor activation affinity, and are being targeted as therapeutic agents since they have higher subunit affinity, bind in less common regions, and are clinically better tolerated¹⁹. One example is the divalent ion zinc (Zn^{2+}). It is naturally present in the synaptic vesicles and acts as a non-competitive allosteric inhibitor of NMDAR binding at the ATD (Figure 1-1)⁵². Unlike Mg^{2+} , Zn^{2+} produces a voltage-independent inhibition decreasing the channel open probability and its dysregulation is believed to be associated with glutamatergic transmission dysfunctions conditions like epilepsy⁵².

Another example are protons that work as endogenous allosteric modulators inhibiting NMDAR. The proton sensor is located at the ATD and is associated with the channel gate⁵³. Like Zn^{2+} , protons are important in regulation of NMDAR under physiologic and pathologic conditions⁵³.

Polyamines like spermine and spermidine are another example of allosteric regulation⁵⁴. They work by enhancing glycine binding in the GluN2A and GluN2B subunits⁵⁴.

Polyamines bind at the ATD and are voltage-independent⁵⁴. However, at the ATD of the GluN2D subunit polyamines favor blocking of the channel in a voltage-dependent manner⁵⁴.

Other key allosteric modulators are neurosteroids, an example of which is pregnanolone sulfate (PAS)⁵⁵. PAS modulates the inhibition of NMDAR by reducing the single-channel open probability⁵⁵. When studied in vivo, PAS displays neuroprotective properties, making it a therapeutic target for pathologies like acute and chronic neurodegeneration.⁵⁵

Arachidonic acid, for example, potentiates the NMDAR increasing the channel open probability without changing the channel current.⁵⁶

Some other examples of NMDAR allosteric modulators are UBP compounds. UBP are a family of agents that potentially target the LBD heterodimer interface of the GluN1/GluN2 subunits¹⁰⁴. UBP compounds exhibit subunit-selectivity and can both inhibit and potentiate the receptors¹⁰⁴. An illustration of this is UBP512 that inhibits the GluN2C and GluN2D subunit having a little response on the GluN2A and GluN2B subunits¹⁰⁵. Contrary to this, UBP 608 that acts as GluN2A subunit antagonist with moderate selectivity towards the GluN2B subunit¹⁰⁵. Also, UBP551 shows potentiation in the GluN2D subunit while inhibiting the other NMDAR subtypes¹⁰⁵. Most of the mode of action of some of these compounds are not well defined. Some inhibitory compounds are voltage-independent and are not competitive with agonist glutamate or glycine; they do not bind to the ATD but show preference to the LBD dimer interface altering the receptor desensitization and agonist unbinding kinetics¹⁰⁴.

An example of negative allosteric modulation is 3-chloro-4-fluoro-N-[4-[[2-(phenylcarbonyl) hydrazino] carbonyl] benzyl] benzenesulphonamide or TCN201^{106,107}. TCN201 preferably blocks the GluN2A subtype with a binding site located at the interface between the GluN1 and GluN2A subunits¹⁰⁷. The degree of inhibition of TCN201 will depend on glycine agonist concentration at the GluN1 subunit, but it is independent from glutamate concentration¹⁰⁶.

And finally, an illustration of a positive allosteric modulation is the tetrahydroisoquinoline CIQ (3-chlorophenyl) (6,7-dimethoxy-1-((4-methoxyphenoxy) methyl)-3,4-dihydroisoquinolin-2(1H)-yl) methanone)¹¹⁰. CIQ binds to the transmembrane helix of the NMDAR and enhances the channel opening in the GluN2C and GluN2D subunit in a concentration dependent manner¹¹⁰. CIQ potentiation has been

tested in mice with doses of MK-801. The mice showed schizophrenic-like symptoms following the application of MK-801 and once CIQ was applied mice demonstrated reversal of behaviors like hyperlocomotion and stereotypy and showed enhancement of memory in a Y maze test¹¹¹. CIQ has been suggested to work as treatment in NMDAR-hypofunction related conditions like SCZ and memory impairment having the advantage of preferably targeting the GluN2C and GluN2D NMDAR subunits¹¹¹.

SUMMARY

NMDAR activity is necessary for normal physiological functions like synaptic plasticity, memory formation, mood control, brain development and neuronal survival⁵⁹, however, when NMDAR are activated in excess, they can contribute to excitotoxicity which leads to neurological disorders and neuronal death^{59,65}. Glutamate serves as NMDAR agonist and glycine as coagonist¹. Synaptic glutamate levels are fluctuant and are the result of the balance between glutamate secretion and glutamate uptake⁹² There is an estimate of extracellular glutamate concentration that ranges from 0.02 to 20 μ M⁹¹. Excessive glutamate activity precipitates NMDAR-mediated cell death after Ca²⁺ influx through membrane depolarization⁶⁵. This excitotoxicity can be observed under both acute and chronic conditions including acute brain injuries, stroke, HD, PD, AD, chronic alcohol exposure and neuropathic pain⁶⁵. Some NMDAR antagonists have been proposed as therapeutic agents to stop the excessive receptor activation like memantine.

On the other hand, several studies indicate that cerebral cortex exhibits an age-related decrease in glutamate concentration⁸⁹ that could contribute to age-related pathologies like PD, AD, ALS and dementia^{88,95}. There are also some pathologic conditions that can be present when the receptor is hypo-activated¹² like autism, cognitive impairments, SCZ

and anti NMDAR encephalitis¹². In an effort to treat some of these conditions 'NMDAR potentiators like CIQ are being studied¹¹⁰.

Overall, strong efforts have been made to develop therapies to control both NMDAR excitotoxicity and hypoactivation¹¹². The resolution of the x-ray structure of the LBD allows a deep understanding into the molecular mechanism of NMDAR ligand binding and channel gating, facilitating the understanding of pharmacological selectivity of the channel and giving an insight to develop modulatory compounds¹¹². Future therapeutic options could arise from modulating different glutamate concentrations at the different NMDAR subunits improving their normal physiological function without producing a complete block or excessively hyperactivating them¹¹².

CHAPTER 3: DOSE DEPENDENT ACTIVITY OF CNS4

INTRODUCTION

The need for allosteric regulation based on glutamate concentration

NMDAR are involved in normal physiological functions like synaptic plasticity, memory formation, mood control, brain development and neuronal survival⁵⁹. Glutamate serves as NMDAR agonist and its concentration in the CNS is highly diverse fluctuating between 0.02 to 20 μ M⁹¹. Excessive glutamate activity precipitates NMDAR-mediated cell death after Ca²⁺ influx through membrane depolarization⁶⁵. This excitotoxicity can be observed under both acute and chronic conditions including acute brain injuries, stroke, HD, PD, AD, chronic alcohol exposure and neuropathic pain⁶⁵. Additionally, several studies indicate that cerebral cortex exhibits an age-related decrease in glutamate concentration⁸⁹. With aging, glutamate concentration decreases altering NMDAR normal function that can contribute to age-related pathologies like PD, AD and ALS^{88,95}. As well, some pathologic conditions that can be present when the receptor is hypo-activated¹² are autism, cognitive impairments, SCZ and anti-NMDAR encephalitis¹². In an effort to treat some of these conditions' NMDAR potentiators like CIQ are being studied¹¹⁰. Likewise, some NMDAR antagonists have been proposed as therapeutic agents to stop the excessive receptor activation like memantine¹⁰³. However, when completely blocking the receptors there is a restriction of the receptor's normal physiological function⁵⁹. Overall, strong efforts have been made to develop therapeutics to control both NMDAR excitotoxicity and hypoactivation¹¹². The resolution of the x-ray structure of the LBD allows a deep understanding into the molecular mechanism of NMDAR ligand binding and

channel gating, facilitating the understanding of pharmacological selectivity of the channel and giving an insight to develop modulatory compounds¹¹². Future therapeutic options could arise from compounds that are able to carefully tune NMDAR without altering its normal physiological function^{65,112}. These compounds are known as allosteric modulators and are more likely to express GluN2 subunit selectivity since they target less conservative binding regions, resulting in diminishment of undesired clinical side effects and avoidance of global NMDAR overactivation^{59,65,122}. In this study, the pharmacologic properties of the a compound developed by Dr. Costa were evaluated. The compound is CNS4, or (4-fluoro-N-(2-(pyridin-3-yl)piperidine-1-carbonothioyl) benzamide (**Figure 3-1**), was developed by Dr. Blaise Costa and synthesized at Siringe International, India. Details about computational modeling of this compound cannot be released due to proprietary reasons, however, it was presumed that CNS4 could possibly bind to the LBD interface of NMDAR suggesting affinity towards different GluN2 subunits. In order to corroborate if CNS4 could have an effect on NMDAR, two-electrode voltage clamp electrophysiology and neuron culture techniques were used.

The first part of this study involves two-electrode voltage clamp electrophysiology. This technique facilitates the study of plasma membrane proteins such as ions channels. The movement of ions through the plasma membrane produces an electrical current that is measured in microamperes¹¹³. Every current or response is recorded facilitating future statistic analysis. We hypothesized that CNS4 selectively modulates NMDA diheteromeric receptors based on glutamate concentration since alterations in glutamate give raise to different pathologies. Eggs from *Xenopus laevis* were used to express recombinant cRNA of the NMDAR diheteromeric receptors (GluN2A, GluN2B, GluN2C and GluN2D). Every

diheteromeric subunit was recorded separately using solutions with different glutamate concentrations and increasing doses of CNS4.

SPECIFIC AIM 1:

To identify agonist concentration dependent activity of CNS4 by using two electrode voltage clamp (TEVC) in *Xenopus laevis* oocytes expressing recombinant NMDA diheteromeric receptors (GluN2A, GluN2B, GluN2C and GluN2D) using three different agonist solutions (named Agonist (0.3 μ M Glu/ 100 μ M Gly), Agonist Max (100 μ M Glu/ 100 μ M Gly) and Agonist Super Max (300 μ M Glu/ 100 μ M Gly)) with an increasing dose of CNS4 (1 μ M, 3 μ M, 10 μ M, 30 μ M and 100 μ M)

MATERIALS AND METHODS

Oocytes:

Stage 4 *Xenopus laevis* oocytes from Xenopus-I, (Ann Arbor, MI, USA)

Solutions:

Ringer's Solution or Recording buffer: 116mM NaCl, 2mM KCL, 0.3mM BaCl₂, 5mM.

HEPES: pH 7.4.

ND-96 Solution: 82mM NaCl, 3M KCL, 1M CaCl₂, 5mM HEPES, 2.5mM, Sodium Pyruvate, Gentamicin, pH to 7.6.

OR-2 Solution: 82mM NaCl, 3M KC, 1M MgCl₂, 5 mM HEPES, pH to 7.6

Compounds

CNS4: The compound 4-fluoro-N-(2-(pyridin-3-yl)piperidine-1-carbonothioyl)benzamide (CNS4) was developed by Dr. Costa from computational modeling and synthesized at Syngene International, India.

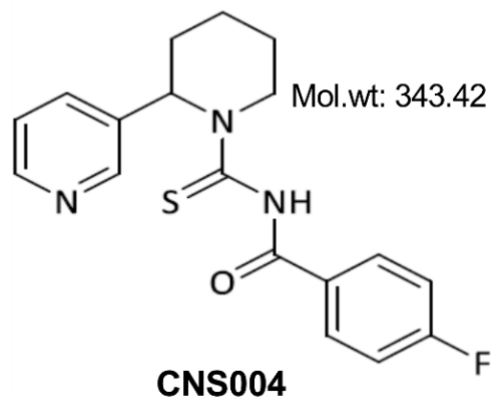


Figure 3. 1 CNS4 (4-fluoro-N-(2-(pyridin-3-yl)piperidine-1-carbonothioyl) benzamide chemical structure

NMDAR Constructs

cDNA encoding the NMDAR1a subunit (GluN1a) was obtained from Dr. Nakanishi (Kyoto, Japan). cDNA encoding the GluN2B (pci_sepGluN2B) was purchased from Addgene, Cambridge, MA. cDNA encoding the GluN2C and GluN2D were purchase from GenScript, New Jersey, USA.

Plasmids were linearized with NotI (GluN1) or StuI (GluN2A), or AvrII (GluN2B), or BstB1 (GluN2C and GluN2D) and transcribed in vitro with T7 (GluN2A, GluN2B, GluN2C & GluN2D) RNA polymerase using the mMessae mMachine transcription kits (Invitrogen by Thermo Fisher Scientific (Waltham, MA, USA) and RNA polymerase using the mMessage mMachine transcription kits (Ambion, Austin, TX, USA).

Oocyte Processing

Once arrived, stage 4 xenopus oocytes from Xenopus-I, (Ann Arbor, MI, USA) were manually selected and washed three times with 13ml of OR-2 solution before being left

overnight with 13ml of ND-96 solution and 5 mg collagenase. The following day, 0.5 μ l of every NMDAR subunit's cRNAs (GluN1A, GluN2B, GluN2C and GluN2D) were mixed in 1:1 ratio. 50 nL of the final cRNA mixture was microinjected into the oocyte cytoplasm. Oocytes were incubated in ND- 96 solution at 18°C prior to electrophysiological recordings (1–3 days).

Electrophysiological Recordings for Dose Response Curve (DRC)

Electrophysiological responses were measured using a standard two-microelectrode voltage clamp [Warner Instruments (Hamden, Connecticut) model OC-725C] designed to provide fast clamp of large cells. An example of a “clamped” oocyte can be observed in **Figure 3.2**. Note the two glass electrodes perforating the membrane which creates a sealing between the cell membrane and the electrode facilitating the recording of ion movements across the NMDAR channel pore.

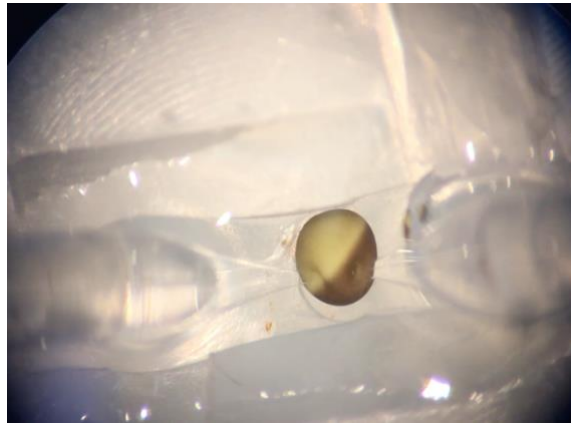


Figure 3. 2 Kwapisz L (2020) Picture of a “clamped” oocyte using two-electrode voltage clamp electrophysiology. Costa lab, Virginia Tech.

Response magnitude of the channel opening, which is measured in microamperes, was determined in xenopus oocytes containing different NMDAR subunits (GluN1/2A, GluN1/2B, GluN1/2C and GluN1/2D) at a holding potential of -60 mV . Three different

agonist solutions were used, either Agonist (0.3 μ M glu / 100 μ M gly), Agonist max (100 μ M glu and 100 μ M gly) or Agonist super max (300 μ M glu and 100 μ M gly) at a holding potential of -60 mV. Once every subunit exhibited a response amplitude between 0.1 and 2 μ A using either of the three Agonist solutions, increasing doses of CNS4 were applied (1 μ M, 3 μ M, 10 μ M, 30 μ M and 100 μ M of CNS4) and the response in amplitude was measure each time. One oocyte was used per every experiment being the application process of solution like this, e.g, Ringer \rightarrow Agonist solution \rightarrow Agonist solution+1 μ M CNS4 \rightarrow Agonist solution +3 μ M CNS4 ... \rightarrow Agonist solution+ 100 μ M CNS4. The solutions were given one at a time at a constant rate and no washes with Ringer between application was made. Recordings were done using 8-channel perfusion system (Automate Scientific, Berkeley, CA), and the amplitude responses were digitized for quantification (Digidata 1550A and pClamp-10, Molecular Devices, Sunnyvale, CA). A summary of the dose-response protocol followed and the amount of oocytes used is found on **Table 3.1**.

	GluN2A	GluN2B	GluN2C	GluN2D
Agonist (0.3 μ M glutamate / 100 μ M glycine	1,3,10,30 and 100 μ M CNS4 5 oocytes used	1,3,10,30 and 100 μ M CNS4 5 oocytes used	1,3,10,30 and 100 μ M CNS4 5 oocytes used	1,3,10,30 and 100 μ M CNS4 6 oocytes used
Agonist Max (100 μ M glutamate / 100 μ M glycine	1,3,10,30 and 100 μ M CNS4 5 oocytes used			
Agonist Super Max (300 μ M glutamate / 100 μ M glycine	1,3,10,30 and 100 μ M CNS4 5 oocytes used	1,3,10,30 and 100 μ M CNS4 5 oocytes used	1,3,10,30 and 100 μ M CNS4 5 oocytes used	1,3,10,30 and 100 μ M CNS4 6 oocytes used

Table 3. 1 Protocol followed for the CNS4 dose response experiment and the amount of oocytes used.

Statistics

Dose- response relationships using at least five independent oocytes per subunit (GluN2A, GluN2B, GluN2C and GluN2D) in three different agonist solutions containing 0.3 μ M Glu/ 100 μ M Gly, 100 μ M Glu/ 100 μ M Gly and 300 μ M Glu/ 100 μ M Gly with increasing doses of CNS4 (1,3,10,30 and 100 μ M) were fit to a single-site with variable slope (GraphPad Prism, ISI Software, San Diego, CA, USA) using a non-linear regression to calculate IC50 or EC50 and percentage maximal inhibition. Statistical Analysis: Values given represent means of relative response of the 5-6 oocytes used per set of recordings (\pm) S.E. In order to present only highly significant results, statistical significance was determined at the alpha level $p < 0.05$ (*) and using a one-way ANOVA with Tukey's multiple comparisons.

RESULTS

A variety of glutamate and glycine containing solutions were used to determine CNS4 dose-dependent activity. The evoked responses were obtained using two-electrode voltage clamp in *Xenopus* Oocytes expressing recombinant diheteromeric receptors. The average of at least six independent sessions were run for each subunit type and the statistical significance determined by one-way ANOVA and Tukey's multiple comparisons test with alpha level $p < 0.05$ (*) unless contrary specified.

The first solution, Agonist, evoked a response between -0.01 μ A and -0.2 μ A in recombinant NMDAR expressing oocytes. The GluN2A and the GluN2B subunit

exhibited a significant difference in amplitude response with 100 μ M CNS4 compared with Agonist alone (**Figure 3.3**). No statistical significance was determined in the GluN2A and GluN2B subunits with 1 μ M, 3 μ M, 10 μ M and 30 μ M of CNS4 (**Figure 3.3**). In contrast, the GluN2C and the GluN2D subunits demonstrated a significant statistical difference with 30 μ M and 100 μ M of CNS4 compared to Agonist alone (**Figure 3.3**). Traces of the GluN2C and GluN2D subunits recordings with Agonist solution, and increasing concentrations of CNS4, are represented in **Figure 3.4**. Once recordings with Agonist were completed, the relative responses of every subunit to increasing doses of CNS4 were plotted at the logarithmic scale. This type of scale facilitates the comparison of all four subunit percent relative responses to increasing doses of CNS4 in a single graph. At the logarithmic scale, the GluN2D subunit exhibited a numerically greater relative response with 30 μ M and 100 μ M CNS4 compared with the GluN2A, GluN2B, and GluN2C subunits (**Figure 3.5**).

The second solution, named Agonist max, evoked a response between -0.01 and -0.5 μ A in recombinant NMDAR expressing oocytes. The GluN2A and GluN2B Agonist max alone responses were not significantly different from any of the following concentrations of CNS4: 1 μ M, 3 μ M, 10 μ M, 30 μ M or 100 μ M (**Figure 3.6**). On the contrary, the GluN2C subunit exhibited an inhibition of relative response with 1 μ M CNS4 compared to Agonist max alone (**Figure 3.6**). Lastly, the GluN2D subunit was the only one that exhibited a significant increase with 30 μ M and 100 μ M of CNS4 compared to Agonist max alone (**Figure 3.6**). Traces for all four diheteromeric subunits can be observed in **Figure 3.7**. At the logarithmic scale it can be observed that the GluN2A

subunit exhibited higher relative response to increasing doses of CNS4, however, this increase in relative response was not statistically significant **Figure 3.8**.

The third solution, named Agonist super max, evoked an average response between -0.02 and -0.1 μ A in recombinant NMDAR expressing oocytes. The GluN2A, GluN2B, and GluN2C subunits were not statistically significant when any of the concentrations of CNS4 (1 μ M, 3 μ M, 10 μ M, 30 μ M or 100 μ M) were compared to Agonist super max alone (**Figure 3.9**). The GluN2D subunit showed a significant inhibition pattern with 30 μ M and 100 μ M of CNS4 (**Figure 3.9**). Traces from all four diheteromeric recordings can be observed in **Figure 3.10**. In the logarithmic scale it can be observed that the GluN2D subunit exhibited the greatest numerical inhibition in relative response with increasing doses of CNS4 in **Figure 3.11**

After completing the first set of recordings with Agonist, Agonist Max and Agonist super max, an effect in some of the diheteromeric GluN2 subunits with increasing doses of CNS4 was observed. However, CNS4 was always applied in company of both glutamate and glycine. In order to clarify if CNS4 was able to potentiate NMDAR in the absence of either glutamate or glycine another set of recordings was done. For this, Agonist max was used as base solution in a minimum of five oocytes expressing either the GluN2A or the GluN2B subunits. After the initial application of Agonist Max solution, a solution containing only glutamate (100 μ M) or glycine (100 μ M) was applied, followed by application of either glutamate (100 μ M) plus CNS4 (100 μ M) or glycine (100 μ M) plus CNS4 (100 μ M) (Top of **Figure 3.12** and **Figure 3.13**). The evoked responses in the GluN2A and GluN2B subunits with every solution application was measured and the mean of the relative responses was used to determine the statistical difference among

groups using ANOVA with Tukey's multiple comparisons test with alpha level $p < 0.05$ (*) (Bottom of **Figure 3.12** and **Figure 3.13**).

Using Agonist Max solution, traces of the GluN2A subunit showed an evoked response of $0.02\mu\text{A}$ (Top of **Figure 3.12**). There was a statistical difference when using glutamate alone versus glutamate plus CNS4 since CNS4 seemed to decrease the relative response with only glutamate in the absence of glycine (Bottom of **Figure 3.12**). The evoked response obtained when adding CNS4 to either glutamate or glycine did not potentiate GluN2A NMDAR receptors at the same level than when using both glutamate and glycine together. It can be suspected then, that CNS4 does not replace either glutamate or glycine in the GluN2A subunit to produce the same effect as Agonist max solution alone (**Figure 3.12**).

The GluN2B subunit with Agonist max solution evoked a response of $0.05\mu\text{A}$ (Top of **Figure 3.13**). Opposed to what happened in the GluN2A subunit, in the GluN2B subunit CNS4 plus glutamate increased the relative response of the receptor compared with glutamate alone. No statistical differences were found with solution only containing glycine versus glycine plus CNS4 (Bottom of **Figure 3.13**). Also, CNS4 in the absence of either glutamate or glycine did not produce the same effect as when used with both glutamate and glycine together in the GluN2B subunit (**Figure 3.13**).

DISCUSSION

Substantial efforts have been made to develop therapies to treat disorders associated with both NMDAR excitotoxicity and hypoactivation^{65,112}. Future therapeutic options could arise from modulating the different NMDAR subunits without producing a complete block or excessively hyperactivating them¹¹². The compound CNS4 exhibited both

potentiation and inhibition in different NMDA diheteromeric receptors when used with both glutamate and glycine compared with the elicited responses obtained with glutamate and glycine alone. With the first solution named Agonist, 100 μ M of CNS4 significantly increased all subunits relative response compared when using Agonist alone. In the GluN2C and GluN2D subunits, 30 μ M of CNS4 also significantly increased the relative response compared to Agonist alone. (**Figure 3.3**)

When using the solution Agonist max, the GluN2C subunit exhibited a decreased in relative response with 1 μ M of CNS4 and in the GluN2D subunit, 30 μ M and 100 μ M of CNS4 significantly increased the relative response compared to Agonist max alone (**Figure 3.6**). When the glutamate concentration was increased from 0.3 μ M to 100 μ M, the significant potentiation in the GluN2A, GluN2B and GluN2C subunits was lost. This emphasizes the differences in CNS4 response based on glutamate concentration.

Furthermore, it is important to note that with the higher concentration of glutamate (300 μ M) using Agonist super max solution, the response to 30 and 100 μ M of CNS4 in the GluN2D subunit is opposite to that seen for the Agonist and Agonist max solutions. Emphasizing the different response of CNS4 at different glutamate concentrations.

In the dose response curve set of recordings it was observed that CNS4 did not exhibit a constant inhibition of relative response like antagonists do, discarding this pharmacologic classification. CNS4 elicited both potentiation and inhibition of the distinct GluN2 subunits depending on the different glutamate concentrations used. This modulatory feature allows labeling CNS4 as an allosteric modulator compound.

Since the relative response of CNS4 in the first set of recordings was obtained in the presence of both glutamate and glycine, a second assay involving the GluN2A and

GluN2B subunits was performed in order to determine whether CNS4 could potentiate the response of glutamate alone and glycine alone. Also, the assay looked to see if CNS4 was able to replace the function of glutamate when combined with glycine and if it could also replace the function of glycine when combined with glutamate. In the GluN2A subunit, CNS4 decreased the evoked relative response with only glutamate in the absence of glycine (bottom of **Figure 3.12**). Contrarily, in the GluN2B subunit CNS4 exhibited the opposite effect increasing the evoked response when given with glutamate in the absence of glycine (bottom of **Figure 3.12**). CNS4 then, displayed differences in relative response between the GluN2A and GluN2B subunits when used with glutamate alone. Additionally, in both subunits, CNS4 was unable to emulate the relative response obtained with Agonist max solution when being used alone with either glutamate or glycine (**Figure 3.12** and **Figure 3.13**). This finding corroborates the inability of CNS4 to replace either glutamate or glycine. Furthermore, it cannot be classified as an agonist compound.

CONCLUSION

Substantial efforts have been made to develop compounds that select distinct GluN2 subunits minimizing overall NMDAR hyperactivation¹²². Using two-electrode clamp electrophysiology, we studied various doses of CNS4 with different glutamate concentrations in NMDA dimeric receptors.

Three different glutamate concentration solutions were used named Agonist (0.3 μ M glu/ 100 μ M gly), Agonist max (100 μ M glu/ 100 μ M gly) and Agonist super max (300 μ M glu/ 100 μ M gly). Using Agonist solution, 100 μ M of CNS4 significantly produced an increase in relative response compared with Agonist alone in all subunits and 30 μ M of CNS4 was

enough to significantly increase the response in GluN2C and GluN2D subunits. (**Figure 3.3**). With Agonist max solution non significant changes in relative response were observed in the GluN2A and GluN2B subunits, 1 μ M of CNS4 inhibited the relative response of GluN2C subunit compared with Agonist max solution alone and in the GluN2D subunit, 30 μ M and 100 μ M of CNS4 produced a significant increase in relative response compared with Agonist max solution (**Figure 3.6**). Finally, when using Agonist Super max solution the only subunit that exhibited a significant change in relative response was the GluN2D subunit with 30 μ M and 100 μ M of CNS4, this time, instead of potentiating the receptor a significant reduction in relative response was observed when compared with Agonist super max solution alone (**Figure 3.9**). The purpose of the first set of recordings was to determine the dose response activity of CNS4 and lead us to conclude that the compound exhibited a dose-dependent activity in diheteromeric NMDAR that differed based on glutamate concentration.

The second set of recordings was made to determine how CNS4 will interact in the receptors in the absence of either glutamate or glycine compared with both native transmitters together. The Agonist max solution was used in the GluN2A and GluN2B subunits followed by the application of either glutamate (100 μ M) or glycine (100 μ M) in the presence and absence of CNS4 (100 μ M). At the GluN2A subunit, CNS4 decreased the relative response when used with glutamate compared with glutamate alone (**Figure 3.12**) and produced the opposite effect in the GluN2B subunit decreasing the relative response when used with glutamate compared with glutamate alone (**Figure 3.13**). In both subunits there were not significant differences in the glycine response when adding CNS4. Additionally, CNS4 did not potentiate the GluN2A and GluN2B subunits to the

same level as Agonist max alone when being used in company of either glutamate or glycine. This finding corroborates the inability of CNS4 to replace either glutamate or glycine based on the reduction of relative response when used with gly alone, Furthermore, it cannot be classified as an agonist compound. To finalize and based on the dose response assay, CNS4 can be still labeled as an allosteric modulator that also behaves differently with distinct glutamate concentrations and exhibits NMDAR subunit selectivity. Increased subunit selectivity decreases the probability of global NMDAR activation which could lead to alteration in normal receptor function^{65,112}.

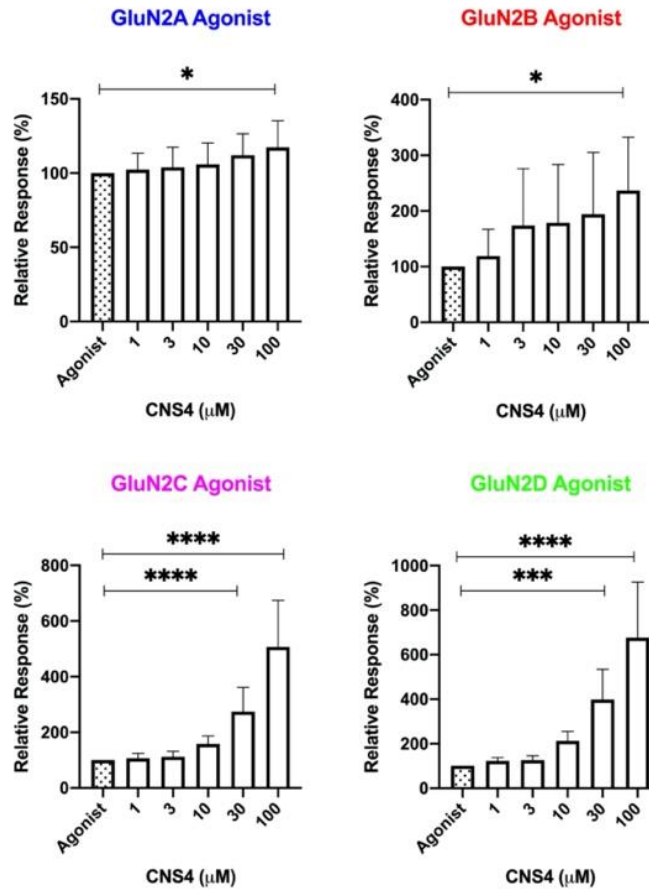
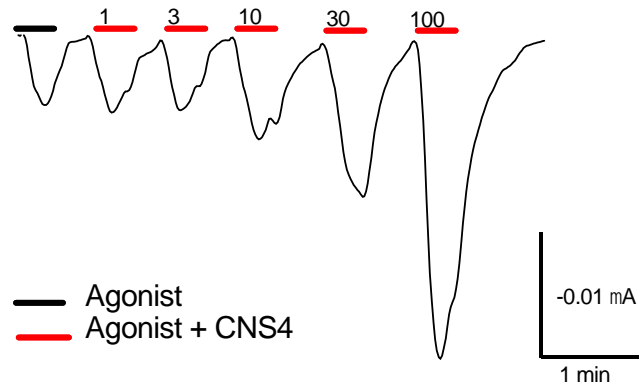


Figure 3. 3 GluN2A (blue), GluN2B (red), GluN2C (pink) and GluN2D (green) relative response with increasing doses of CNS4 (1μM, 3μM, 10μM, 30μM and 100μM) in Agonist solution (0.3μM Glu/ 100μM Gly). Statistical significance was determined comparing means, for at least five oocytes, of the evoked response using Agonist solution alone to every CNS4 dose at the alpha level $p < 0.05$ (*)using a one-way ANOVA with Tukey's multiple comparisons.

GluN2C (0.3mM Glu/ 100mMGly)



GluN2D (0.3mM Glu/ 100mM Gly)

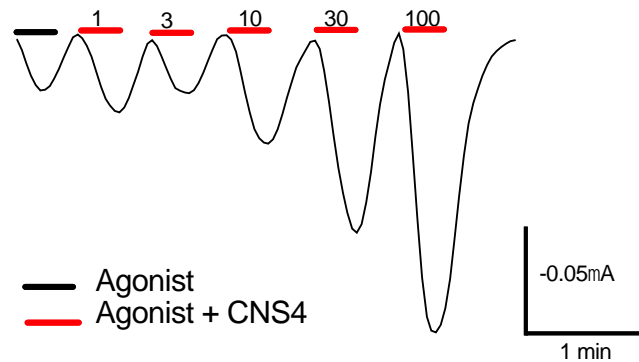


Figure 3. 4 Traces from GluN2C (pink) and GluN2D (green) dose response curve recordings with increasing doses of CNS4 (1 μ M, 3 μ M, 10 μ M, 30 μ M and 100 μ M) in agonist solution (0.3 μ M Glu/ 100 μ M Gly). Every trace represents a single experiment using one oocyte.

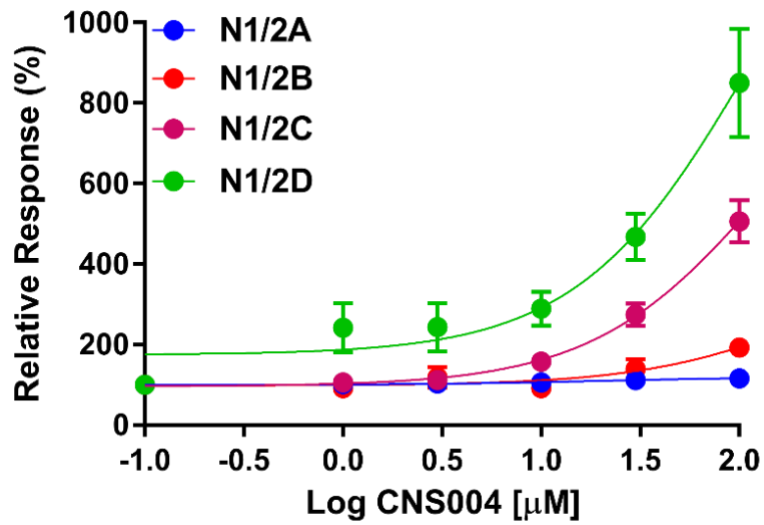


Figure 3. 5 Relative response (y axis) of the GluN2A (blue), GluN2B, (red), GluN2C (pink) and GluN2D (green) in Agonist solution with increasing doses of CNS4 converted to the logarithmic scale (x axis). The GluN2D subunit exhibits the greatest numerical increase in relative response.

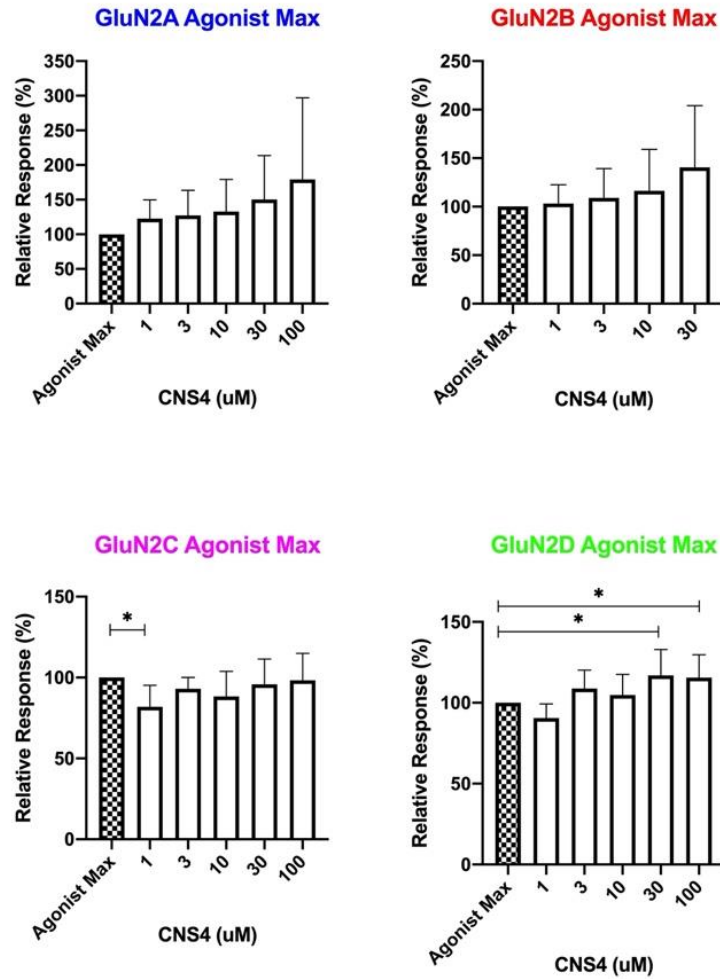


Figure 3. 6 GluN2A (blue), GluN2B (red), GluN2C (pink) and GluN2D (green) relative response with increasing doses of CNS4 (1 μ M, 3 μ M, 10 μ M, 30 μ M and 100 μ M) in Agonist max solution (100 μ M Glu/ 100 μ M Gly). Statistical significance was determined comparing means, for at least five oocytes, of the evoked response using Agonist solution alone to every CNS4 dose at the alpha level $p < 0.05$ (*)using a one-way ANOVA with Tukey's multiple comparisons.

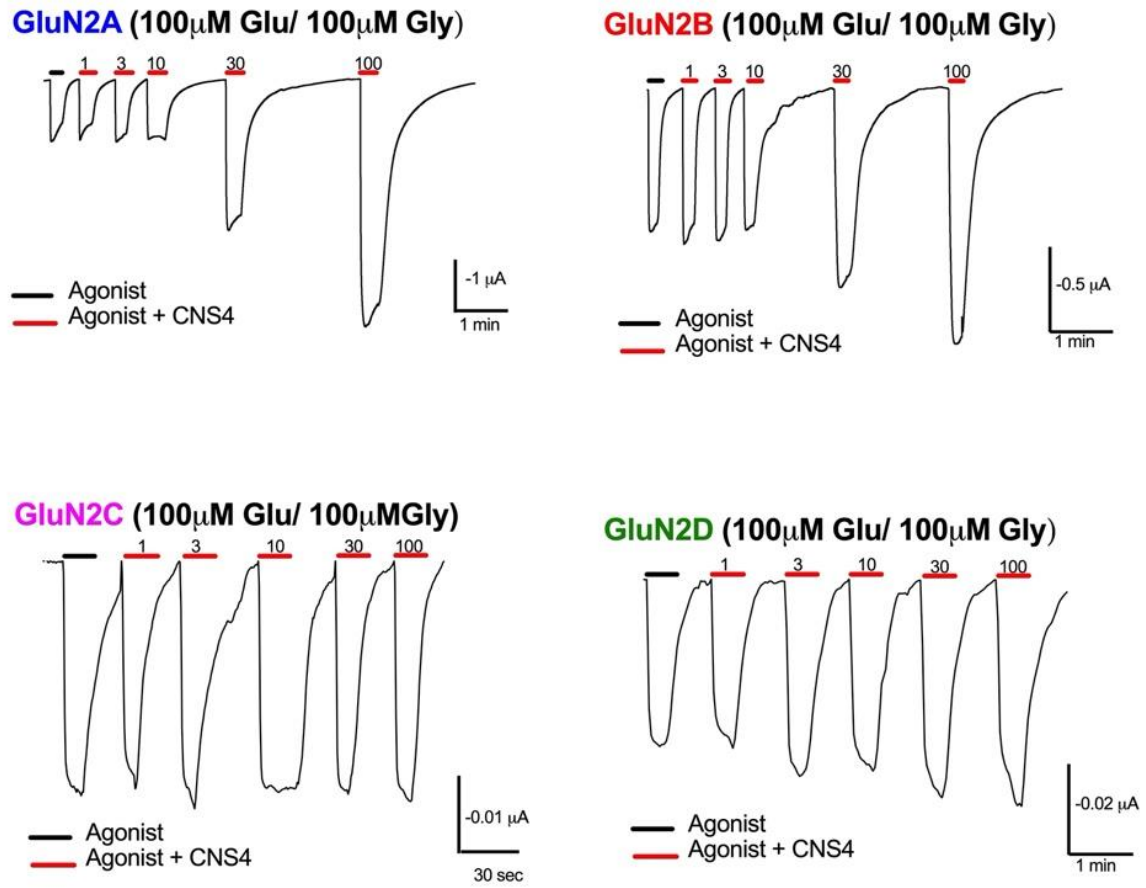


Figure 3. 7 Traces from GluN2C (pink) and GluN2D (green) dose response curve recordings with increasing doses of CNS4 (1 μM , 3 μM , 10 μM , 30 μM and 100 μM) in agonist max solution (100 μM Glu/ 100 μM Gly). Every trace represents a single experiment using one oocyte.

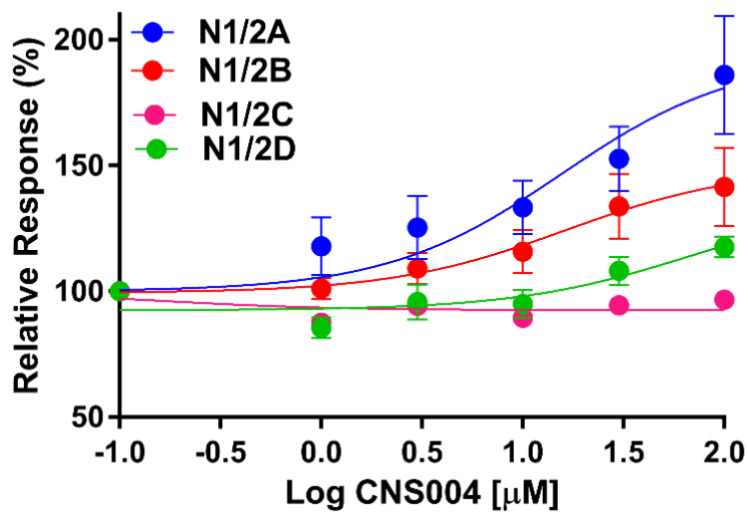


Figure 3. 8 Relative response (y axis) of the GluN2A (blue), GluN2B, (red), GluN2C (pink) and GluN2D (green) in Agonist max solution with increasing doses of CNS4 converted to the logarithmic scale (x axis). The GluN2A subunit exhibits the greatest increase in relative response, however, it was non statistically significant.

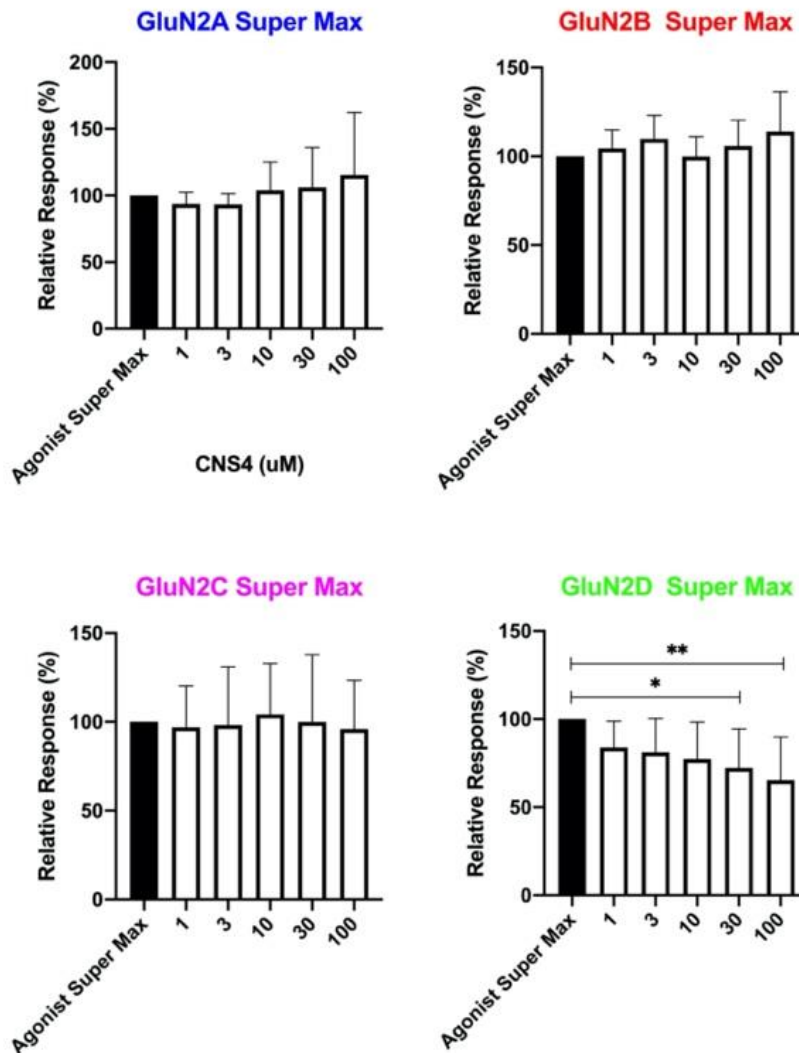
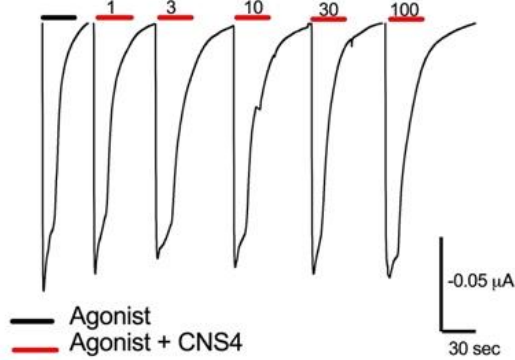
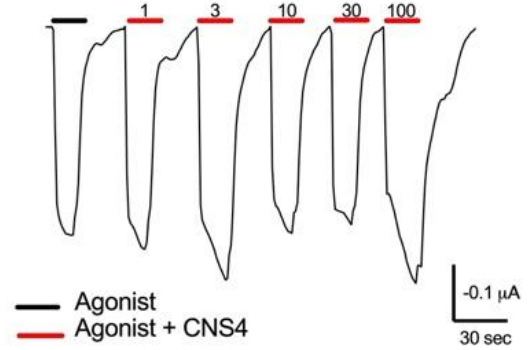


Figure 3.9 GluN2A (blue), GluN2B (red), GluN2C (pink) and GluN2D (green) relative response with increasing doses of CNS4 (1μM, 3μM, 10μM, 30μM and 100μM) in Agonist super max solution (300μM Glu/ 100μM Gly). Statistical significance was determined comparing means, for at least five oocytes, of the evoked response using Agonist solution alone to every CNS4 dose at the alpha level $p < 0.05$ (*)using a one-way ANOVA with Tukey's multiple comparisons.

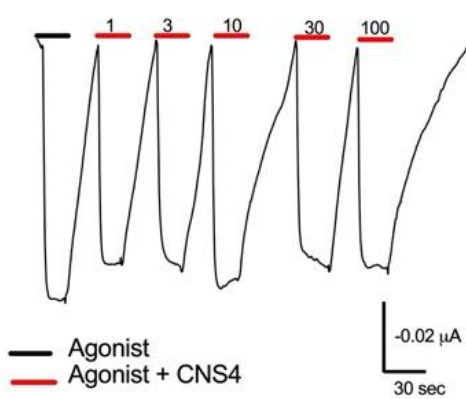
GluN2A (300 μ M Glu/ 100 μ M Gly)



GluN2B (300 μ M Glu/ 100 μ M Gly)



GluN2C (300 μ M Glu/ 100 μ M Gly)



GluN2D (300 μ M Glu/ 100 μ M Gly)

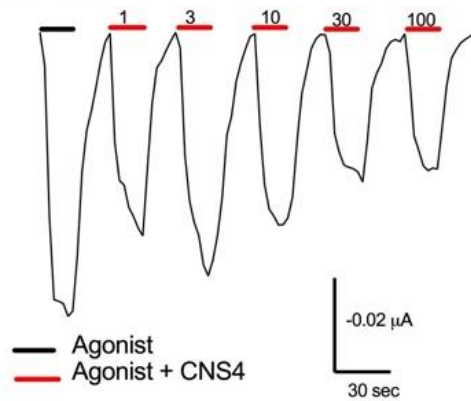


Figure 3. 10 Traces from GluN2C (pink) and GluN2D (green) dose response curve recordings with increasing doses of CNS4 (1 μ M, 3 μ M, 10 μ M, 30 μ M and 100 μ M) in agonist super max solution (300 μ M Glu/ 100 μ M Gly)., Every trace represents a single experiment using one oocyte

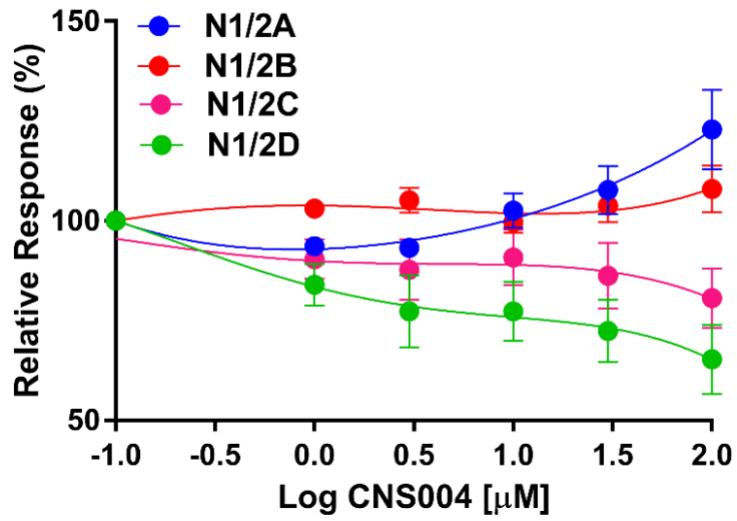
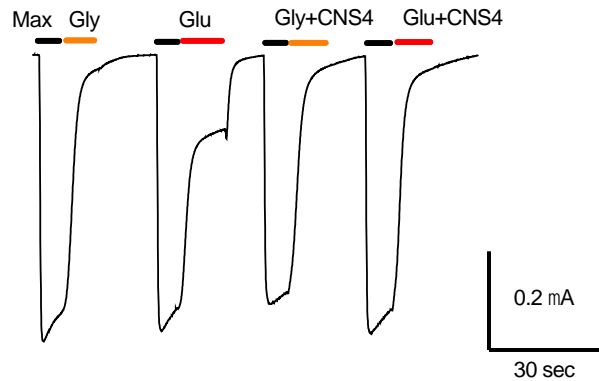


Figure 3. 11 Relative response (y axis) of the GluN2A (blue), GluN2B, (red), GluN2C (pink) and GluN2D (green) in Agonist super max solution with increasing doses of CNS4 converted to the logarithmic scale (x axis). The GluN2D subunit exhibits the greatest numerical decrease in relative response.

GluN1/2A +/- glutamate, glycine and CNS4



GluN1/2A

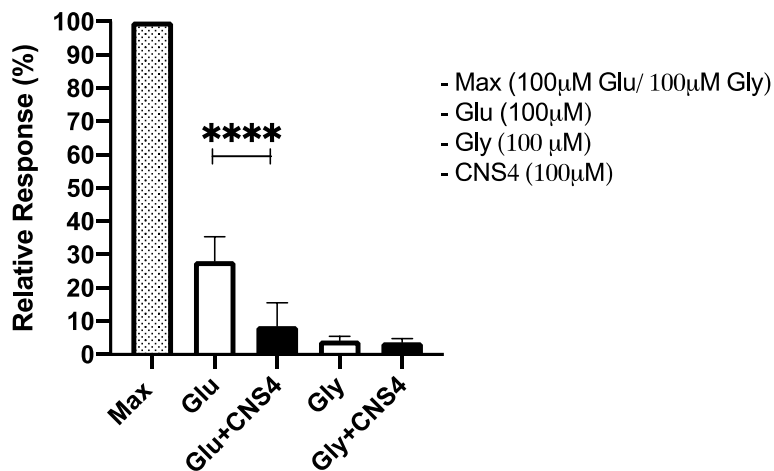


Figure 3. 12 Top, Traces from GluN2A subunit with Agonist max solution, glycine alone (100 μ M), glutamate alone (100 μ M), glycine + CNS4 (100 μ M each) and glutamate + CNS4 (100 μ M each) representing a single experiment using one oocyte. **Bottom**, GluN2A relative response with Agonist max, glutamate alone (100 μ M), glutamate + CNS4 (100 μ M each), glycine alone (100 μ M) and glycine + CNS4 (100 μ M each). Agonist max alone is significantly different from Glu+CNS4 and gly+CNS4. Statistical significance was determined comparing means of the evoked response with every solution in at least five oocytes at the alpha level $p < 0.05$ (*) using ANOVA with Tukey's multiple comparisons test.

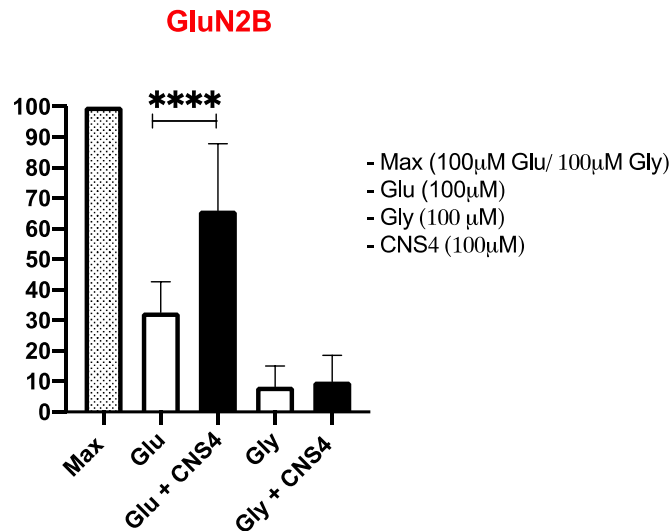
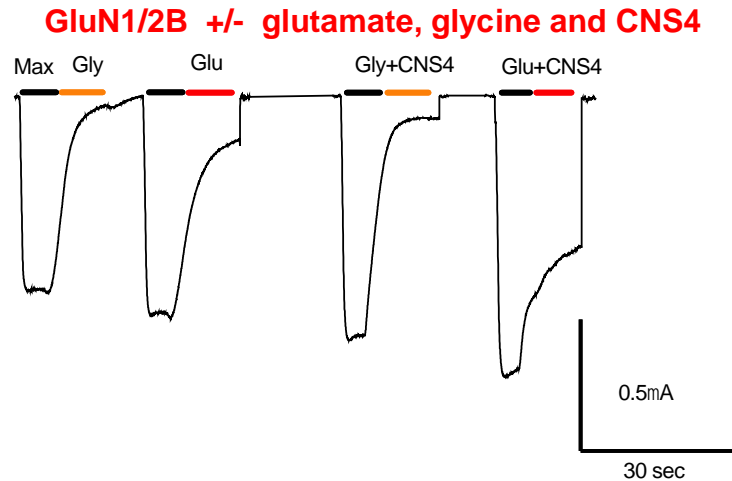


Figure 3. 13 Top, Traces from GluN2A subunit with Agonist max solution, glycine alone (100µM), glutamate alone (100µM), glycine + CNS4 (100µM each) and glutamate + CNS4 (100µM each) representing a single experiment using one oocyte. **Bottom**, GluN2A relative response with Agonist max, glutamate alone (100µM), glutamate + CNS4 (100µM each), glycine alone (100µM) and glycine + CNS4 (100µM each). Agonist max alone is significantly different from Glu+CNS4 and gly+CNS4. Statistical significance was determined comparing means of the evoked response with every solution in at least five oocytes at the alpha level $p < 0.05(*)$ using ANOVA with Tukey's multiple comparisons test

CHAPTER 4: CNS CHANNEL ACTIVITY IN NMDA RECEPTORS

INTRODUCTION

Understanding NMDAR channel properties

Physiological activity of NMDAR is essential for normal neuronal function¹¹⁹. Each NMDAR subunit (GluN2A, GluN2B, GluN2C and GluN2D) has unique structural and functional properties^{16,17,18}. The different subunits have assembly and conformational differences in the M2 loop of the TMD that alter the correct function of ligand binding, activation and desensitization^{19,20}. For example, the deactivation kinetics among subunits differs from one another and can be ranked from faster to slower beginning with GluN2A > GluN2B > GluN2C > GluN2D¹¹. A fast desensitization is considered critical in shaping inhibitory synaptic currents and a slow desensitization could decrease the synaptic efficacy during prolonged exposure to glutamate^{116,117}. Nevertheless, alteration in NMDAR normal function can contribute to neuronal injury and death¹¹⁹.

Potential neuroprotective agents that block all NMDAR like antagonists have unacceptable clinical side effects¹¹⁹. Uncompetitive antagonists like channel blockers obstruct the NMDAR when the channel is open and function in a use-dependent way, the more open the receptor is the more inhibition will be produced⁵¹. However, different compounds exhibit different clinical effects. Memantine for example, is a partial channel blocker that exhibits less deleterious effects on perception and consciousness than MK-801 or PCP¹¹⁸. When the channels release the agents in a fast way, more channels become available for synaptic activation and response¹¹⁸. In addition, the different NMDAR subunits assembly produces different functional properties¹¹⁸. The NMDAR

channel is naturally blocked by Mg^{2+} , nevertheless, the affinity of the blockage will be lower for the GluN2C and GluN2D subunits^{2,51}.

In order to better understand how CNS4 affects channel properties, a current-voltage plot was performed. The relationship between current and voltage permits one to analyze the ion currents (measured in microamperes) with respect to the voltage (measured in millivolts) of the cell membrane¹¹⁴. The cell membrane conductance changes with voltage, meaning that ion channels carrying current are open at some membrane potentials and closed at others¹¹⁵.

SPECIFIC AIM 2

To identify the current- voltage (I-V) activity of CNS4 by using two-electrode voltage clamp (TEVC) in *Xenopus laevis* expressing recombinant NMDA diheteromeric receptors (GluN2A, GluN2B, GluN2C and GluN2D) using four different solutions of Agonist and Agonist max: (1) either Agonist (0.3 μ M Glu/ 100 μ M Gly) or Agonist max solution (100 μ M Glu/ 100 μ M Gly) alone (2) either Agonist or Agonist max solution plus CNS4 (100 μ M) (3) either Agonist or Agonist max solution plus 40 μ M $MgCl_2$ and (4) either Agonist or Agonist max solution plus $MgCl_2$ (40 μ M) plus CNS4 (100 μ M), with a manual increase in holding membrane potential from -90mV to +30mV in 10mV intervals.

MATERIALS AND METHODS

Oocytes:

Stage 4 *Xenopus laevis* oocytes from Xenopus-I, (Ann Arbor, MI, USA)

Solutions:

Ringer's Solution or Recording buffer: 116mM NaCl, 2mM KCL, 0.3mM BaCl₂, 5mM. HEPES: pH 7.4.

ND-96 Solution: 82mM NaCl, 3M KCL, 1M CaCl₂, 5mM HEPES, 2.5mM, Sodium Pyruvate, Gentamicin, pH to 7.6.

OR-2 Solution: 82mM NaCl, 3M KC, 1M MgCl₂, 5 mM HEPES, pH to 7.6

Compounds

CNS4: The compound 4-fluoro-N-(2-(pyridin-3-yl)piperidine-1-carbonothioyl)benzamide (CNS4) was developed by Dr. Costa from computational modeling and synthesized at Syngene International, India (**Figure 3.1**).

NMDAR Constructs

cDNA encoding the NMDAR1a subunit (GluN1a) was obtained from Dr. Nakanishi (Kyoto, Japan). cDNA encoding the GluN2B (pci_sepGluN2B) was purchased from Addgene, Cambridge, MA. cDNA encoding the GluN2C and GluN2D were purchased from GenScript, New Jersey, USA.

Plasmids were linearized with NotI (GluN1) or StuI (GluN2A), or AvrII (GluN2B), or BstB1 (GluN2C and GluN2D) and transcribed in vitro with T7 (GluN2A, GluN2B, GluN2C & GluN2D) RNA polymerase using the mMessage mMachine transcription kits (Invitrogen by Thermo Fisher Scientific (Waltham, MA, USA) and RNA polymerase using the mMessage mMachine transcription kits (Ambion, Austin, TX, USA).

Oocyte Processing

Once arrived, stage 4 xenopus oocytes from Xenopus-I, (Ann Arbor, MI, USA) were manually selected and washed three times with 13ml of OR-2 solution before being left overnight with 13ml of ND-96 solution and 5 mg collagenase. The following day, 0.5µl

of every NMDAR subunit's cRNAs GluN1A, GluN2B, GluN2C and GluN2D were mixed in 1:1 ratio. 50 nL of the final cRNA mixture was microinjected into the oocyte cytoplasm. Oocytes were incubated in ND- 96 solution at 18°C prior to electrophysiological recordings (1–3 days).

Electrophysiological Recordings for Current Voltage (IV) plot

I-V relationships have been used to clarify the changes in ion flow that take place during an experimental situation, giving a better understanding of the operation of the channel¹¹⁴. Electrophysiological recordings using the voltage-clamp technique were used to study ion movement across diheteromeric NMDAR in the presence of CNS4 and MgCl₂. Recombinant cRNA with NMDAR diheteromeric subunits (GluN2A, GluN2B, GluN2C and GluN2D) was injected into *Xenopus laevis* eggs. Either Agonist (0.3μM glu/ 100μM gly) or Agonist max solution (100μM glu/ 100μM gly) was first applied followed by Agonist or Agonist max solutions containing CNS4 (100μM), MgCl₂ (40μM) and a combination of CNS4 (100μ) plus MgCl₂ (40μM). The solutions were given one at a time and no washes with Ringer between application was made. One oocyte was used with all four solutions (containing either Agonist or Agonist max solution) and the total of oocytes used per every NMDAR diheteromeric subunit was five. The holding potential was manually changed with every solution application beginning at -90mV and ending at +30mV going up in 10mV intervals with the intention of producing cell membrane depolarization and observing the movement of ions going across the cell. To give a better idea of how to identify whether ions are moving in or out the cell an explanatory diagram can be found in **Figure 4.1**.

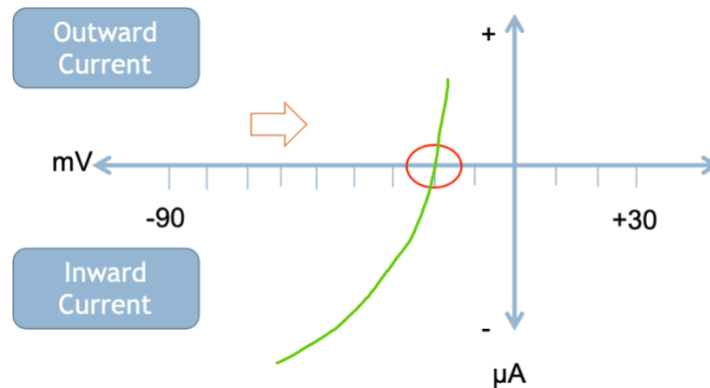


Figure 4. 1 Explanatory diagram of ion movement across the cell membrane (green line) when doing I-V plot electrophysiology. The y axis represent electrophysiological responses in current which is measured in microamperes. Negative values represent inward current (ions going outside the cell). The x axis represents different membrane holding potentials. Negative values are plotted to the left and positive values to the right. The red circle points out when the y axis is equal to zero, meaning that no ions are crossing the cell membrane, and this is referred as Reversal potential.

Recordings were done using an 8-channel perfusion system (Automate Scientific, Berkeley, CA). Electrophysiological current responses obtained after every change in membrane holding potential were measured in microamperes using a standard two-microelectrode voltage clamp [Warner Instruments (Hamden, Connecticut) model OC-725C, and the amplitude responses were digitized for quantification (Digidata 1550A and pClamp-10, Molecular Devices, Sunnyvale, CA).

Statistics

Every NMDAR diheteromeric subunit had two different types of statistical analysis..

The first one involved the plotting of ion movement across the channel pore with the different holding membrane potentials using the four different solutions mentioned in Specific Aim Two. The movement of ions was plotted using linear regression with variable slope (GraphPad Prism, ISI Software, San Diego, CA, USA). In the second part of the analysis statistical significance was determined by the average of at least six recordings per NMDAR subunit comparing the reversal potential of Agonist solution with Agonist solution plus CNS4 and comparing Agonist solution containing MgCl₂ with Agonist solution containing both CNS4 and MgCl₂. The same comparisons were made for the Agonist max solutions. Significant differences were determined at the alpha level $p < 0.05$ (*) using ANOVA with Tukey's multiple comparisons test (GraphPad Prism, ISI Software, San Diego, CA, USA).

RESULTS

The response in xenopus oocytes containing different NMDAR subunits, GluN1/2A, GluN1/2B, GluN1/2C and GluN1/2D, was determined by the response elicited by bath application of either Agonist or Agonists max solution. The first set of recordings included four solutions, Agonist solution (0.3 μ M glu / 100 μ M gly) Agonist solution with 100 μ M CNS4, Agonist solution with 40 μ M MgCl₂ and finally Agonist solution with 40 μ M MgCl₂ plus 100 μ M CNS4.

The reversal potential for every solution helped determine at which membrane potential ions stop moving across the membrane. If any significant difference is seen with CNS4 application it means that CNS4 could increase or decrease the ion current (**Figure 4.1**). Since depolarization naturally releases magnesium block from NMDAR¹¹, solutions with magnesium were given in the presence and absence of CNS4 in order to determine if

CNS4 will interact with the magnesium block in the channel pore and if it would express the same voltage-dependent activity that magnesium has.

With Agonist solution, the GluN2A and GluN2B did not exhibit a significant change in reversal potential in the presence of CNS4. Additionally, when comparing CNS4 plus Agonist solution with just Agonist solution, CNS4 did not numerically decrease the ion inward current suggesting a non blockage of the channel. And in Agonist solution, when CNS4 was used with Mg^{2+} the blockage did not appear to be numerically increased compared to the absence of CNS4, nor was the reversal potential significantly changed, suggesting that CNS4 did not alter the potency of the Mg^{2+} (**Figure 4.2** and **Figure 4.3**).

On the contrary, in the GluN2C and GluN2D subunits the presence of CNS4 significantly reduced the reversal potential, meaning that with CNS4 the ion inward current will flow at more positive membrane holding potential values (**Figure 4.4** and **4.5**). Since this assay produces a manual depolarization, keeping the cell membrane at more positive values produces less Mg^{2+} block and more ions flowing inside the cell.

In order to better understand the ion movement across the channel with a different glutamate concentration, the second set of recordings was performed with a solution named Agonist max (100 μ M Glu/ 100 μ M Gly); the other three solutions applied were similar to the first set of recordings.

No significant differences in reversal potential were found in the GluN2A (**Figure 4.6**), GluN2B (**Figure 4.7**) and GluN2D (**Figure 4.9**) subunits when comparing Agonist max solution with CNS4 to Agonist max solution alone, or when comparing Agonist max solution with 40 μ M $MgCl_2$ plus 100 μ M CNS4 to Agonist max solution containing only $MnCl_2$. To the contrary, Agonist max containing CNS4 in the GluN2C subunit

significantly reduced the reversal potential when comparing to Agonist max alone, meaning that ions were coming into the cell at a more positive membrane holding potential. Likewise, CNS4 reduced the reversal potential when added to Agonist max solution containing MgCl₂ and it did not exhibit a voltage-dependent effect (**Figure 4.8**)

DISCUSSION

NMDA ionotropic receptors are key in physiological and pathological processes in the CNS¹²⁰. The ion movement through the receptor channel is involved in synaptic processes since this is highly permeable to Ca²⁺ and exhibits a voltage-dependent block by Mg²⁺¹²⁰. Once there is significant depolarization, the Mg²⁺ block is relieved, allowing Ca²⁺ to enter the cell¹²⁰. Mg²⁺ also exhibits more affinity towards the GluN2A and GluN2B subunits than the GluN2C and GluN2D due to mutations in the M2 loop of the TMD^{121, 135}. In general, little is known about Mg²⁺ interaction with other compounds that interact with NMDAR, like channel blockers¹²⁰. In this study, we evaluated CNS4 (100µM) channel interactions using two-electrode voltage clamp electrophysiology in the presence or absence of 40 mM MgCl₂ using two different agonist solutions at different holding membrane potentials¹³⁴.

There was no statistical difference in reversal potential for the GluN2A and GluN2B subunits when comparing Agonist solution (0.3µM Glu/ 100µM Gly) with Agonist solution plus CNS4 nor when comparing MgCl₂ in the presence of CNS4 with CNS4 alone (both in Agonist solution (**Figure 4.2 Figure 4.3**). In contrast, these comparisons were significantly different in both GluN2C and GluN2D subunits. In these subunits, when the manual depolarization is being made from -90mV to +30mV, ions expressed a prolonged inward current with numerically more positive membrane potential values in

the presence of CNS4 (**Figures 4.4** and **Figure 4.5**). Additionally, a linear-like I-V relationship of x axis membrane holding potential compared with y axis microamperes in any of the subunits supports the non-voltage-dependent activity of CNS4¹³⁴.

Additionally, in order to clarify if CNS4 will alter the reversal potential in some subunits with different glutamate concentrations, a second set of recordings using Agonist max solution (100 μ M glu/ 100 μ M gly) was performed. The comparisons made were similar to those using Agonist solution. This time, neither the GluN2A, GluN2B or GluN2D subunits exhibited a statistical difference in reversal potential in the presence of CNS4 (**Figure 4.6** **Figure 4.7** and **Figure 4.9**). In contrast, only the GluN2C revealed a significant difference when CNS4 was added to either Agonist max alone or to Agonist max with MgCl₂ (**Figure 4.8**). The presence of CNS4 numerically increased the ion inward current in Agonist max solution containing MgCl₂ with more positive values of membrane potential. In general, CNS4 did not seem to block the channel with agonist max solution since ion inward current was not altered and the comparisons were made with magnesium since it is the ion that naturally blocks the receptor.

When using both Agonist and Agonist max solution in all four diheteromeric subunits, CNS4 in the presence of either Agonist solution did not numerically decrease the ion inward current when compared to either Agonist solution alone, suggesting that CNS4 does not block the channel pore. Also, in all diheteromeric subunits when CNS4 was used in the solutions containing Mg²⁺, the blockage was not numerically increased suggesting that CNS4 does not increase the Mg²⁺ blockage. Finally, CNS4 altered the reversal potential in a different complement of subunits when using different glutamate

concentrations, corroborating with the findings in the dose response curve assay of Specific Aim 1.

Overall, development of compounds that are subunit-selective is ideal since it can target distinct GluN2 subunits without global NMDAR overactivation¹²². For the most part, NMDAR antagonists are dissociative anesthetics, drugs of abuse and are a high target for treatment of neuropsychiatric diseases⁹⁶. Many NMDAR antagonists are positively charged and voltage-dependent channel blockers¹³⁶. Subunit specificity is ideal since not all NMDAR subunits exhibit equal sensitivity to Mg^{2+} block and different subunits are linked to specific disorders like GluN2C hyperactivation to schizophrenic like behaviors¹³⁷. The ideal approach is to develop a new set of allosteric modulator compounds that can influence channel conductance among distinct NMDA subtypes¹²². Some compounds like endogenous neurosteroid pregnenolone sulfate ($3\alpha5\beta S$) inhibit NMDAR activity in a voltage-independent manner by reducing the channel probability with a lower effect on the GluN2A and GluN2B subunits compared to the GluN2C and GluN2D subunits¹³³. Like neurosteroids, CNS4 exhibited a more selective activity on the GluN2C and GluN2D subunits. Although CNS4 binding site could not be identified from this study, we are planning on doing a cryo-electronmicroscopy or x-ray crystallography, or an artificial intelligence algorithm to define the CNS4 binding site (s).

CONCLUSION

NMDAR are essential for normal brain function and are naturally blocked by Mg^{2+} ¹²⁰,¹²². Nevertheless, the GluN2A and GluN2B subunits exhibit more affinity towards Mg^{2+} than the GluN2C and GluN2D subunits¹²¹². Thus, the development of compounds that are

subunit-selective are ideal to modulate GluN2 function without global NMDAR overactivation having better therapeutic effects¹²².

We studied the compound CNS4 using a two-electrode voltage-clamp technique changing the membrane holding potential from -90mV to +30 mV to understand the ions inward and outward current in the presence and absence of 40 μ M MgCl₂ (**Figure 4.1**). With Agonist solution, the presence of CNS4 significantly decreased the reversal potential in the GluN2C (**Figure 4.4**) and GluN2D (**Figure 4.5**) subunits, and non significant change was observed in the GluN2A (**Figure 4.2**) and GluN2B (**Figure 4.3**) subunit. And when using Agonist max solution a significant difference in reversal potential was only observed in the GluN2C subunit (**Figure 4.8**). Numerical decreases in reversal potential findings suggest that inward current of ions in presence of CNS4 occurs with more positive membrane holding potentials in manual depolarization. Additionally in all diheteromeric subunits and with both Agonist solutions, CNS4 in the absence of Mg²⁺ was unable to mimick the blockage seen when Mg²⁺ is used alone suggesting the possibility that CNS4 alone is unable to block the channel pore. Overall, in the current voltage plot it can also be observed that the linear-like relationship between the y axis (current) and x axis (voltage) for CNS4 with any of the solutions given, and in all diheteromeric subunits, suggests a lack of voltage-dependent activity of this compound. And finally, CNS4-induced significant differences in reversal potential among diheteromeric subunits varied based on the amount of glutamate used, corroborating the findings from the dose response assay made in Chapter 3 in which a glutamate dose dependent acitivity of CNS4 is found.

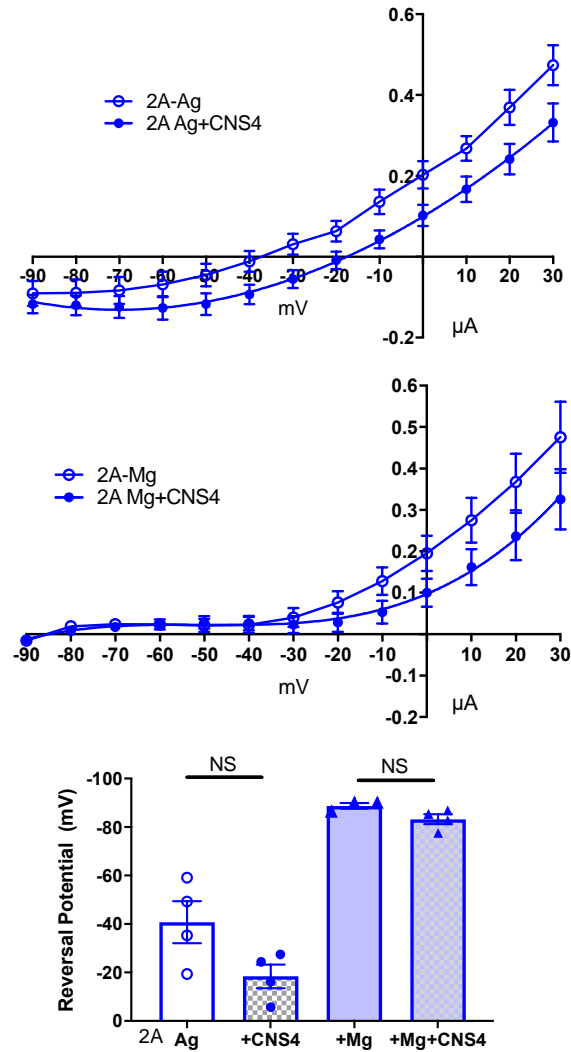


Figure 4. 2 Upper two, current (y axis) and voltage (x axis) relationship in the GluN2A subunit for 1) Agonist solution (0.3 μM Glu/100 μM Gly) in the presence and absence of CNS4 (100 μM) and for 2) Agonist solution with 40 μM MgCl₂ in the presence and absence of CNS4 , allowing visualizing of the ion movements across the channel.

Bottom, comparison of reversal potential from at least five recordings in the presence and absence of CNS4, in the GluN2A subunit, for Agonist solution with and without MgCl₂ . Statistical significance of differences in reversal potential were determined at the alpha level $p < 0.05(*)$ using one way ANOVA with Tukey's multiple comparisons

test .

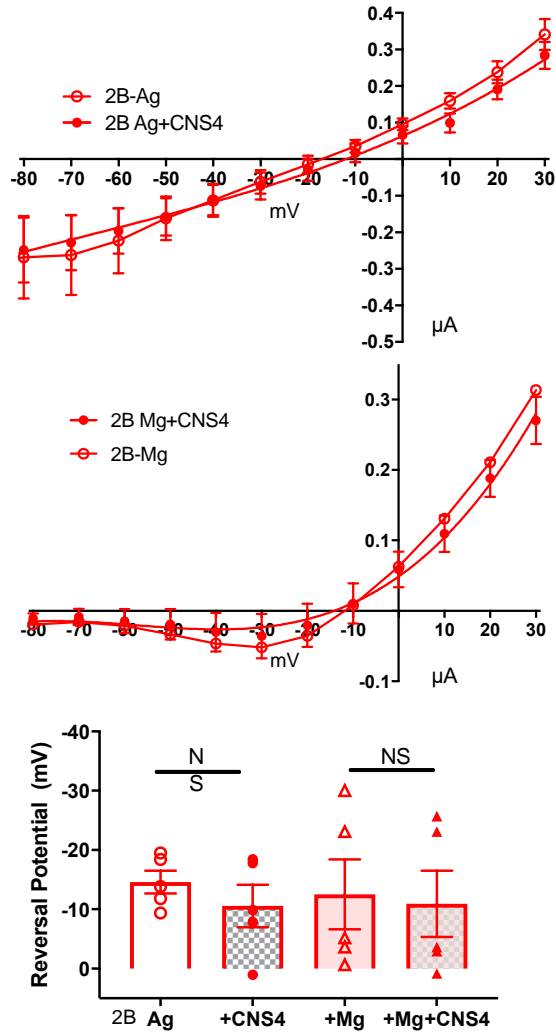


Figure 4.3 Upper two, current (y axis) and voltage (x axis) relationship in the GluN2B subunit for 1) Agonist solution (0.3 μ M Glu/100 μ Gly) in the presence and absence of CNS4 (100 μ M) and for 2) Agonist solution with 40 μ M MgCl₂ in the presence and absence of CNS4 , allowing visualizing of the ion movements across the channel. **Bottom**, comparison of reversal potential from at least five recordings in the presence and absence of CNS4, in the GluN2B subunit, for Agonist solution with and without MgCl₂ . Statistical significance of differences in reversal potential were determined at the alpha level $p < 0.05$ (*) using one way ANOVA with Tukey's comparisons test .

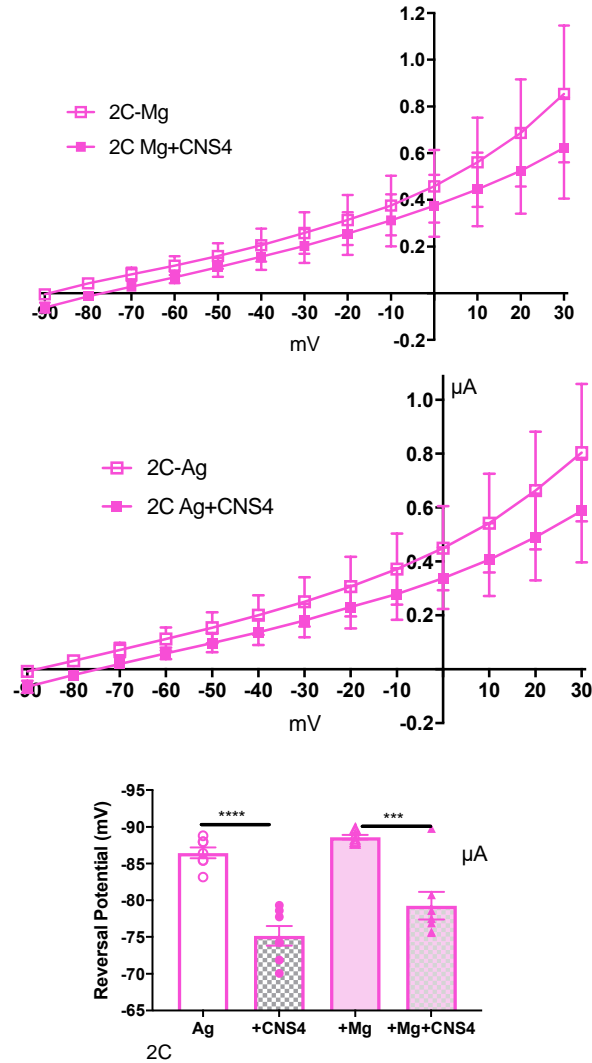


Figure 4. 4 Upper two, current (y axis) and voltage (x axis) relationship in the GluN2C subunit for 1) Agonist solution ($0.3\mu\text{M}$ Glu/ $100\mu\text{Gly}$) in the presence and absence of CNS4 ($100\mu\text{M}$) and for 2) Agonist solution with $40\mu\text{M}$ MgCl_2 in the presence and absence of CNS4 , allowing visualizing of the ion movements across the channel.

Bottom, comparison of reversal potential from at least five recordings in the presence and absence of CNS4, in the GluN2C subunit, for Agonist solution with and without MgCl_2 . Statistical significance of differences in reversal potential were determined at the alpha level $p < 0.05(*)$ using one way ANOVA withTukey’s multiple comparisons

test.

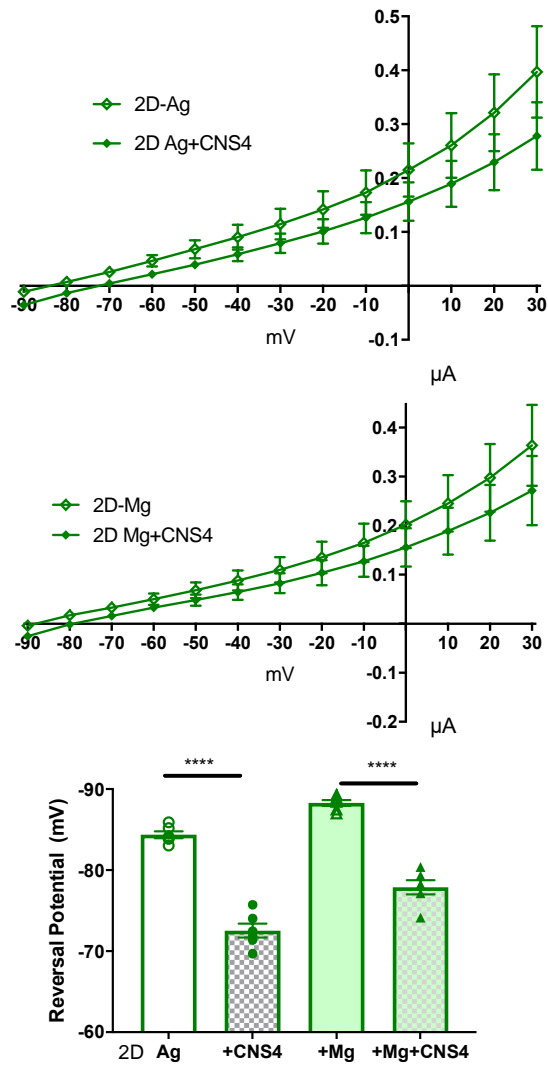


Figure 4. 5 Upper two, current (y axis) and voltage (x axis) relationship in the GluN2D subunit for 1) Agonist solution (0.3μM Glu/100μGly) in the presence and absence of CNS4 (100 μM) and for 2) Agonist solution with 40μM MgCl₂ in the presence and absence of CNS4 , allowing visualizing of the ion movements across the channel.

Bottom, comparison of reversal potential from at least five recordings in the presence and absence of CNS4, in the GluN2D subunit, for Agonist solution with and without MgCl₂ . Statistical significance of differences in reversal potential were determined at the alpha level $p < 0.05(*)$ using one way ANOVA withTukey’s multiple comparisons

test

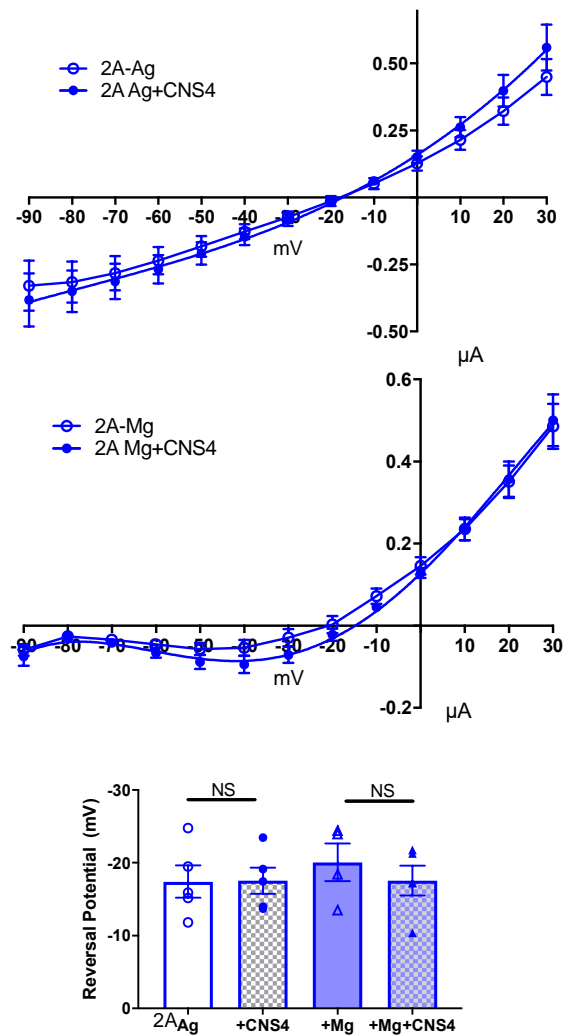


Figure 4. 6 Upper two, current (y axis) and voltage (x axis) relationship in the GluN2A subunit for 1) Agonist max solution (Ag) (0.3μM Glu/100μGly) in the presence and absence of CNS4 (100 μM) and for 2) Agonist max solution with 40μM MgCl₂ in the presence and absence of CNS4 , allowing visualizing of the ion movements across the channel. **Bottom**, comparison of reversal potential from at least five recordings in the presence and absence of CNS4, in the GluN2A subunit, for Agonist max solution with and without MgCl₂. Statistical significance of differences in reversal potential were determined at the alpha level $p < 0.05(*)$ using one way ANOVA with Tukey's multiple comparisons test.

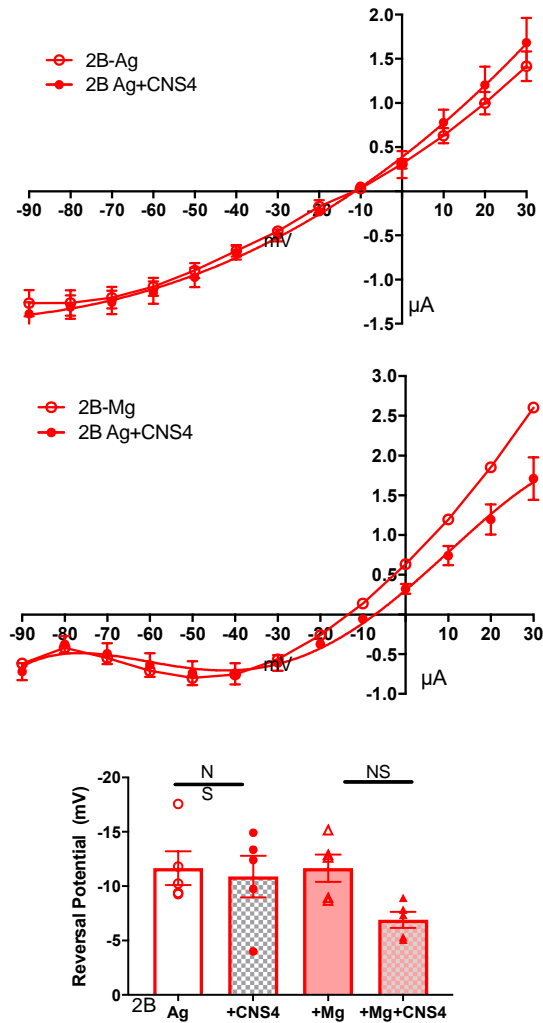


Figure 4. 7 Upper two, current (y axis) and voltage (x axis) relationship in the GluN2B subunit for 1) Agonist max solution (Ag) ($0.3\mu\text{M}$ Glu/ $100\mu\text{Gly}$) in the presence and absence of CNS4 ($100\mu\text{M}$) and for 2) Agonist max solution with $40\mu\text{M}$ MgCl_2 in the presence and absence of CNS4 , allowing visualizing of the ion movements across the channel. **Bottom**, comparison of reversal potential from at least five recordings in the presence and absence of CNS4, in the GluN2B subunit, for Agonist max solution with and without MgCl_2 . Statistical significance of differences in reversal potential were determined at the alpha level $p < 0.05(*)$ using one way ANOVA with Tukey's multiple comparisons test.

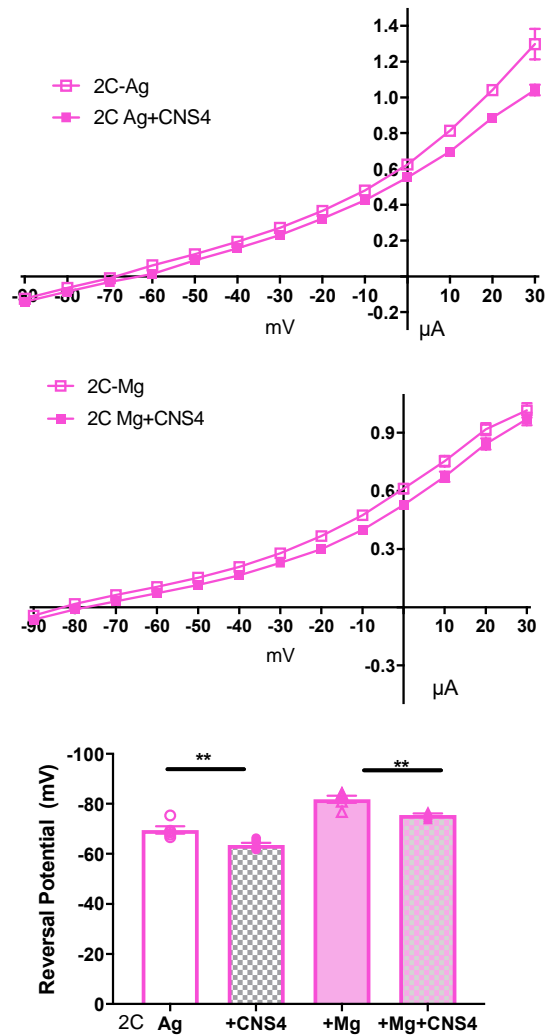


Figure 4. 8 Upper two, current (y axis) and voltage (x axis) relationship in the GluN2C subunit for 1) Agonist max solution (Ag) ($0.3\mu\text{M}$ Glu/ $100\mu\text{Gly}$) in the presence and absence of CNS4 ($100\mu\text{M}$) and for 2) Agonist max solution with $40\mu\text{M}$ MgCl_2 in the presence and absence of CNS4 , allowing visualizing of the ion movements across the channel. **Bottom**, comparison of reversal potential from at least five recordings in the presence and absence of CNS4, in the GluN2C subunit, for Agonist max solution with and without MgCl_2 . Statistical significance of differences in reversal potential were determined at the alpha level $p < 0.05(*)$ using one way ANOVA with Tukey's multiple comparisons test.

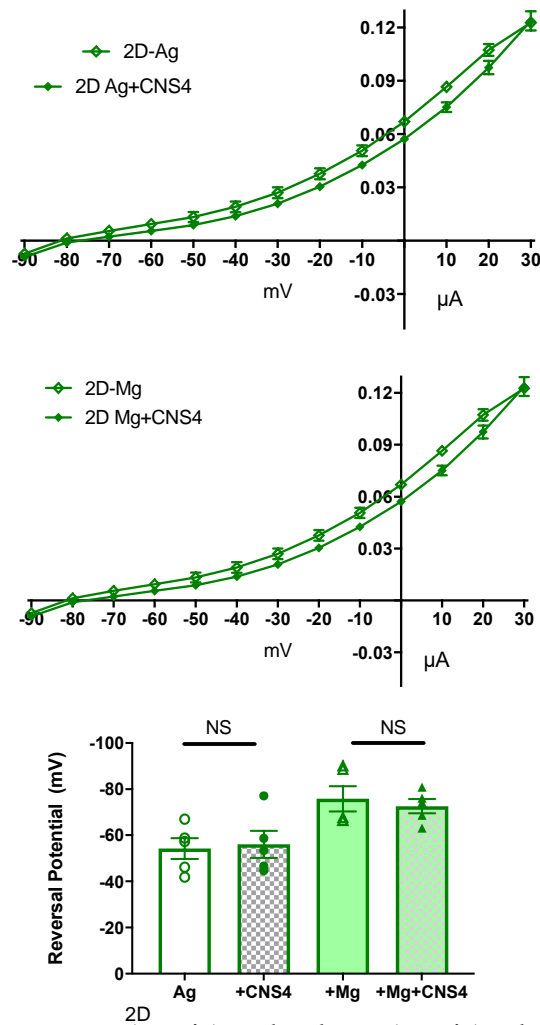


Figure 4. 9 Upper two, current (y axis) and voltage (x axis) relationship in the GluN2D subunit for 1) Agonist max solution (Ag) ($0.3\mu\text{M}$ Glu/ $100\mu\text{Gly}$) in the presence and absence of CNS4 ($100\mu\text{M}$) and for 2) Agonist max solution with $40\mu\text{M}$ MgCl_2 in the presence and absence of CNS4 , allowing visualizing of the ion movements across the channel. **Bottom**, comparison of reversal potential from at least five recordings in the presence and absence of CNS4, in the GluN2D subunit, for Agonist max solution with and without MgCl_2 . Statistical significance of differences in reversal potential were determined at the alpha level $p < 0.05(*)$ using one way ANOVA with Tukey's multiple comparisons test.

CHAPTER 5: CNS4 ACTIVITY IN PRIMARY NEURONS

INTRODUCTION

NMDAR mediated excitotoxicity

NMDAR activity is necessary for normal physiological functions like synaptic plasticity, memory formation, mood control, brain development, and neuronal survival⁵⁹. Each subunit provides distinct physiological and pharmacological properties¹²³. The receptor's activation is important in neuronal processes of long-term potentiation (LTP) and long-term depression (LTD), which are crucial for learning and memory¹²⁵. In fact, the GluN2B subunit is required for LTD activation¹²⁴. In contrast, the GluN2A subunit, which is predominately expressed in the adult cortex, is required for LTP induction^{124,125}. Some NMDAR blockers like ifenprodil, which selectively block the GluN2B subunit, impede the induction of LTD but have no effect on the induction of LTP⁹⁴.

In abnormal conditions like brain trauma or stroke, there is the reduction of blood flow that leads to oxygen and glucose shortage that eventually depletes available ATP for neurons and glial cells, which are in control of regulating normal glutamate levels¹²⁶. Consequently, extracellular glutamate level increases, triggering NMDAR, which results in excessive Ca^{2+} influx that starts multiple intracellular cascades that cause damage and death to neurons¹²⁶. This excitotoxicity can be observed under both acute and chronic conditions, including acute brain injuries, Huntington's disease, PD, AD, chronic alcohol exposure, and neuropathic pain⁶⁵.

Ca^{2+} ions also generate intracellular signals that determine a variety of functions including exocytosis of neurotransmitter-containing synaptic vesicles and induction of activity-dependent synaptic plasticity¹²⁷. Nevertheless, an increase in Ca^{2+} uptake is related to the

degradation of structural proteins in neurons¹²⁶. NMDAR blockers like memantine have been used to protect neurons by blocking all NMDAR subtypes. However, completely blocking the receptors can produce undesired side effects¹²⁶.

Since overactivation of the receptor leads to several side effects, CNS4 was used in neurons with induced neurotoxicity to evaluate if CNS4 could have an effect on calcium uptake, through a calcium assay, and on cellular viability, through a MTS colorimetric assay. Cortical and striatal neurons were used by primary culture from rat brains and induced excitotoxicity was obtained with using the synthetic agonist NMDA.

SPECIFIC AIM 3

To demonstrate the effect of CNS4 activity on NMDAR from neurons of primary culture from rat brain by performing neurotoxicity assay through excessive NMDAR activation with increasing doses of synthetic agonist NMDA in the presence of CNS4. Ca²⁺ and MTS assays are done in order to determine Ca²⁺ influx and cellular viability.

MATERIALS AND METHODS

Neuronal culture

Two days before the neuronal culture, 96 well plates (Costar 3603, Germany) were coated with 0.1mg/ml Poly-D-Lysine (PDL) (Gibco A3890401, Germany). One day before culture, the 96 well plates were washed three times with autoclaved dd H₂O and left to dry overnight at 37°C. On the day of the culture, a pregnant female rat from Charles River (MA, USA) was handled according to institutional guidelines and permission of IACUC (Virginia Tech, USA). The female rat was put under anesthesia with isoflurane (Fluriso,

Vetone) in a glass anesthesia jar and heads from embryos day-19 (E19) were retrieved in accordance to Virginia Tech IACUC guidelines and kept in 1xHBSS (Gibco 1470-112)

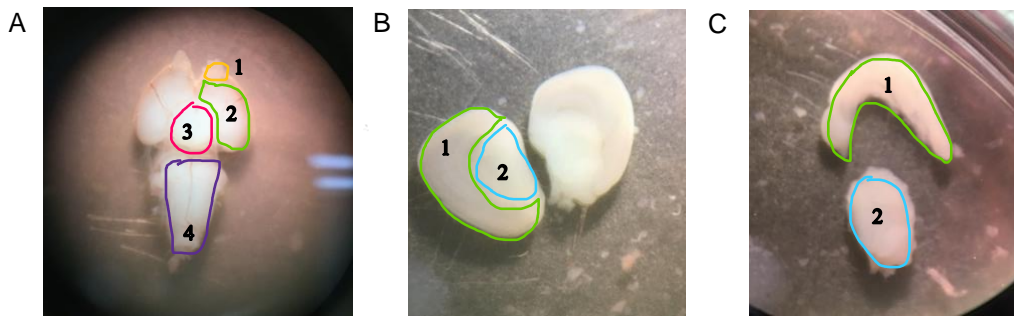


Figure 5.1 Kwapisz L (2020) Pictures of E19 rat embryo dissection with anatomic characterization of different brain regions. **A.** Ventral view of an E19 rat brain under the microscope, (1) olfactory bulb (2) left hemisphere (3) midbrain (4) medulla and spinal cord. **B.** Ventral view of one of the two hemispheres separated from the brain (1) brain cortex (2) striatum. **C.** Ventral view of one hemisphere with (1) cortex region separated from (2) striatum region. Costa Lab, Virginia Tech.

Under the microscope anatomic differentiation of different brain regions was made (**Figure 5.1**) and cortex and striatum brain regions were dissected in a 35mm dish containing HBSS with forceps and tweezers. Following this and under the hood, the brain samples were homogenized by hand, and 4.5ml trypsin-EDTA (ATCC 30-2101) was added to the sample and incubated at 37°C for 10min. At the end of the incubation, 500µM FBS (Sigma MFCD00132239) was added to the tube and agitated by tapping for 5 min. Big clots were broken using a glass pipet and put into a new 50ml tube using 100µl of prepared Neuronal Media which contained 500ml neuronal media (Gibco A35829-01) + 10ml B27 (Gibco A35828-01) + 5ml Pen-Strep (Millipore Sigma P078) + 5ml GlutaMAX (Gibco 35050-061). The resulting sample was centrifuged at 1000RPM for 10min at 4°C. After this, the

supernatant was poured off and pellet was resuspended in 10ml of our Neuronal Media. Cell count was done using trypan blue (0.4% Trypan blue stain: Invitrogen 2086739). Cells were plated with a density of 5×10^4 cells per well in 200 μ l of Neurobasal Media over 96 well plates. Neuronal media was partially changed every 3 days leaving neurons to grow for 14 days.

Calcium assay

A quantitative assay to measure calcium concentration in neurons was done by using Fluo-8 dye (Abcam ab112129). The dye was prepared by combining reagents according to the manufacturer's protocol. Neurons were treated on day 15. All neuronal media was removed from wells and replaced with 100 μ l of 1xHBSS (Gibco 14170-112) plus 100 μ l Fluo-8 dye. The plate (Costar 3603) was incubated for 1 hour, first 30 minutes at 37°C and remaining 30min at room temperature. The treated columns had the following order: (1) Control vehicle containing 1xHBSS (2) 50 μ M Memantine + 100 μ M NMDA (3) 300 μ M NMDA (4) 100 μ M CNS4 (5) 300 μ M NMDA+ 100 μ M CNS4 (6) 100 μ M NMDA + 100 μ M CNS4 (7) 30 μ M NMDA + 100 μ CNS4 (8) 10 μ M NMDA + 100 μ M CNS4 (9) 3 μ M NMDA + 100 μ M CNS4 (10) 1 μ M NMDA + 100 μ M CNS4 (11) 0.3 μ M NMDA + 100 μ M CNS4. After incubation time, the calcium concentration for plates containing cortical and striatal neurons was measured by reading optical density one plate at a time at 490/525nm (BioTek Synergy H1 plate reader 17032020).

MTS tetrazolium cell proliferation assay

A quantitative assay to assess neuronal viability was done using an MTS assay kit (Abcam ab197010). In this assay neurons are given tetrazolium dye that is converted into formazan

dye in metabolically active neurons. The formazan dye is quantified by measuring the absorbance at 490-500nm based on manufacturer's recommendations. Neurons from neuronal culture were treated on day 15. Every well of the 96 well plates from neuronal culture had 100µl of Neuronal Media removed and replaced with 100µl of treatment, leaving the plate overnight at 37°C. The treated columns of the 96 well plates (Costar 3603) had the following order: (1) Control containing neuronal media only (2) 100µM NMDA (3) 50µM Memantine + 100µM NMDA (4) 100µM NMDA + 100µM CNS4 (5) 100µM NMDA + 10µM CNS4 (6) 100µM NMDA + 1µM CNS4. The next day, 200µl of dye from MTS assay kit (Abcam ab197010) was applied to each well and left in an incubator for 3 hours at 37°C. Formazan dye quantification of plates containing cortical and striatal neurons was read at 490nm (BioTek Synergy H1 plate reader 17032020)

Statistics

There were two plates per assay. The calcium assay had one plate with cortical neurons and one plate with striatal neurons and the MTS assay had one plate with cortical neurons and one plate with striatal neurons. The quantified calcium concentration (Calcium assay) and formazan dye (MTS assay) were obtained from reading the 96 well plates at 490/525nm (BioTek Synergy H1 plate reader 17032020). Comparisons of the average of eight repetitions, corresponding to the eight wells in every treated column in the 96 well plates, were done using ANOVA with Tukey's multiple comparisons test at the alpha level $p < 0.05(*)$ and T-Test significance level $P < (0.001)$ when specified (GraphPad Prism, ISI Software, San Diego, CA, USA).

RESULTS

Physiologically, the amount of Ca^{2+} ions are essential for normal neuronal activity and brain function¹²⁷. However, excessive NMDAR activation triggers Ca^{2+} uptake leading to cellular death¹²⁶. To better understand CNS4 activity in native neurons undergoing induced excitotoxicity, primary rat brain culture of two different brain regions, cortex, with predominately expression of GluN2B and GluN2A subunits, and striatum, with predominately GluN2D and GluN2C subunit expression, was made. Neurons were treated with increasing doses of NMDA in the presence of CNS4 to further determine Ca^{2+} influx, and with increasing doses of CNS4 in the presence of a presumed excitotoxic dose of NMDA to examine effects on metabolic activity.

In neurons from the cortex region, NMDA (300 μM) alone significantly increased Ca^{2+} uptake compared with control and with NMDA + memantine (50 μM). CNS4 (100 μM) used alone did not have an effect in the amount of Ca^{2+} uptake compared to control. However, when CNS4 was given with 300 μM of NMDA there was a significant increase in Ca^{2+} uptake compared with NMDA (300 μM) alone (**Figure 5.2**).

In the striatal region, CNS4 alone (100 μM) did not alter the amount of Ca^{2+} uptake compared to control. Nevertheless, 100 μM of CNS4 significantly increased the amount of Ca^{2+} uptake when given with 100 and 300 μM of NDMA compared with 300 μM of NMDA alone and 3 μM of NMDA with CNS4 decreased Ca^{2+} uptake compared to control (**Figure 5.3**) suggesting that CNS4 could facilitate Ca^{2+} influx.

Since Ca^{2+} uptake is linked with neuronal death¹²⁶, a metabolic assay (MTS) was performed to evaluate neuronal viability. In cortical neurons, NMDA alone (100 μM) decreased OD compared with control suggesting a decrease in cellular viability. On the contrary, when memantine was used (50 μM) with NMDA there was an increase in cellular viability

compared to NMDA (300 μ M) alone and no difference compared with control (**Figure 5.4**). The further treatments were done with constant NMDA (100 μ M) with increasing doses of CNS4 (1 μ M, 10 μ M and 100 μ M). Even though the presence of CNS4 did not improve neuronal viability compared to NMDA alone, it did not increase further cellular death (**Figure 5.4**). The same MTS assay was done in striatal neurons with similar results. Additionally, memantine (50 μ M) not only increased cellular viability compared with NMDA (300 μ M) alone but also compared with control (**Figure 5.5**)

It is important to point out that all MTS assay treatment groups for both cortical and striatal neurons contained NMDA. Furthermore, to have a better idea of CNS4 influence on neuronal viability in neurons, a different MTS assay was performed comparing CNS4 (100 μ M) alone with untreated neurons. In both cortical and striatal neurons, when CNS4 was used by itself it did not alter cellular viability (**Figure 5.6**) leading us to think that CNS4 activity in primary neurons could be non-toxic.

DISCUSSION

NMDAR participate in many physiological and pathological conditions¹²⁶. Different subunits exhibit unique features in neuroprotection and neurotoxicity^{130,132}. The GluN2A and GluN2B, for example can form a complex with transient receptor potential cation channel subfamily M member 4 (TRPM4) that is required for excitotoxic damage induced by excessive glutamate¹³⁰. In contrast, tonic activation of GluN2C and GluN2D subunits in vivo by ambient glutamate can facilitate cortical interneuron maturation¹³². The NMDAR is a key component in leading ions like Ca²⁺ to enter the cell and initiate numerous intracellular processes². However, excessive NMDAR hyperactivation can lead to neuronal death¹²⁶. Even though the molecular basis for toxic NMDAR signaling is

unknown, a high Ca^{2+} influx has been implicated^{126,130}. There are numerous neuropathological conditions related to NMDAR-mediated excitotoxicity making the receptor an important target for disorders like autism, depression, SCZ, and PD^{57,65}. There is a need to find compounds that interact with NMDAR without completely blocking the receptor like antagonists do since it can compromise physiological synaptic functions¹³⁰.

To better understand the effect of the compound CNS4 in neurons with ongoing excitotoxicity, a primary brain culture was made in cortical neurons with predominately GluN2A and GluN2B expression and striatal neurons with predominant GluN2C and GluN2D expression^{11,14,15}.

The use of synthetic agonist NMDA was used to induce excitotoxicity. Since the EC_{50} of this compound ranges between 6.5- 25.0 μM ¹³⁹, a higher dose (100 μM) was used in the MTS assay to induce NMDAR overactivation, which has been linked with neuronal excitotoxicity.

In both neuron types, high doses of NMDA (100 μM) decreased cellular viability compared with control (**Figure 5.4** and **Figure 5.5**). These results corroborate the fact that neuronal survival decreases with NMDAR overactivation¹²⁶. Memantine is currently used as an NMDAR blocker with neuroprotective properties in conditions like AD^{101,102}. When memantine was used with NMDA it restored viability to control levels for cortical neurons and even surpassed control levels in striatal neurons. The presence of CNS4 (300 μM) by itself did not seem to alter Ca^{2+} influx compared to control in both cortical and striatal neurons (**Figure 5.2** and **Figure 5.3**). There was also a substantial increment in Ca^{2+} influx compared to control, in a dose dependent manner, using constant CNS4 (100 μM) with

increasing NMDA. Furthermore, CNS4 was able to potentiate NMDAR Ca^{2+} influx produced by NMDA alone in both cortical and striatal tissue.

Some NMDAR antagonists like MK-801 and Ketamine decreased metabolic activity altering proper NMDAR function¹²⁹. In order to clarify the effect of CNS4 in primary brain neurons with ongoing excitotoxicity, two different MTS assays were done for cortical and striatal neurons. In both regions, increasing doses of CNS4 with constant NMDA (100 μM) did not enhance nor decrease neuronal viability (**Figure 5.4, Figure 5.5**). Since all treatments contained NMDA, another assay was done in order to determine if CNS4 (100 μM) by itself could alter neuronal viability compared to untreated primary cortical and striatal neurons (**Figure 5.6**). The results did not show a statistical difference, leading us to think that CNS4 does not alter viability in untreated primary neurons and that the decreases in viability, compared to control, observed in **Figure 5.4** and **Figure 5.5** is due to presence of high doses of NMDA (100 μM). This is concordant with the fact that NMDAR hyperactivation by NMDA synthetic agonist leads to toxicity and neuronal death¹³¹.

CONCLUSION

NMDAR participate in many physiological and pathological conditions and different subunits exhibit unique features in neuroprotection and neurotoxicity¹²⁶. Many disorders are associated with NMDAR-mediated excitotoxicity like Autism, PD, and SCZ^{12,57,65}. For this reason, there is a need to find compounds that interact with NMDAR without completely blocking the receptor like antagonists do since it can compromise physiological synaptic functions¹³⁰.

To better understand the effect of the compound CNS4 in neurons with ongoing excitotoxicity, a primary brain culture was made in cortical neurons with predominately

GluN2A and GluN2B expression and striatal neurons with predominant GluN2C and GluN2D expression^{11,14,15}.

Quantification of calcium uptake was measured in both cortical and striatal regions. In both regions, NMDA doses of 300 μ M increased Ca²⁺ uptake compared to control (**Figure 5.2** and **Figure 5.3**). In cortex, when NMDA (300 μ M) was used with CNS4 (100 μ M) a significant increase in Ca²⁺ uptake was observed compared with NMDA (300 μ M) alone (**Figure 5.2**) and in the striatal region, CNS4 (100 μ M) increased Ca²⁺ uptake in company of both 100 and 300 μ M NMDA (**Figure 5.3**) compared to NMDA alone, suggesting that CNS4 facilitates NMDA-induced Ca²⁺ influx.

In the MTS assay, CNS4 did not alter neuronal viability in either cortical nor striatal neurons compared with NMDA alone (**Figure 5.4, Figure 5.5**). Since all treatments contained NMDA, another assay was done in order to determine if CNS4 (100 μ M) by itself could alter neuronal viability. The results did not show a statistical effect in either region (**Figure 5.6**), leading us to think that the decrease in viability in the previous assay was due to the presence of high doses (100 μ M) of NMDA. This is concordant with the fact that NMDAR hyperactivation by NMDA synthetic agonist leads to toxicity and neuronal death¹³¹.

CORTEX

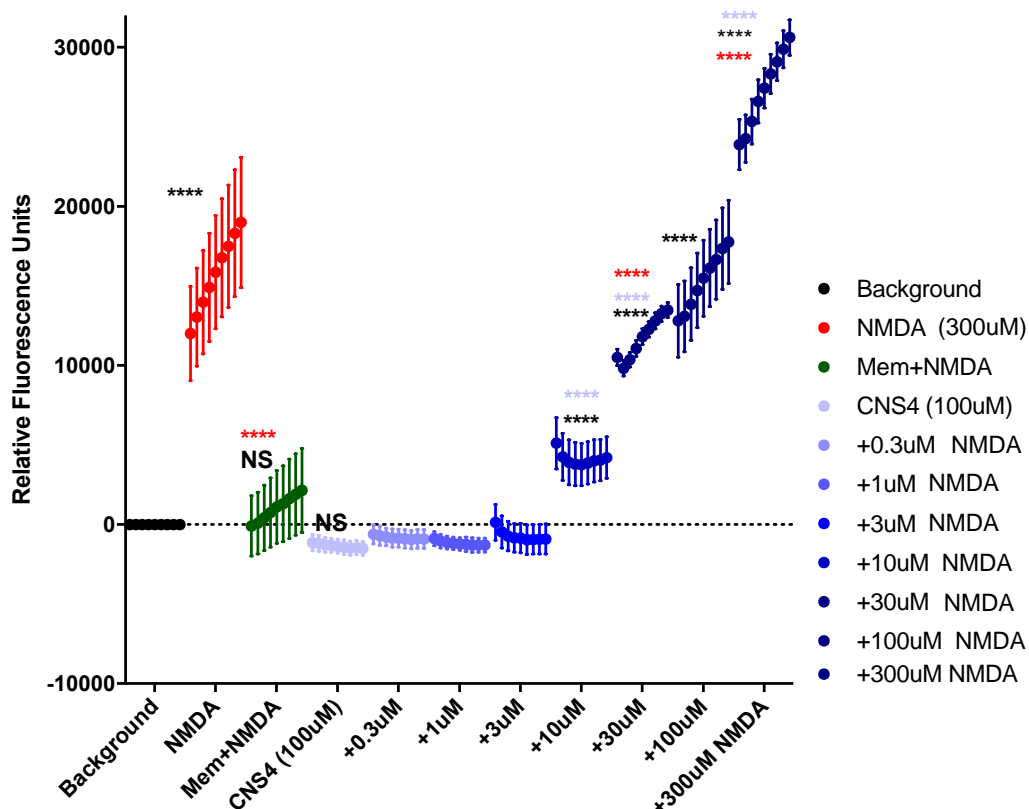


Figure 5. 2 Cortex Ca²⁺ assay in neurons with increasing doses of NMDA and constant (100μM) CNS4. Every treatment group has eight dots representing the eight wells of every column of the 96 well plate. Color of stars on top of the dots represent the group that is being compared with. The presence of CNS4 (100μM) alone did not alter Ca²⁺ uptake compared to control, however, it increased Ca²⁺ uptake when used with NMDA (300μM) compared with NMDA (300μM) alone. Statistical difference was determined at the alpha level $p < 0.05(*)$ using one way ANOVA with Tukey's multiple comparisons.

• •

STRIATUM

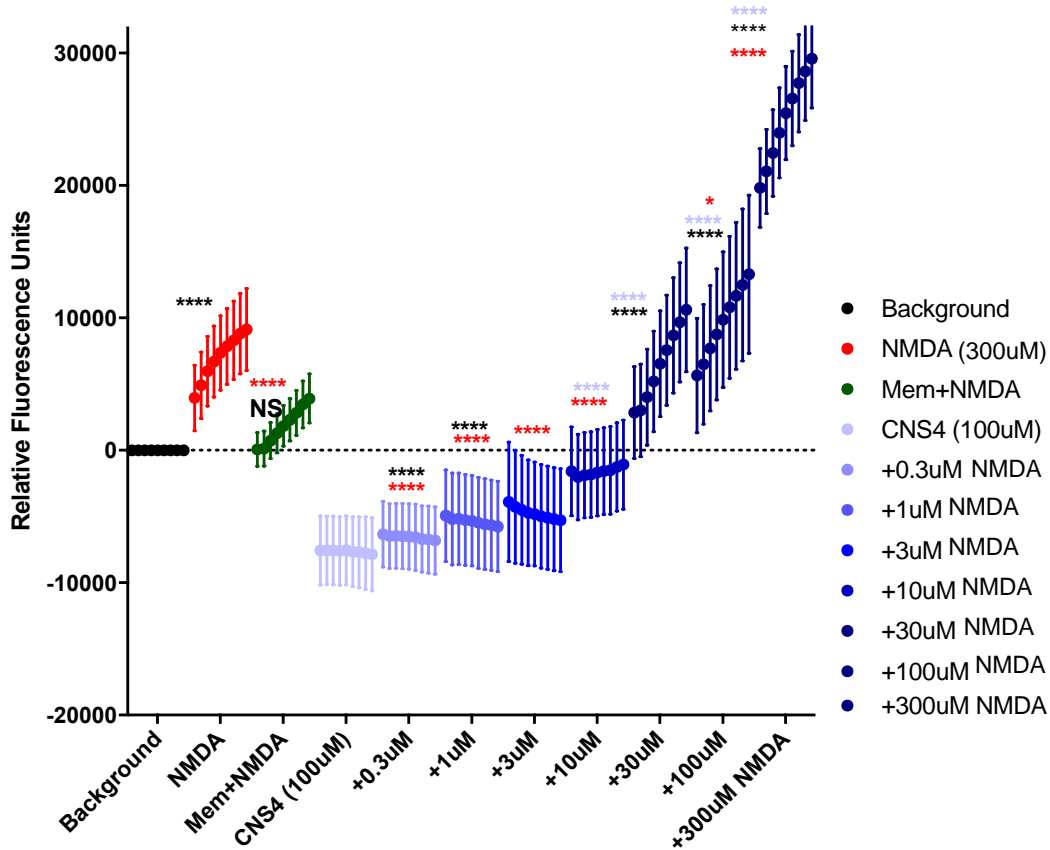


Figure 5. 3 Striatum Ca²⁺ assay in neurons with increasing doses of NMDA and constant 100μM CNS4. Every treatment group has eight dots representing the eight wells of every column of the 96 well plate. Color of stars on top of the dots represent the group that is being compared with. The presence of CNS4 (100μM) alone did not alter Ca²⁺ uptake compared to control, however, it increased Ca²⁺ uptake when used with NMDA (100μM and 300μM) compared to NMDA (300μM) alone. Statistical difference was determined at the alpha level $p < 0.05$ (*) using one way ANOVA with Tukey’s multiple comparisons.

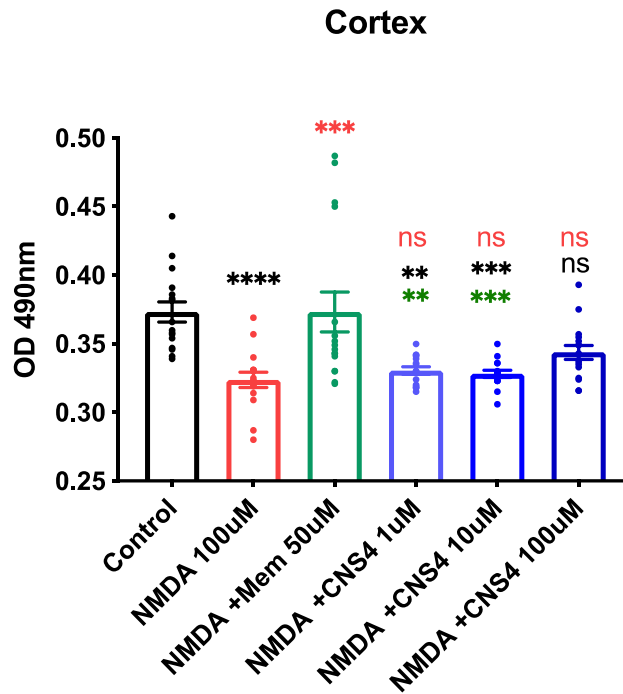


Figure 5. 4 Cortex MTS Assay. Y axis represents quantification of cellular metabolic activity measured by OD at 490nm. X axis represents treatment groups and color of stars represents the group that is being compared with. NMDA (100µM) reduced metabolic activity in neurons compared with control. Increasing doses of CNS4 (1, 10 and 100µM) with NMDA (100µM) did not have an effect in neuronal viability compared with NMDA (100µM) alone. Statistical differences were analyzed by comparing means of every treatment group with ANOVA followed Tukey’s multiple comparisons test at the alpha level $p < 0.05$ (*).

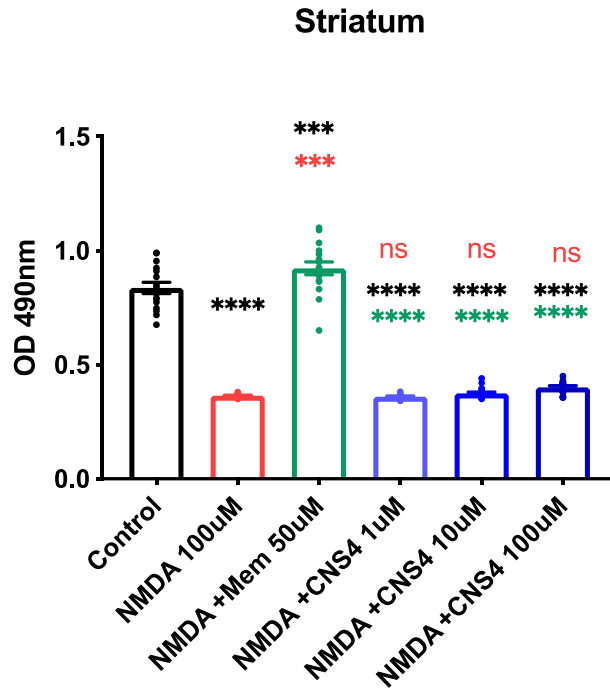


Figure 5. 5 Striatum MTS Assay. Y axis represents quantification of cellular metabolic activity measured by OD at 490nm. X axis represents treatment groups and color of stars represents the group that is being compared with. NMDA (100µM) reduced metabolic activity in neurons compared with control and memantine (50 µM) increased it. Increasing doses of CNS4 (1, 10 and 100µM) with NMDA (100µM) did not have an effect in neuronal viability compared with NMDA (100µM) alone. Statistical differences were done comparing means of every treatment group with ANOVA Tukey’s multiple comparisons test at the alpha level $p < 0.05$ (*)

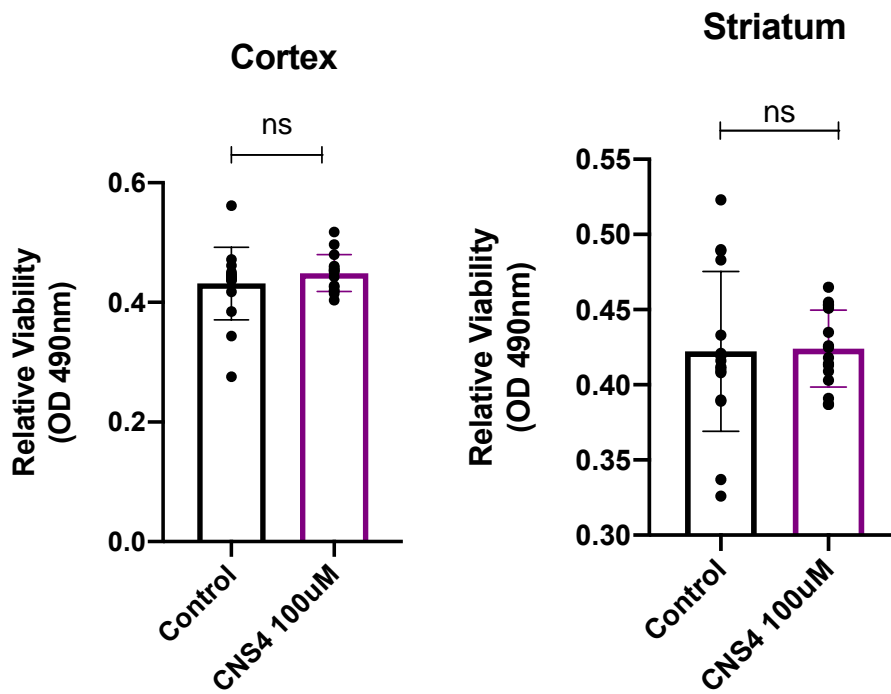


Figure 5. 6 Cortex and Striatum MTS assay in untreated neurons versus 100 μ M CNS4.

Statistical difference was determined with unpaired T-Test at alpha level of $P < 0.005$

CHAPTER 6: CONCLUSION

NMDAR participate in many physiological and pathological conditions and different subunits exhibit unique features in neuroprotection and neurotoxicity¹²⁶. Many disorders are associated with NMDAR-mediated excitotoxicity when excessive glutamate activates the receptor like Autism, PD, and SCZ^{12,57,65}. Substantial efforts have been made to develop compounds that select distinct GluN2 subunits minimizing overall NMDAR hyperactivation that is linked with several disorders¹²². The search for compounds with increased subunit selectivity is ideal since those compounds might decrease the probability of global NMDAR activation which could lead to alteration in normal receptor function^{65,112}. In this project, we studied the effect of the compound CNS4 (**Figure 3.1**) in NMDAR diheteromeric receptors.

The first part of the project used two-electrode clamp electrophysiology to determine the dose response activity of CNS4 using different glutamate concentrations named Agonist (0.3 μ M glu/ 100 μ M gly), Agonist max (100 μ M glu/ 100 μ M gly) and Agonist super max (300 μ M glu / 100 μ M gly) in NMDA diheteromeric receptors (GluN2A, GluN2B, GluN2C and GuN2D) and measuring ionic current. Using Agonist solution, 100 μ M of CNS4 significantly produced an increase in relative response compared with Agonist alone in all subunits and 30 μ M of CNS4 was enough to significantly increase the response in GluN2C and GluN2D subunits (**Figure 3.3**). With Agonist max solution 30 μ M and 100 μ M of CNS4 produced a significant increase in relative response compared with Agonist max solution alone for GluN2D, while 1 μ M produced a significant decrease for GluN2D (**Figure 3.6**). When using Agonist super max 30 μ M and 100 μ M of CNS4

significantly reduced relative response in the GluN2D subunit when compared with Agonist super max solution alone (**Figure 3.9**) but did not produce significant changes for any of the other subunits. This first set of recordings lead us to conclude that the compound exhibited a dose-dependent activity in diheteromeric NMDAR based on glutamate concentration.

Another set of recordings was made to determine how CNS4 will interact in the receptors in the absence of either glutamate or glycine compared with both native transmitters together in the absence of CNS4. The Agonist max solution was used in the GluN2A and GluN2B subunits followed by the application of either glutamate (100 μ M) or glycine (100 μ M) in the presence and absence of CNS4 (100 μ M). At the GluN2A subunit, CNS4 decreased the relative response when used with glutamate compared with glutamate alone (**Figure 3.12**) and produced the opposite effect in the GluN2B subunit increasing the relative response when used with glutamate compared with glutamate alone (**Figure 3.13**). CNS4 did not appear to numerically potentiate the GluN2A and GluN2B subunits to the same response level as when using Agonist max when used in company of either glutamate or glycine alone. This finding corroborates the inability of CNS4 to replace either glutamate or glycine based on the reduction of relative response when used with glu alone at the NMDAR. Furthermore, it cannot be classified as an agonist compound. CNS4 can be labeled as an allosteric modulator that also behaves differently with distinct glutamate concentrations and exhibits NMDAR subunit selectivity.

In order to understand how CNS4 alters the ions inward and outward current a second set of electrophysiological recordings was made. This time, instead of changing solutions with different glutamate concentration, a manual change in membrane holding potential

was done (from -90mV to +30 mV) in order to recreate membrane depolarization which normally expels a Mg^{2+} ion block from NMDAR and allows ion flow across the membrane. Changes in reversal potential in the presence of CNS4 were studied helping us determine changes in the membrane holding potential at which there is no net ion flow across the receptor . This comparison was made in the presence and absence of Mg^{2+} . Using Agonist solution, the presence of CNS4 significantly decreased the reversal potential in the GluN2C (**Figure 4.4**) and GluN2D (**Figure 4.5**) subunits, and non significant change was observed in the GluN2A (**Figure 4.2**) and GluN2B (**Figure 4.3**) subunit. And when using Agonist max solution a significant difference in reversal potential was only observed in the GluN2C subunit (**Figure 4.8**). Numerical decreases in reversal potential findings suggest that inward current of ions in presence of CNS4 occurs with more positive membrane holding potentials in manual depolarization. Additionally in all diheteromeric subunits and with both Agonist solutions, CNS4 in the absence of Mg^{2+} was unable to mimick the blockage seen when Mg^{2+} is used alone suggesting the possibility that CNS4 alone is unable to block the channel pore. Overall, in the current voltage plot it can also be observed that the linear-like relationship between the y axis (current) and x axis (voltage) for CNS4 with any of the solutions given, and in all diheteromeric subunits, suggests a lack of voltage-dependent activity of this compound. And finally, CNS4-induced significant differences in reversal potential among diheteromeric subunits varied based on the amount of glutamate used, corroborating the findings from the dose response assay made in Chapter 3 in which a glutamate dose dependent activity of CNS4 is found.

A final experiment was performed to better understand the effect of CNS4 on Ca^{2+} uptake and the effect of CNS4 in neurons that were given excessive doses of synthetic agonist NMDA in order to hyperactivate native NMDAR. To do so, a primary brain culture was made from cortical neurons with predominately GluN2A and GluN2B expression and striatal neurons with predominant GluN2C and GluN2D expression^{11,14,15}.

Quantification of calcium uptake was measured in both cortical and striatal regions. In cortex, when NMDA (300 μM) was used with CNS4 (100 μM) a significant increase in Ca^{2+} uptake was observed compared with NMDA (300 μM) alone (**Figure 5.2**) and in the striatal region, CNS4 (100 μM) increased Ca^{2+} uptake in company of both 100 and 300 μM NMDA (**Figure 5.3**) compared to NMDA alone, suggesting that CNS4 facilitates NMDA-induced Ca^{2+} influx.

In the MTS assay, CNS4 did not alter neuronal viability in either cortical nor striatal neurons compared with NMDA alone (**Figure 5.4, Figure 5.5**). Since all treatments contained NMDA, another assay was done in order to determine if CNS4 (100 μM) by itself could alter neuronal viability. The results did not show a statistical effect in either region (**Figure 5.6**), leading us to think that the decrease in viability in the previous assay was due to the presence of high doses (100 μM) of NMDA. This is concordant with the fact that NMDAR hyperactivation by NMDA synthetic agonist leads to toxicity and neuronal death¹³¹.

REFERENCES

1. Burnashev N, Szepietowski P (2017) NMDA receptors methods and protocols. Mairselle, France: Humana Press, 11-20
2. Hashimoto K (2017) The NMDA receptors. Malta, Italy: Series editor, 11-15
3. Popescu G. (2016) Ionotropic glutamate receptor technologies. New York, USA: Humana press, 45-70.
4. Bledsoe D, Tamer C, Mesic I, Madry C, Klein B, Laube B and Costa BM (2017) Positive Modulatory Interactions of NMDA Receptor GluN1/2B Ligand Binding Domains Attenuate Antagonist Activity. *Frontiers in Pharmacology*. 8;229
5. Alvin Y and Albert L (2018) Glutamate and Glycine Binding to the NMDA Receptor. *Structure*; 26, 1035-1043
6. Mayer M (2017) The Challenge of Interpreting Glutamate-Receptor Ion-Channel Structures. *Biophysical Journal*; 113, 2143- 2151
7. Burnell E, Irvine M, Fang G, Sapkota K, Jane D and Monaghan D (2019) Positive and Negative Allosteric Modulators of N-Methyl-D-aspartate (NMDA) Receptors: Structure- Activity Relationships and Mechanisms of Action. *Journal of Medicinal Chemistry*; 62, 3-23
8. Hayashi T, Thomas G and Haganir R (2009) Dual Palmitoylation of NR2 Subunits Regulates NMDA Receptor Trafficking. *Neuron*; 64, 213-226
9. Burnashev N, Schoepfer R, Monyer H, Ruppersberg P, Günther W, Seeburg P and Sakmann B (1992) Control by Asparagine Residue of Calcium Permeability and Magnesium Blockade in the NMDA Receptor. *Science*; 257, 1415.
10. Ulbrich M and Isacoff E (2007) Subunit counting in membrane-bound proteins. *Nature Methods*; 4(4), 319-321.
11. Paoletti P (2011) Review Molecular Basis of NMDA receptor functional diversity. *European Journal of Neuroscience*; 33, 1351- 1365.
12. Paoletti P, Bellone C and Zhou Qiang (2013) NMDA receptor subunit diversity: impact on receptor properties, synaptic plasticity and disease. *Nature Reviews*;14, 383- 400
13. Wollmuth L and Sobolevsky A (2004) Structure and gating of the glutamate receptor ion channel. *Trends in Neuroscience*; 27 [6], 321- 328

14. Akazawa C, Shigemoto R, Bessho Y, Nakanishi S and Mizuno N (1994) Differential Expression of Five N-Methyl-D-Aspartate Receptor Subunit mRNAs in the Cerebellum of Developing and Adult Rats. *The Journal of Comparative Neurology*; 347, 150- 160
15. Law A, Weickert C, Webster M, Herman M, Kleinman J and Harrison Paul (2003) Expression of NMDA receptor NR1, NR2A and NR2B subunit mRNAs during development of the human hippocampal formation. *European Journal of Neuroscience*; 18, 1197- 1205
16. Cull-Candy S, Brickley S and Farrant Mark (2001) NMDA receptor subunits: diversity, developmental and disease. *Current Opinion in Neurobiology*; 11(3), 327- 335
17. Cull-Candy S and Leszkiewicz D (2004) Role of Distinct NMDA Receptor Subtypes at Central Synapses. *Sciences STKE*; 255 (16), 1-9
18. Glasgow N, Retchless B and Johnson J (2015) Molecular bases of NMDA receptor subtype-dependent properties. *The Journal of Physiology*; 593(1), 83- 95
19. Traynelis S, Wollmuth L, McBain C, Menniti F, Vance K, Ogden K, Hansen K, Yuan H, Myers S and Dingledine R (2010) Glutamate Receptor Ion Channels: Structure, Regulation, and Function. *Pharmacological Reviews*; 62, 405-496
20. Quick M and Lester R (2002) Desensitization of Neuronal Nicotinic Receptors. *Journal of Neurobiology*; 1(53), 457- 478
21. Lüscher C and Malenka R (2012) NMDA Receptor-Dependent Long-Term Potentiation and Long-Term Depression (LTD/LTD). *Cold Spring Harbor Perspectives in Biology*; 4(6), 1- 15
22. Castillo P (2012) *Cold Spring Harbor perspectives in biology*; 4 (2), 1- 23
23. Malenka R and Bear M (2004) LTP and LTD: An Embarrassment of Riches. *Neuron*; 44, 5-21
24. Brecht D and Nicoll R (2003) AMPA Receptor Trafficking at Excitatory Synapses. *Neuron*; 40, 361-379
25. Dudek S and Bear M (1992) Homosynaptic long-term depression in area CA1 of hippocampus and effects of N-methyl-D-aspartate receptor blockage. *Neurobiology*; 89, 4363- 4367
26. Hrabetova S, Serrano P, Blace N, Tse H, Skifter D, Jane D, Monaghan D and Charlton T (2000) Distinct NMDA Receptor Subpopulations Contribute to Long-Term Potentiation and Long-Term Depression Induction. *The Journal of Neuroscience*; 20, 1-6
27. Van Dam E, Ruiter B, Kamal A, Ramakers G, Gispen W and Graan P (2002) N-methyl-D-aspartate-induced long-term depression is associated with a decrease in postsynaptic protein kinase C substrate phosphorylation in rat hippocampal slices. *Neuroscience letters*; 320, 129- 132
28. Lee H, Barbarosie M, Kameyama K, Bear M and Huganir R (2002) Regulation of distinct AMPA receptor phosphorylation sites during bidirectional synaptic plasticity. *Letters to nature*; 405, 955- 959
29. Kleckner N and Dingledine R (1988) Requirement for Glycine in activation of NMDA-Receptors Expressed in *Xenopus* Oocytes. *Science*; 241, 835-837

30. Inanobe A, Furukawa H and Gouaux E (2005) Mechanism of Partial Agonist Action at the NR1 Subunit of NMDA Receptors. *Neuron*; 47, 71-84
31. Panatier A, Theodosis D, Mothet J, Touquet B, Pollegioni L, Poulain D and Oliet S (2006) Glia-Derived D-Serine Controls NMDA Receptor Activity and Synaptic Memory. *Cell*; 125, 775- 784
32. Basu A, Tsai G, Ma C, Ehmsen J, Mustafa A, Han L, Jiang Z, Benneyworth M, Froimowitz M, Lange N, Snyder S, Bergeron R and Coyle J (2009) Targeted disruption of serine racemase affects glutamatergic neurotransmission and behavior. *Molecular Psychiatry*; 14, 719- 727
33. Sheinin A, Shavit S and Benveniste M (2001) Subunit specificity and mechanism of action of NMDA partial agonist D-cycloserine. *Neuropharmacology*; 41, 151- 158
34. Chen P, Geballe M, Katz E, Errenger K, Livesey M, O'Toole K, Le P, Lee J, Snyder J, Traynelis S and Wyllie D (2008) *The Physiological Society*; 586 (1), 227- 245
35. Errico F, Rossi S, Napolitano F, Catuogno V, Topo E, Fisone G, D'Aniello A, Centonze D and Usiello A (2008) D-Aspartate Prevents Corticostriatal Long-Term Depression and Attenuates Schizophrenia-Like Symptoms Induced by Amphetamine and MK-801. *The Journal of Neuroscience*; 28 (41), 10404-10414
36. Zhang X and Nadler V (2009) Postsynaptic response to stimulation of the Schaffer collaterals with properties similar to those of synaptosomal aspartate release. *Brain Research*; 1295, 13-20
37. Clausen R, Christensen C, Hansen K, Greenwood J, Jorgensen L, Micale N, Madsen J, Nielsen B, Egebjerg J, Brauner-Osborne H, Traynelis S and Kristensen J (2008) N-Hydroxypyrazolyl Glycine Derivates as Selective N-Methyl-D-aspartic Acid Receptor Ligands. *Journal of Medicinal Chemistry*; 51 (14), 4179- 4187
38. Yao Y, Harrison C, Freddolino P, Schulten K and Mayer M (2008) Molecular mechanism of ligand recognition by NR3 subtype glutamate receptors. *The EMBO Journal*; 27, 2158- 2170
39. Furukawa H and Gouaux E (2003) Mechanisms of activation, inhibition and specificity: crystal structures of the NMDA receptor NR1 ligand-binding core. *The EMBO Journal*; 22 (12), 2873- 2885
40. Kutsuwanda T, Kashibuchi N, Mori H, Sakimura K, Kushiya E, Araki K, Meguro H, Masaki H, Kumanishi T, Arakawa M and Mishina M (1992) Molecular diversity of the NMDA receptor channel. *Nature*; 358, 36- 41
41. Dravid S, Erreger K, Yuan H, Nicholson K, Le P, Lyboslavsky P, Almonte A, Murray E, Mosley C, Barber J, French A, Balster R, Murray T and Traynelis S (2007) Subunit-specific mechanisms and proton sensitivity of NMDA receptor channel block. *Journal of Physiology*; 581, 107- 128
42. Clausen R, Christensen C, Hansen K, Greenwood J, Jorgensen L, Micale N, Madsen J, Nielsen B, Egebjerg J, Brauner-Osborne H, Traynelis S and Kristensen J (2008) N-Hydroxypyrazolyl Glycine Derivates as Selective N-Methyl-D-aspartic Acid Receptor Ligands. *Journal of Medicinal Chemistry*; 51, 4179- 4187

43. Dickinson R, Peterson B, Banks P, Simillis C, Sacristan M, Valenzuela C, Maze M and Franks N (2007) Competitive Inhibition at the Glycine Site of the N-Methyl-D-aspartate Receptor by the Anesthetics Xenon and Isoflurane. *Anesthesiology*; 107, 756- 767
44. Furukawa H, Singh S, Mancusso R and Gouaux E (2005) Subunit arrangement and function in NMDA receptors. *Nature*; 438, 185- 192
45. Feng B, Tse H, Skifter D, Morley R, Jane D and Monaghan D (2004) Structure-activity analysis of a novel NR2C/ NR2D-preferring NMDA receptor antagonist: 1-(phenanthrene-2-carbonyl) piperazine-2,3-dicarboxylic acid. *British Journal of Pharmacology*; 141, 508- 516
46. Prorok M and Castellino F (1998) Thermodynamics of Binding of Calcium, Magnesium, and Zinc to the N-Methyl-D-aspartate Receptor Ion Channel Peptidic Inhibitors, Conantokin-G and Conantokin-T. *The Journal of Biological Chemistry*; 273 (31), 19573- 19578
47. Gallagher M, Huang H, Pritchett D and Lynch D (1996) Interactions between Ifenprodil and the NR2B Subunit of the N-Methyl-D-aspartate Receptor. *The Journal of Biological Chemistry*; 271 (16), 9603- 9611
48. Barton M and White S (2004) The effect of CGX-1007 and CI-1041, novel NMDA receptor antagonists, on kindling acquisition and expression. *Epilepsy Research*; 59, 1-12
49. Lovinger D, White G and Weight F (1989) Ethanol Inhibits NMDA-Activated Ion Current in Hippocampal Neurons. *Science*; 243 (4899), 1721- 1724
50. Woods A, Kaminski R, Oz M, Wang Y, Hauser K, Goody R, Wang H, Jackson S, Zeitz P, Zeitz K, Zolkowska D, Schepers R, Nold M, Danielson J, Graslund A, Vukojevic V, Bakalkin G, Basbaum A and Shippenberg T (2006) Decoy Peptides that Bind Dynorphin Noncovalently Prevent NMDA Receptor-Mediated Neurotoxicity. *Journal of Proteome Research*; 5, 1017- 1023
51. Parsons C, Quack G, Bresink I, Baran L, Przegalinski E, Kostowski W, Krzascik P, Hartmann S and Danysz W (1995) Comparison of the Potency, Kinetics and Voltage-dependency of a Series of Uncompetitive NMDA Receptor Antagonist In Vitro with Anticonvulsive and Motor Impairment Activity In Vivo. *Neuropharmacology*; 34 (10), 1239- 1258
52. Paoletti P, Vergnano A, Barbour B and Casado M (2009) Zinc at Glutamatergic Synapses. *Neuroscience*; 158, 126- 136
53. Gielen M, Siegler B, Mony L, Johnson J and Paoletti P (2009) Mechanism of differential control of NMDA receptor activity by NR2 subunits. *Nature*; 459 (4), 703- 709
54. Han X, Tomitori H, Mizuno S, Higashi K, Full C, Fukiwake T, Terui Y, Leewanich P, Nishimura K, Toida T, Williams K, Kashiwagi K and Igarashi K (2008) Binding of spermine and ifenprodil to a purified, soluble regulatory domain of the N-methyl-D-aspartate receptor. *Journal of Neurochemistry*; 107, 1566- 1577
55. Kussius C, Kaur N and Popescu G (2009) Pregnanolone Sulfate Promotes Desensitization of Activated NMDA Receptors. *The Journal of Neuroscience*; 29, 6819- 6827

56. Miller B, Sarantis M, Traynelis S and Attwell D (1992) Potentiation of NMDA receptor currents by arachidonic acid. *Nature*; 355, 722- 725
57. Weita T, Shyu W and Wang Y (2011) Stroke intervention pathways: NMDA receptors and beyond. *Cell Press*; 17 (5), 266- 275
58. Wu Land Zhuo M (2009) Targeting the NMDA Receptor Subunit NR2B for the Treatment of Neuropathic Pain. *The American Society for Experimental NeuroTherapeutics*; 6, 693- 702
59. Malinow R (2012) New developments on the role of NMDA receptors in Alzheimer's disease. *Current Opinion in Neurobiology*; 22, 559- 563
60. Milnerwood A, Gladding C, Pouladi M, Kaufman A, Hines R, Boyd J, Ko R, Vasuta O, Graham R, Hayden M, Murphy T and Raymond L (2010) Early Increase in Extrasynaptic NMDA Receptor Signaling and Expression Contributes to Phenotype Onset in Huntington's Disease Mice. *Neuron*; 65, 178- 190
61. Zhang Z, Shang S, Fu P, Zhang Z, Lin, K, Ko J and Yung K (2019) Roles of Glutamate Receptors in Parkinson's Disease. *International Journal of Molecular Sciences*; 20, 1- 17
62. Zarate C, Singh J, Quiroz J, De Jesus G, Denicoff K, Luckenbaugh D, Manji H and Charney D (2006) A Double-Blinded, Placebo-Controlled Study of Memantine in the Treatment of Major Depression. *The American Journal of Psychiatry*; 163, 153- 155
63. Li N, Lee B, Li R, Banasr M, Dwyer J, Iwata M, Li X, Aghjanian G and Duman R (2010) mTOR-Dependent Synapse Formation Underlies the Rapid Antidepressant Effects of NMDA Antagonists. *Science*; 329 (5994), 959- 964
64. Autry A, Adachi M, Nosyreva E, Na E, Los M, Cheng P, Kavalali E and Monteggia L (2011) NMDA receptor blockage at rest triggers rapid behavioral antidepressant responses. *Nature*; 475, 91- 97
65. Henson M, Roberts A, Perez-Otano I and Philpot Benjamin (2010) Influence of the NR3A subunit on NMDA receptor functions. *Progress in Neurobiology*; 91, 23- 37
66. Lipton S (2004) Failures and Successes of NMDA Receptor Antagonists: Molecular Basis for the Use of Open-Channel Blockers like Memantine in the Treatment of Acute and Chronic Neurologic Insults. *NeuroRx: The Journal of the American Society for Experimental NeuroTherapeutics*; 1, 101- 110
67. Pachernegg S, Strutz-Seebohm N and Hollmann M (2011) GluN3 subunit-containing NMDA receptors: not just one-trick ponies; 35 (4), 240- 247
68. Won H, Lee H, Gee H, Mah W, Kim J, Lee J, Ha S, Chung C, Jung E, Cho Y, Park S, Lee J, Lee K, Kim D, Bae Y, Kaang B, Lee M and Kim E (2012) Autistic-like social behaviour in Shank2-mutant mice improved by restoring NMDA receptor function. *Nature*; 486, 261- 265
69. Berkel S, Marshall C, Weiss B, Howe J, Roeth R, Moog U, Endris V, Roberts W, Szatmari P, Pinto D, Bonino M, Riess A, Engels H, Sprengel Rm Scherer S and Rappold G (2010) Mutations in the SHANK2 synaptic scaffolding gene in autism spectrum disorders and mental retardation. *Nature Genetics*; 42 (6), 489- 491

70. Schmeisser M, Ey E, Wegener S, Bockmann J, Stempel A, Kuebler A, Janssen A, Uvardi P, Shiban E, Spilker C, Balschum D, Skryabin B, Dieck S, Smalla K, Montag D, Leblond C, Faure P, Torquet N, Le Sourd A, Toro R, Grabrucker A, Schoichet S, Schmitz D, Kreutz M, Bourgeron T, Gundelfinger E and Boeckers T (2012) Autistic-like behaviours and hyperactivity in mice lacking ProSAP2/Shank2. *Nature*; 486, 256- 261
71. Tovar K, Sprouffske K and Westbrook G (2000) Fast NMDA Receptor-Mediated Synaptic Currents in Neurons from Mice Lacking the NR2B Subunit. *Journal of Neurophysiology*; 83 (1), 616- 620
72. Clayton D, Mesches M, Alvarez E, Bickford P and Browning M (2002) A Hippocampal NR2B Deficit Can Mimic Age-Related Changes in Long-Term Potentiation and Spatial Learning in the Fischer 344 Rat. *The Journal of Neuroscience*; 22 (9), 3628- 2637
73. Magnusson K, Brim B and Das S (2010) Selective vulnerabilities of N-methyl-D-aspartate (NMDA) receptors during brain aging. *Frontiers in Aging Neuroscience*; 2 (11), 1- 15
74. Magnusson K, Scruggs B, Zhao X and Hammersmark R (2007) Age-related declines in a two-day reference memory task are associated with changes in NMDA receptor subunits in mice. *BMC Neuroscience*; 8 (43), 1- 13
75. Castorina M, Ambrosini A, Pacifici L, Ramacci M and Angelucci L (1994) Age-Dependent Loss of NMDA Receptors in Hippocampus, Striatum and Frontal Cortex of the Rat: Prevention By Acetyl-L-Carnitine. *Neurochemical Research*; 19 (7), 795- 798
76. Wu Y and Johnson S (2015) Memantine selectively blocks extrasynaptic NMDA receptors in rat substantia nigra dopamine neurons. *Brain Research*; 1(603), 1-7
77. Martinez B, Paniagua M, Fernandez A and Calvo P (2006) Effect of d-aminolevulinic acid and vitamin E treatments on the N-methyl-D-aspartate receptor at different ages in the striatum of rat brain. *Brain Research*; 1114, 19- 23
78. Beracochea D, Boucard A, Tromcme-Thibierge C and Morain P (2008) Improvement of contextual memory by S 24795 in aged mice: comparison with memantine. *Psychopharmacology*; 196, 555- 564
79. Moghaddam B and Javitt D (2012) From Revolution to Evolution: The Glutamate Hypothesis of Schizophrenia and its Implication for Treatment. *Neuropsychopharmacology*; 37, 4- 15.
80. Mohn A, Gainetdinow R, Caron M and Koller B (1999) Mice with Reduced NMDA Receptor Expression Display Behaviors Related to Schizophrenia. *Cell*; 98, 427- 436
81. Woo T, Walsh J and Benes F (2004) Density of Glutamic Acid Decarboxylase 67 Messenger RNA-Containing Neurons That Express the N-Methyl-D-Aspartate Receptor Subunit NR2A in the Anterior Cingulate Cortex in Schizophrenia and Bipolar Disorder. *Archives of Genetic Psychiatry*; 61, 649- 657
82. Lakhan S, Caro M and Hadzimichalis N (2013) NMDA receptor activity in neuropsychiatric disorders. *Frontiers in Psychiatry*; 4 (52), 1-8

83. Dalmau J, Gleichman A, Hughes E, Rossi J, Peng X, Lai M, Dessain S, Rosenfeld M, Balice-Gordon R and Lynch D (2008) Anti-NMDA-receptor encephalitis: case series and analysis of the effects of antibodies. *The Lancet*; 7, 1091- 1098
84. Hughes E, Peng X, Gleichman A, Lai M, Tsou R, Parsons T, Lynch D, Dalmau J and Balice-Gordon R (2010) Cellular and Synaptic Mechanism of Anti-NMDA Receptor Encephalitis. *The Journal of Neuroscience*; 30 (17), 5866, 5875
85. Mikasova L, De Rossi P, Bouchet D, Georges F, Rogemond V, Didelot A, Meissirel C, Honnorat J and Groc L (2012) Disrupted surface cross-talked between NMDA and Ephrin-B2 receptors in anti-NMDA encephalitis. *Brain*; 135, 1606- 1621
86. Dalva M, Takasu M, Lin M, Shamah S, Hu L, Gale N and Greenberg M (2000) EphB Receptors Interact with NMDA Receptors and Regulate Excitatory Synapse Formation. *Cell*; 103, 945- 956
87. Taraschenko O, Fox H, Pittock S, Zekeridou A, Gafurova M, Eldridge E, Liu J, Dravid S and Dingleline R (2019) A mouse model of seizures in anti-N-methyl-D-aspartate receptor encephalitis. *Epilepsy*; 60, 452- 463
88. Kaiser L, Schuff N, Cashdollar N and Weiner M (2005) Age-related glutamate and glutamine concentration changes in normal human brain: H MR spectroscopy study at 4T. *Neurobiology Aging*; 26(5), 665- 672
89. Benedetti M, Marrari P, Cini M, Prada M and Dostert P (1990) The effects of lifelong treatment with MAO inhibitors on amino acid levels in rat brain. *Journal of Neural Transmission*; 2, 239- 248
90. Heath P and Shaw P (2002) Update on the Glutamatergic Neurotransmitter system and the role of excitotoxicity in Amyotrophic Lateral Sclerosis. *Muscle and Nerve*; 26(4), 438- 458
91. Moussawi K, Riegel A, Nair S and Kalivas (2011) Extracellular glutamate: Functional compartments operate in different concentration ranges. *Frontiers in System Neuroscience*; 5 (94), 1-9
92. Featherstone D and Shippy S (2008) Regulation of Synaptic Transmission by ambient Extracellular Glutamate. *The Neuroscientist*; 14 (2), 171- 181
93. Montana V, Malarkey E, Verderio C, Matteoli M and Parpura V (2006) Vesicular Transmitter Release from Astrocytes. *Glia*; 54, 700- 715.
94. Parpura V, Scemes E and Spray D (2004) Mechanisms of glutamate release from astrocytes: gap junction “hemichannels”, purinergic receptors and exocytotic release. *Neurochemistry International*; 45, 259- 264.
95. Buchanan R, Darrow D, Meier K, Robinson J, Schiehser D, Glahn D and Nadasdy Z (2014) Changes in GABA and glutamate concentrations during memory tasks in patients with Parkinson’s disease undergoing DBS surgery. *Frontiers in Human Neuroscience*; 8 (81), 1- 8.
96. Charousaei A, Nasehi M, Babapour V, Vasehi S and Zarrindast M (2020) The effect of 5-HT4 serotonin receptors in the CA3 hippocampal region on D-AP-5-induced anxiolytic-like effects: isobolographic analyses. *Brain Research Bulletin*; 20, 1- 34.

97. Lodge D, Watkins J, Bortolotto Z, Jane D and Volianskis A (2019) The 1980s: D-AP5, LTP and a Decade of NMDA Receptor Discoveries. *Neurochemical Research*; 44, 516- 530.
98. Tajima N, Karakas E, Grant T, Simorowski N, Diaz-Alvalos R, Griforieff N and Furukawa H (2016) Activation of NMDA receptors and the mechanism of inhibition by ifenprodil. *Nature*; 534, 63- 69.
99. Perin-Dureau F, Rachline J, Neyton J and Paoletti P (2002) Mapping the Binding Site of the Neuroprotectant Ifenprodil on NMDA Receptors. *The Journal of Neuroscience*; 22 (14), 5955- 5965
100. Kalmoe M, Janski A, Zorumski C, Nagele P, Palanca B and Conway C (2020) Ketamine and nitrous oxide: The evolution of NMDA receptor antagonist as antidepressant agents. *The Journal of Neurological Sciences*; 412, 1- 8.
101. Johnson J and Kotermanski S (2006) Mechanism of action of Memantine. *Current Opinion in Pharmacology*; 6, 61- 67.
102. Sharp F, Tomitaka M, Bernaudin M and Tomitaka S (2001) Psychosis: Pathological activation of limbic thalamocortical circuits by psychomimetics and schizophrenia. *Trends in Neurosciences*; 24 (6), 330- 334.
103. Sonkusare S, Kaul C and Ramarao P (2005) Dementia of Alzheimer's disease and other neurodegenerative disorders- memantine, a new hope. *Pharmacological Research*; 51, 1- 17.
104. Zhu S and Paoletti P (2015) Allosteric modulators of NMDA receptors: Multiple sites and mechanisms. *Current Opinion in Pharmacology*; 20, 14- 23.
105. Costa B, Irvine M, Fang G, Eaves R, Mayo-Martin M, Skifter D, Jane D and Monaghan D (2010) A Novel Family of Negative and Positive Allosteric Modulators of NMDA Receptors. *The Journal of Pharmacology and Experimental Therapeutics*; 335 (3), 614- 621.
106. Edman S, McKay S, McDonald L, Samadi M, Livesey M, Hardingham G and Wyllie D (2012) TCN 201 selectively blocks GluN2A-containing NMDARs in a GluN1 co-agonist dependent but non-competitive manner. *Neuropharmacology*; 63, 441- 449.
107. Muller S, Schreiber J, Schepmann D, Strutz-Seebohm N, Seeborhm G and Wunsch B (2017) Systematic variation of the benzenesulfonamide part of the GluN2A selective NMDA receptor antagonist TCN-201. *European Journal of Medicinal Chemistry*; 129, 124- 134
108. Seillier A and Giuffrida A (2009) Evaluation of NMDA receptor models of Schizophrenia: Divergences in the behavioral effects of sub-chronic PCP and MK-801. *Behavioural Brain Research*; 204, 410- 415.
109. Song X, Jensen M, Jogini V, Stein R, Lee C, Mchaourab H, Shaw D and Gouaux E (2018) Mechanisms of NMDA receptor channel block by MK-801 and memantine. *Nature*; 556, 515- 519
110. Mullasseril P, Hansen K, Vance K, Ogden K, Yuan Hm Kurtkaya N, Santangelo R, Orr A, Le P, Vellano K, Liotta D and Traynelis S (2010) A subunit-selective potentiator of NR2C- and NR2D- containing NMDA receptors. *Nature*; 1038, 1-8.
111. Suryabanshi P, Ugale R, Yilmazer-Hanke D, Stairs D and Dravid S (2014) GluN2C and GluN2D subunit-selective NMDA receptor potentiator CIQ

- reverses MK-801-induced impairment in pre pulse inhibition and working memory in Y-maze test in mice. *British Journal of Pharmacology*; 171, 799-809.
112. Villman C and Becker C (2007) On the Hypes and Falls in Neuroprotection: Targeting the NMDA Receptor. *The Neuroscientist*; 13 (6), 194- 615.
 113. Papke R and Smith C (2009) High Throughput Electrophysiology with *Xenopus* oocytes. *Combinatory Chemistry & High Throughput Screening*; 12 (1), 38-50
 114. Yelhekar T, Druzin M, Karlsson U, Blomqvist E and Johansson S (2016) How to Properly Measure a current- voltage relation? – Interpolation vs. Ramp methods applied to studies of GABA_A Receptors. *Frontiers in cellular neuroscience*; 10 (10), 1-10
 115. Hille B (2002) *Ion Channels of Excitable Membrane*. Massachusetts, USA: Sinauer Associates, 17-20.
 116. Karlsson R, Druzin M and Johansson S (2011) Cl⁻ concentration changes and desensitization of GABA receptors. *The Journal of General Physiology*; 138 (6), 609- 626
 117. Bianchi M and Macdonald R (2002) Slow phases of GABA (A) receptor desensitization: structural and possible relevance for synaptic function. *The Journal of Physiology*; 544 (1), 3-18
 118. Albeni C and Ilkanich E (2004) Open-Channel Blockers of the NMDA Receptor Complex. *Drugs News Perspect*; 17 (9), 1- 6.
 119. Lipton S (2004) Failures and Successes of NMDA Receptor Antagonist: Molecular Basis for the Use of Open-Channel Blockers like Memantine in the Treatment of Acute and Chronic Neurologic Insults. *The American Society for Experimental NeuroTherapeutics*; 1, 101- 110.
 120. Nicolaev M, Magazanik L and Tikhonov D (2012) Influence of external magnesium ions on the NMDA receptor channel block by different types of organic cations. *Neuropharmacology*, 62, 2078- 2085.
 121. Otton H, McLean A, Pannozzo M, Davies C and Wyllie D (2011) Quantification of the Mg²⁺ - induced potency shift of amantadine and memantine voltage-dependent block in human recombinant GluN1/ GluN2A NMDARs. *Neuropharmacology*; 60, 388- 396.
 122. Perszyk R, Swanger S, Shelley C, Khatri A, Fernandez-Cuervo G, Epplin M, Zhang J, Le P, Bulow P, Garnier-Amblard E, Reddy P, Bassel G, Yuan H, Menaldino D, Liotta D, Liebeskind L and Traynelis S (2020) Biased modulators of NMDA receptors control channel opening and ion selectivity. *Nature Chemical Biology*; 16, 188- 196
 123. Liu Y, Wong T, Aarts M, Rooyackers A, Liu L, Lai T, Wu D, Lu J, Tymianski M, Craig A and Wang Y (2007) NMDA Receptor Subunits Have Differential Roles In Mediating Excitotoxic Neuronal Death Both *In Vitro* and *In Vivo*. *The Journal of Neuroscience*; 27 (11), 2846- 2857
 124. Liu L, Wong T, Pozza M, Lingenhoehl K, Wang Y, Sheng M, Auberson Y and Wang Y (2004) Role of NMDA Receptor Subtypes in Governing the Direction of Hippocampal Synaptic Plasticity. *Science*: 304, 1021- 1024

125. Massey P, Johnson B, Moulton P, Auberson Y, Brown M, Molnar E, Collingridge G and Bashir Z (2004) Differential Roles of NR2A and NR2B-Containing NMDA Receptors in Cortical Long-Term Potentiation and Long-Term Depression. *The Journal of Neuroscience*; 24 (36), 7821- 7828
126. Luo T, Wu W and Chen B (2011) NMDA receptor signaling: death of survival? *Frontiers in Biology*; 6 (6), 468- 476
127. Grienberger C and Konnerth A (2012) Imaging Calcium in Neurons. *Neuron*; 73 (5), 862- 885
128. Priyadashini M, Nikkila O, Lagas S, Kolehmainen S and Castren E (2019) Culturing primary neurons from rat hippocampus and cortex. *Neuronal signaling*; 3 (2), 1- 10
129. Duncan G, Miyamoto S, Leipzig J and Lieberman J (1999) Comparison of brain metabolic activity patterns induced by ketamine, MK-801 and amphetamine in rats: support for NMDA receptors involvement in responses to subanesthetic dose of ketamine. *Brain Research*; 843, 171- 183
130. Yan J, Bengtson P, Buchthal B, Hagenston A and Bading H (2020) Coupling of NMDA receptors and TRPM4 guides discovery of unconventional neuroprotectants. *Science*; 370, 1- 7
131. Shibata K, Imanishi D, Abe K, Suzuki M, Takahashi S and Kera Y (2020) D-Aspartate N-methyltransferase catalyses biosynthesis of N-methyl-D-aspartate (NMDA), a well-known selective agonist of the NMDA receptor in mice. *BBA-Proteins and Proteomics*; 1868 (12), 1- 6
132. Hanson E, Armbruster M, Lau L, Sommer M, Klaf Z, Swanger S, Traynelis S, Moss S, Noubary F, Chadchankar J and Dulla C (2019) Tonic Activation of GluN2C/GluN2D-Containing NMDA receptors by ambient glutamate facilitates cortical interneuron maturation. *The Journal of Neuroscience*; 39 (19), 3611- 3626
133. Vyklicky V, Korinek M, Smejkalova T, Balik A, Krausova B, Kaniakova M, Lichnerova K, Cerny J, Krusek J, Dittert I, Horak M and Vyklicky L (2014) Structure, Function and Pharmacology of NMDA Receptor Channels. *Physiological Research*; 63, 191- 203
134. Madry C, Betz H, Geiger J and Laube B (2010) Potentiation of glycine-gated NR1/NR3A NMDA receptors relieves Ca²⁺-dependent outward rectification. *Frontiers in molecular neuroscience*; 3 (6), 1- 8
135. Kloda A and Adams D (2005) Voltage-dependent inhibition of recombinant NMDA receptor-mediated currents by 5-hydroxytryptamine. *British Journal of Pharmacology*; 144, 323- 330
136. Linsenhardt A, Chisari M, Yu A, Shu H, Zorumski C and Mennerick S (2013) Noncompetitive, Voltage-Dependent NMDA Receptor Antagonism by Hydrophobic Anions. *Molecular Pharmacology*; 83, 354- 366
137. Shelkar G, Pavuluri R, Gandhi P, Ravikrishnan A, Gawande D, Liu J, Stairs D, Ugale R and Dravid S (2019) Differential effect of NMDA receptor GluN2C and GluN2D subunit ablation on behavior and channel blocker-induced schizophrenia phenotypes. *Nature Scientific Reports*; 9 (7572), 1- 11
138. Chatterton J, Awobuluyi M, Premkumar L, Takahashi H, Talantova M, Shin Y, Cui J, Tu S, Sevarino K, Nakanishi N, Tong G, Lipton S and Zhang D (2002)

Excitatory glycine receptors containing the NR3 family of NMDA receptor subunits. *Nature*; 415, 793- 798.

139. NMDA receptor agonist (n.d.) An NMDA receptor agonist overview. Retrieved 05/01/2021 from <https://www.alomone.com/p/nmda/N-170>